

**Screening extracts of indigenous South African plants
for the presence of anti-cancer compounds.**

Magbubah Essack



A thesis submitted in fulfillment of the requirements for the degree of
Masters in Science in the Department of Biotechnology, Faculty of
Science, University of the Western Cape

Supervisor: Prof. DJG Rees

December 2006

ABSTRACT

Screening extracts of indigenous South African plants for the presence of anti-cancer compounds.

MSc. thesis, Department of Biotechnology, Faculty of Science, University of the Western Cape

Early man dabbled with the use of plant extracts to cure ailments. This practice has been passed down from generation to generation and today more than 50 % of the worlds' drugs are natural products or derivatives thereof. Scientists have thus established a branch of research called natural product research. This branch of research involves the identification and purification of secondary metabolites with a specific biological activity. The methodology involves the screening of plant products for a specific biological activity, purification of the biologically active natural product by separation technology and structure determination. The biologically active natural product/s is then further scrutinized to serve as a novel drug or lead compound for the development of a novel drug.

This research exploited this research methodology. I screened nine indigenous South African plants for anti-cancer 'pro-apoptotic' activity chosen on the basis of cytotoxicity and well-known ethno-medicinal value. It has been documented that choosing plants to be screened on this basis provides an increased possibility of finding biologically active compounds. The nine plants screened were *Cotyledon*

orbiculata, *Oxalis pes caprae*, *Echium plantagineum*, *Cissampelos capensis*, *Euphobia mauritanica*, *Haemanthus pubescens*, *Cynanchum africanum*, *Lessertia frutescens* and *Elytropappus rhinocerotis*. Their extracts were screened via the cytotoxicity assay and numerous apoptosis assays namely; the APOPercentage™ assay, Annexin V-PE Detection assay, Active Caspase-3 Detection assay and the APO-DIRECT™ Kit. *E. rhinocerotis* is the only extract that exhibited significant pro-apoptotic activity in all of three cell lines (MCF7, HeLa and CHO) used. It is for this reason that this plant had been selected for further study.

Anti-cancer activities associated with *E. rhinocerotis* plant extracts from different geographical locations were then assessed to ascertain the superlative extract to be used for the purification process. The aqueous extract from the *E. rhinocerotis* collected from Tulbagh in the Western Cape displayed the highest activity. The significant variation in pro-apoptotic activity induced by the same plant from different geographical locations may be a consequence of environmental variation or genetic variation. Thus, this study shows preliminary data that suggest a possible link between variation in apoptosis activity and genetic variation.

The secondary metabolites in the extract from the *E. rhinocerotis* collected from Tulbagh were then purified by bio-activity guided fractionation. The fractionation or separation technology used includes organic extraction, Liquid Column Chromatography (LCC), Thin Layer Chromatography (TLC) and High Performance Liquid Column Chromatography (HPLC). The success of this purification process was monitored and ascertained by serial dilution assays of the active fraction after

each fractionation step. This process successfully transformed a complex mixture of secondary metabolites represented by numerous peaks on a chromatograph to a single peak. This warranted an attempt at structure determination by MS and NMR.

NMR data allowed the elucidation of a partial structure. However, further purification is necessary for the elucidation of two side chains. Once these side chains are known, the pro-apoptotic activity of this compound (if novel) or commercially available compound must be verified.

This research established that this research methodology is successful and provides optimism for the development of an anti-cancer drug.

December 2006



KEYWORDS:

Anti-cancer

Apoptosis

Apoptosis pathways

Cytotoxicity

Bio-assay guided fractionation

Cell cycle

Chromatography

Elytropappus rhinocerotis

Sutherlandia frutescens

Flow cytometry

Natural products



UNIVERSITY *of the*
WESTERN CAPE

For my family

Especially Taskeen, Haaniem, Gabieb, Ameera, Mariam, Kauthar, Ameer, Zubair,

Isma-eel, Riedaa, Ayoub and Bilqees



DECLARATION

I declare "**Screening extracts of indigenous South African plants for the presence of anti-cancer compounds**" to be my work, which has not been submitted for any degree or examination in any other institution, and that all the sources I have used or quoted have been indicated and acknowledged by references.

Magbubah Essack



December 2006

Signed:.....

TABLE OF CONTENTS

Page

ABSTRACT.....	II
KEYWORDS.....	V
DEDICATION.....	VI
DECLARATION.....	VII
TABLE OF CONTENTS.....	VIII
LIST OF FIGURES AND TABLES.....	XIII
ABBREVIATIONS.....	XVIII
ACKNOWLEDGEMENTS	XXI

CHAPTER 1: LITERATURE REVIEW..... 1

1.1) Introduction 1

1.2) Apoptosis 3

1.2.1) Historical overview of the term apoptosis 3

1.2.2) Morphological features of apoptosis 4

1.2.3) Physiological significance of apoptosis 5

1.2.4) Molecular mechanisms of apoptosis signaling pathways 6

1.2.4.1) Various death signals activate common signaling..... 6

1.2.4.2) Key regulatory componenets in apoptosis signaling 8

1.2.4.2.1) *The Caspase family: central initiators and executioners of apoptosis* 8

1.2.4.2.2) *The Bcl-2 family* 9

1.2.4.2.3) Regulation of apoptosis by inhibitors of apoptosis proteins (IAP's) 10

1.2.4.2.4) *Regulation of apoptosis by heat shock proteins (Hsp)* 11

1.2.4.3) The most extensively researched apoptosis pathways	11
1.2.4.3.1) The death receptor or "extrinsic" apoptosis pathway of type I and type II	12
1.2.4.3.2) The mitochondrial or "intrinsic" apoptosis pathway.....	16
1.2.4.3.3) The ER stress signaling pathway.....	17
1.2.5) Genes implicated in cancer	18
1.3) Plants as sources of anti-cancer drugs	20
1.3.1) Cell cycle regulation.....	22
1.3.2) Current plant-derived anti-cancer drugs	25
1.3.2.1) Paclitaxel and docetaxel.....	25
1.3.1.2) Camptothecin and topotecan.....	27
1.3.1.3) Colchicine	28
1.3.1.4) Podofilox and etoposide.....	29
1.3.1.5) Vinblastine, vincristine, vindesine and vinorelbine.....	30
CHAPTER 2: MATERIALS AND METHODS	33
2.1) General chemicals and assay kits.....	33
2.2) Stock solutions and buffers	34
2.3) Tissue culture media and cell lines	35
2.4) Culturing of cells	36
2.4.1) Thawing of cells.....	36
2.4.2) Trypsinization of cells	36
2.4.3) Freezing of cells	37
2.4.4) Seeding of cells	37

2.5) Tests authenticating the induction of apoptosis	37
2.5.1) Cytotoxicity assay	37
2.5.2) APOPercentage™ assay	38
2.5.3) Annexin V- PE Apoptosis Detection assay.....	38
2.5.4) Active Caspase 3 - PE Mab Apoptosis	39
2.5.5) APO-DIRECT™ Kit	40
2.6) Phylogenetic studies.....	41
2.6.1) 2x CTAB DNA extraction	41
2.6.2) Polymerase Chain Reaction (PCR).....	42
2.6.3) Agarose gel electrophoresis of DNA.....	43
2.6.4) Purification of DNA fragments	43
2.6.5) Cloning PCR fragments into pGEM®-T Easy.....	43
2.6.6) Colony PCR and sequence analysis.....	44
2.7) Methods of fractionation	46
2.7.1) Aqueous extraction.....	46
2.7.2) Organic solvent extraction	46
2.7.3) Thin Layer Chromatography (TLC)	47
2.7.3.1) Determining the solvent system need to separate extract by TLC	47
2.7.3.2) Concentrated compound fractionation by TLC.....	48
2.7.4) Liquid Column Chromatography (LCC)	49
2.7.5) Reverse-Phase High Performance Liquid Chromatography (RP-HPLC).....	49
 CHAPTER 3: SCREENING INDIGENOUS SOUTH AFRICAN PLANTS FOR	
PRO-APOPTOTIC ACTIVITY	51
3.1) Introduction	51
3.2) Aqueous extraction of plant secondary metabolites	54

3.3) Analysis of the cytotoxic and pro-apoptotic effects of plant extracts.....	55
3.3.1) Screening cytotoxic effects of plant aqueous extracts using the neutral red (NR) assay	55
3.3.2) Ascertaining if cytotoxicity is as a consequence of apoptosis induction using the APOPercentage™ assay.....	56
3.4) Screening <i>E. rhinocerotis</i> aqueous extract for the ability to induce specific markers of apoptosis	60
3.4.1) Externalization of phosphatidylserine (PS).....	60
3.4.2) Caspase-3 activation.....	61
3.4.3) DNA fragmentation.....	63
3.3.4) Summary.....	64
CHAPTER 4: INVESTIGATING WHETHER THE VARIATION IN BIOACTIVITY WITHIN THE <i>E. RHINOCEROTIS</i> SPECIES IS ASSOCIATED WITH GENETIC VARIATION.....	66
4.1) Introduction	66
4.2) Pro-apoptotic activity of <i>E. rhinocerotis</i> from different geographical location	68
4.3) Genetic study.....	69
4.3.1) Cloning ITS1 into pGEM® –T Easy vector.....	69
4.3.2) Phylogenetic analysis of ITS1.....	70
4.4) Summary.....	71

CHAPTER 5: THE PARTIAL PURIFICATION OF THE PRO-APOPTOTIC SECONDARY METABOLITE/S ISOLATED FROM E. RHINOCEROTIS.....	73
5.1) Introduction	73
5.2) Organic extraction used to fractionate the aqueous extract from E. rhinocerotis.....	75
5.3) Chromatography.....	76
5.3.1) Thin Layer Chromatography (TLC).....	77
5.3.2) Liquid Column Chromatography (LCC)	77
5.3.3) Reverse-Phase High Performance Liquid Chromatography	79
5.4) Structure Determination.....	82
5.3) Summary	85
CHAPTER 6: GENERAL DISCUSSION.....	87
6.1) Introduction	87
6.2) Screening extracts of indigenous South African plants for the presence of anti-cancer compounds.....	88
6.3) Investigating whether the variation in bioactivity within the E. rhinocerotis species is associated with genetic variation.....	91
6.4) The partial purification of the pro-apoptotic secondary metabolite/s isolated from the extract of the E. rhinocerotis plant from Tulbagh.....	93
6.5) Summary	94
REFERENCES	96



LIST OF FIGURES AND TABLES

Tables

Chapter 1

Table 1.1: Morphological and biochemical characteristics of apoptosis versus necrosis

Table 1.2: Cancer Pre-disposition genes

Table 1.3: Plant derived pharmaceutical drugs

Chapter 2

Table 2.1: The cell lines used

Table 2.2: APO-DIRECT™ kit staining solution

Table 2.3: Experimental set up of the PCR reactions

Table 2.4: Experimental set up of the ligation reactions

Table 2.5: Experimental set up of the colony PCR

Chapter 3

Table 3.1: Plants screened to treat conditions consistent with cancer symptoms

Table 3.2: Yields associated with the aqueous extraction of the dry plant material

Chapter 5

Table 5.1: Serial dilutions of the active fractions used to verify the success of the purification process

Figures

Chapter 1

- Figure 1.1:** Tumor-suppressor genes involved in Human cancers
- Figure 1.2:** Sketch representation hallmarks of the apoptotic and necrotic cell death:
- Figure 1.3:** During limb formation separate digits evolve by death of interdigital mesenchymal tissue
- Figure 1.4:** Current nomenclature for human caspase and their corresponding sub-family groups based on phylogenetic analysis
- Figure 1.5:** Bcl2 family members possess up to four Bcl-2 homology domains
- Figure 1.6:** There are three major delineated pathways namely; the death receptor pathway, the mitochondrial pathway and the ER stress pathway.
- Figure 1.7:** Cell cycle phases
- Figure 1.8:** DNA repair mechanisms
- Figure 1.9:** The Chemical structure of (A) paclitaxel and (B) docetaxel
- Figure 1.10:** The Chemical structure of (A) Camptothecin and (B) Topotecan
- Figure 1.11:** The Chemical structure of Colchicine
- Figure 1.12:** The Chemical structure of (A) Podophyllotoxin and (B) Etoposide.
- Figure 1.13:** The Chemical structure of (A) Vinblastine and (B) Vincristine
- Figure 1.14:** The Chemical structure of (A) Vinorelbine and (B) Vindesine

Chapter 3

- Figure 3.1:** Pictorial representation of the nine indigenous South African plants screened for apoptosis activity
- Figure 3.2:** Screening plant aqueous extracts for induction of cytotoxicity and apoptosis activity on the MCF7 cell line
- Figure 3.3:** Screening plant aqueous extracts for induction of cytotoxicity and apoptosis activity on the HeLa cell line
- Figure 3.4:** Screening plant aqueous extracts for induction of cytotoxicity and apoptosis activity on the CHO cell line
- Figure 3.5:** Flow cytometric analysis demonstrating the externalization of phosphatidylserine in CHO cells treated for 6 h with 3.5 mg/ml of plant aqueous extract
- Figure 3.6:** Flow cytometric analysis demonstrating the presence of active caspase-3 in CHO cells treated for 6 h with 3.5 mg/ml of plant aqueous extract
- Figure 3.7:** Flow cytometric analysis of DNA fragmentation

Chapter 4

- Figure 4.1:** Flow cytometric analysis of the *E. rhinocerotis* extracts from different geographical locations by APOPercentage™ staining.
- Figure 4.2:** Agarose gel electrophoretic representation of the gDNA extracted from the *E. rhinocerotis* collected from different geographical locations

Figure 4.3: PCR screening for the presence of the ITS1 sequence of *E. rhinocerotis* collected from different geographical locations

Figure 4.4: Colony PCR screening for the presence of the ITS1 sequence of *E. rhinocerotis* collected from different geographical locations

Figure 4.5: Sequence alignment of the ITS1 sequences of *E. rhinocerotis* collected from different geographical locations

Figure 4.6: Phylogenetic tree of the aligned ITS1 sequences of the *E. rhinocerotis* and homologous sequences that were retrieved using BLAST

Chapter 5

Figure 5.1: Flow cytometric analysis of the effects of methanol using the APOPercentage™ assay

Figure 5.2: Flow cytometric analysis of the organic fractions by APOPercentage™ staining

Figure 5.3: Flow cytometric analysis of the LCC fractions by APOPercentage™ staining

Figure 5.4: Flow cytometric analysis of the TLC fractions by APOPercentage™ staining

Figure 5.5a: Flow cytometric analysis of the HPLC fractions by APOPercentage™ staining

Figure 5.5b: A HPLC chromatograph representing the active TLC fraction, nB 67.2.

Figure 5.6: Chromatographs illustrating the complexity of the active fractions identified in the purification process.

Figure 5.7: ^{13}C NMR spectrum

Figure 5.8: ^1H - ^{13}C HMBC NMR spectrum

Figure 5.9: ^1H ^{13}C NMR spectrum

Figure 5.10: ^1H - ^{13}C HSQC NMR spectrum

Figure 5.11: ^1H - ^1H COSY NMR spectrum

Figure 5.12: Compound structure 6-(4'-hydroxyphenyl)-2,3-di(R)tetrahydro-4H-pyran-4-one elucidated by NMR data.



ABBREVIATIONS

7-AAD	7-Amino-actinomycin D
AIF	Apoptosis inducing factor
Apaf-1	Apoptotic protease-activating factor-1
Bax	Bcl-2-associated x protein
Bcl-2	B cell leukaemia-2
BLAST	Basic local alignment search tool
bp	base pair
BPB	Bromophenol blue
CAD	caspase-activated deoxyribonuclease
CARD	caspase recruitment domain
Caspase	cysteine aspartic-specific protease
CED	cell death defective
c-FLIP	Cellular-Fas-associated death domain-like ICE inhibitory protein
CHO cells	Chinese hamster ovary cells
Daxx	Fas death domain associated protein
DD	Death domain
DED	death effector domain
dH ₂ O	distilled water
DIABLO	Direct IAP-binding protein with low pI
DISC	death-inducing signaling complex
DMEM	Dulbecco's modified eagle medium

DMSO	Dimethylsulphoxide
DNA	deoxyribonucleic acid
EDTA	ethylene diamine tetra-acetic acid
EGL-1	external germinal layer-1
ER	endoplasmic reticulum
EtBr	Ethidium bromide
FACS	fluorescence activated cell sorter
FADD	fas associated death domain
Fas	fibroblast-associated
FCS	foetal calf serum
FITC	fluorescein isothiocyanate
h	hours
HCl	Hydrochloric acid
HPLC	High Performance Liquid Chromatography
Hsp	heat shock proteins
IAP	inhibitors of apoptosis
ICAD	inhibitor of CAD
ICE	interleukin-1- β -converting caspase enzyme
LB	Luria broth
LCC	Liquid column chromatography
mg/ml	milligrams per millilitre
min	minutes
MS	Mass Spectroscopy
MPTP	mitochondrial permeability transition pore

NaCl	Sodium chloride
NMR	Nuclear Magnetic Resonance
NR	neutral red
PARP	Poly (ADP-ribose) Polymerase
PBS	phosphate buffered saline
PCR	Polymerase chain reaction
PE	Phycoerythrin
PS	phosphatidylserine
RADD	RIP associated ICH/CED-3 homologous protein with a death domain
Rb	Retinoblastoma
RIP	Receptor interacting protein
RT	room temperature
Smac	Second mitochondrial-derived activator of caspase
tBid	truncated BH3 Interacting Domain Death Agonist
TNF	Tumor necrosis factor
TRADD	TNFR-associated death domain
TRAIL	TNF-related apoptosis-inducing ligand
Tris	Tris [hydroxymethyl] aminoethane
UV	Ultra violet
VDAC	Voltage-dependent anion channel

ACKNOWLEDGEMENTS

I begin in the name of Allah, the Most Compassionate, the Most Merciful

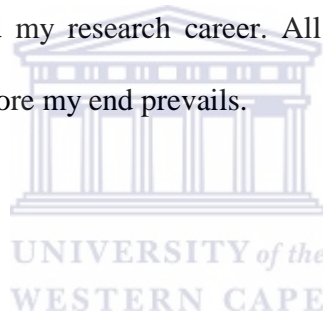
My most fervent appreciation is extended to my friend and colleague Dr. Mervin Meyer for his intellectual insight and overwhelming support. You have been my pillar of strength, my inspiration and my exemplar; thus, nurturing my personal growth that has made my completion of this thesis possible.

To my supervisor, Prof. DJG Rees, I express my gratitude for his guidance, support and intellectual input. My appreciation is also extended to Prof. IR Green for his assistance and intellectual input with regards to the separation technology used. My gratitude is extended to the National Research Foundation for the financial support of this project. I am also indebted to Raymond Daniels, Moegammat Faghrie February, Joseph Mfofo, Stonard Kanyanda, Andrew Faro, Sunil Sagar and Dr. Mandeep Kaur for their never-ending assistance. My boundless appreciation goes to all the members of the Jasper Rees Laboratory, and the entire Applied Biotechnology department; who have carved their memory in my heart with a mere greeting or a smile.

To my siblings and their kids (all twelve of you) my life and accomplishments would be meaningless without you.

Last, but not least to my mother, my mother, my mother... so much to say too little words. My mother lost the love of her life exactly 23 years ago this December to meningitis. With five children to support ranging from 1 to 16 years, my mother had much to cry about but never allowed us to see. All she shared with us was tears of happiness, laughter, an unwavering moral compass and a rigid support structure to ensure that her childrens dreams are realized. Yet, this is not where giving of herself ends, as I have seen her literally help thousands of people in their time of need; she even befriends the homeless whom most try to avoid. How many kids can say that they are astounded at their mothers' excellence on a daily basis or that their mother is their best friend? I can and now that I am older and hopefully wiser, my ultimate ambition extends beyond my research career. All I hope for is that I am half the women my mother is, before my end prevails.

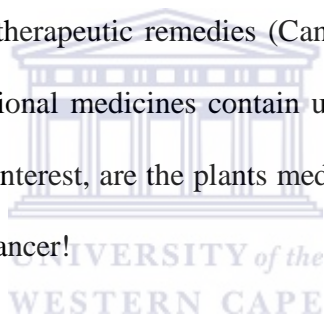
I love you, mom.



CHAPTER 1: LITERATURE REVIEW

1.1) Introduction

Reflection and Wisdom! Can wisdom exist without reflection? The wise reflect on the past to ensure that the mistakes of the past do not recur, so too, do they reflect upon its milestones that serve as the building blocks of the future. Accordingly, we will visit the past and find wisdom in the practices of the ancestors. Traditionally indigenous plant species and their extracts were the primary source of medicine. Today, natural products or derivatives thereof constitute more than 50% of internationally approved therapeutic remedies (Cannell, 1998). It is therefore highly probable that these traditional medicines contain useful substances with unexplored medicinal properties. Of interest, are the plants medicinal values to one of the world's leading causes of death, cancer!



Cancer is a genetic disease characterized by uncontrolled cell growth in the absence of cell cycle regulation. Aberrant cell cycle regulation can arise as a consequence of DNA damage. Under normal physiological conditions the uncontrolled growth of damaged cells is restricted by apoptosis. However these cells can escape the regulatory mechanisms of apoptosis as a result of secondary mutations to genes that regulate apoptosis. This DNA damage can be a result of several environmental factors such as stress, smoking, pollution, diet, toxins and endogenous processes such as errors in replication of DNA and chemical instability of certain DNA bases (Thompson, 1995). Gene mutations may also be inherited (illustrated in [figure 1.1](#)).

TUMOR-SUPPRESSOR GENE	CHROMOSOMAL LOCUS	LOCATION/PROPOSED FUNCTION	SOMATIC MUTATIONS		INHERITED MUTATIONS		
			MAJOR TYPES	EXAMPLES OF NEOPLASMS	SYNDROME	HETEROZYGOTE CARRIER RATE PER 10 ⁵ BIRTHS†	TYPICAL NEOPLASMS
p53	17p13.1	Nucleus/transcription factor	Missense	Most types of human cancer	Li-Fraumeni syndrome	~2	Carcinomas of breast and adrenal cortex; sarcomas; leukemia; brain tumors
<i>RBI</i>	13q14	Nucleus/transcription modifier	Deletion and nonsense	Retinoblastoma; osteosarcoma; carcinomas of the breast, prostate, bladder, and lung	Retinoblastoma	~2	Retinoblastoma; osteosarcoma
<i>APC</i>	5q21	Cytoplasm/unknown	Deletion and nonsense	Carcinoma of the colon, stomach, and pancreas	Familial adenomatous polyposis coli	~10	Carcinomas of colon, thyroid, and stomach
<i>WT1</i>	11p13	Nucleus/transcription factor	Missense	Wilms' tumor	Wilms' tumor	~0.5-1	Wilms' tumor
<i>NF1</i>	17q11	Cytoplasm/guanosine triphosphatase-activating protein	Deletion	Schwannomas	Neurofibromatosis type 1	~30	Neural tumors
<i>NF2</i>	22q	Cytoplasm/cytoskeleton-membrane link	Deletion and nonsense	Schwannomas and meningiomas	Neurofibromatosis type 2	~3	Central schwannomas and meningiomas
<i>VHL</i>	3p25	Unknown/unknown	Deletion	Unknown	von Hippel-Lindau disease	~3	Hemangioblastoma and renal-cell carcinoma

*Data obtained from Weinberg,¹ Latif et al.,² Trowfater et al.,³ and Rouleau et al.⁴ (and Knudson A: personal communication).

†Data obtained from Schimke⁵ (and Knudson A: personal communication).

Figure 1.1. Tumour suppressor genes involved in Human cancers (from Harris and Holstein. 1993)

Orthodox cancer treatments include chemotherapy, radiotherapy, and surgery (McWhirter *et al.*, 1996). These treatments have proved to be ineffective cancer treatments as a result of its toxicity and cells developing resistance (Curtis *et al.*, 1992). Kaldor *et al.*, (1990) reported 114 cases of leukemia developing in patients treated with concurrent chemoradiotherapy (chemoRT) for ovarian cancer (Kaldor *et al.*, 1990). Recent studies in Non-Small-Cell Lung Cancer (NSCLC) demonstrates that treatment with chemoRT yields a survival rate of 21% (Le Chevalier *et al.*, 1991) while a Phase II study of induction chemotherapy with gemcitabine and vinorelbine followed by concurrent chemoradiotherapy with oral etoposide and cisplatin in patients with inoperable stage III non-small-cell lung cancer yields a survival rate of 43,9% (Lee *et al.*, 2005). This multi-drug approach provides a glimmer of hope but still leaves much to be desired, as the ideal anti-cancer drug must be selective and cytotoxic to cancer cells. Many anti-cancer drugs are derived from natural sources, including marine, microbial origin and plants. The FDA approved plant derived drugs include Combretastatin A-4 phosphate (*Combretum caffrum*), Taxol (*Taxus brevifolia*), Velban (*Catharanthus roseus*) and so on. These chemotherapeutic drugs have diverse mechanisms of action. However, their ability to induce programmed cell death (PCD) is the unifying event for the mechanisms of chemoprevention (Hadfield *et al.*, 2003).

PCD (also referred to as apoptosis) consists of a set of pathways leading to non-inflammatory cell suicide, as apposed to chaotic, unstructured cell death coined necrosis (Kerr *et al.*, 1972). Substantial down-regulation and up-regulation of apoptosis leads to cancer and neurodegenerative diseases, respectively. Thus

apoptosis is critical to the development and maintenance of homeostasis in multicellular organisms. Apoptosis has been documented to play a crucial role in embryogenesis, metamorphosis and morphogenesis (Renehan *et al.*, 2001; Steller, 1995). Necrotic cell death results from physical injury or disease that causes cell membrane damage, with the ensuing cell swelling due to the influx of water and sodium ions and consequently inflammation (Kroemer *et al.*, 1998). Distinctively, apoptosis displays phenotypic characteristics such as cell shrinkage, chromatin condensation, plasma membrane blebbing and DNA fragmentation (Zhao *et al.*, 2001). The apoptotic bodies resulting from the plasma membrane blebbing are phagocytosed thus preventing inflammation (Savill, 1996). These phenotypic characteristics result from specific cascading events and are thus proof of the existence of distinct pathways for apoptosis.

Apoptotic pathways are being delineated, for the purpose of identifying novel apoptosis targets. Inducers or inhibitors of the apoptotic pathways can be used to control the substantial up-regulation and down-regulation of apoptosis and consequently influence disease states.

1.2) Apoptosis

1.2.1) Historical overview of the term apoptosis

Hippocrates of Cos, the father of Western medicine (*ca.* 460-370 BC) used the term, apoptosis for the first time in the textual translation, "the falling off of the bones"

describing structural changes (bone erosion) related to tissue and cell death (Degli-Esposti, 1998). Another notable use of the word apoptosis was in textual translation the "dropping of the scabs" denoted by Galen (129-201 AD). This use of the term apoptosis relates it to wound healing and inflammation (Hetts, 1998). The term programmed cell death was introduced in 1964, proposing that cell death during development is not of accidental nature but follows sequential, controlled steps leading to defined self-destruction (Lockshin and Williams, 1964). In 1972, the term apoptosis was re-introduced into modern scientific writing by Kerr *et al* and had been coined to describe the morphological processes leading to controlled cellular self-destruction distinct from necrotic cell death (Kerr *et al.*, 1972).

1.2.2) Morphological features of apoptosis

Apoptosis is initiated in normal cells by a variety of stimuli such as, ligation of cell surface receptors, a lack of survival signals, developmental death signals, DNA damage as a result of defects in DNA repair mechanisms or treatment with cytotoxic drugs and/or irradiation. These stimuli leads to the activation of several apoptotic pathways with characteristic morphological and biochemical changes (listed in [table 1.1](#)) that are used in the identification of apoptosis (Kerr *et al.*, 1972; Zhao *et al.*, 2001). An important distinction between necrosis and apoptosis is the fact that cells that had undergone apoptosis forms apoptotic vesicles that are phagocytosed by macrophages or neighboring cells preventing inflammation ([figure 1.2.](#)) (Ren and Savill, 1998).

Table1.1. Morphological and biochemical characteristics of apoptosis versus necrosis

	Differences		Similarity / variables
	Apoptosis	Necrosis	
Nuclei	Dense condensation of chromatin	Irregular chromatin clumping	Damage occur in both
Cytoplasmic organelles	Morphologically intact	Disrupted	Secondary damage in apoptosis
Cell membrane	Cell blebbing	Loss of integrity	Changes seen in both
Cell volume	Cells shrink	Cells swell	Occasionally no change
In tissues	Individual cells affected	Groups of cells affected	Superficial epithelial cells are apoptotic.
Tissue response	None	Inflammation	N/A
Nuclear DNA damage	DNA fragmentation (+-200bp), ladder visible on gel	Random DNA fragmentation, smears on gel	Takes place in both
Mitochondrial DNA damage	Occurs late	Occurs early	N/A
Cell membrane	Intact	Loss of function	N/A
Cell internal milieu	Na ⁺ /K ⁺ pump intact and ATP required	Defective Na ⁺ /K ⁺ pump and no ATP	N/A

(Studzinski, 1999)

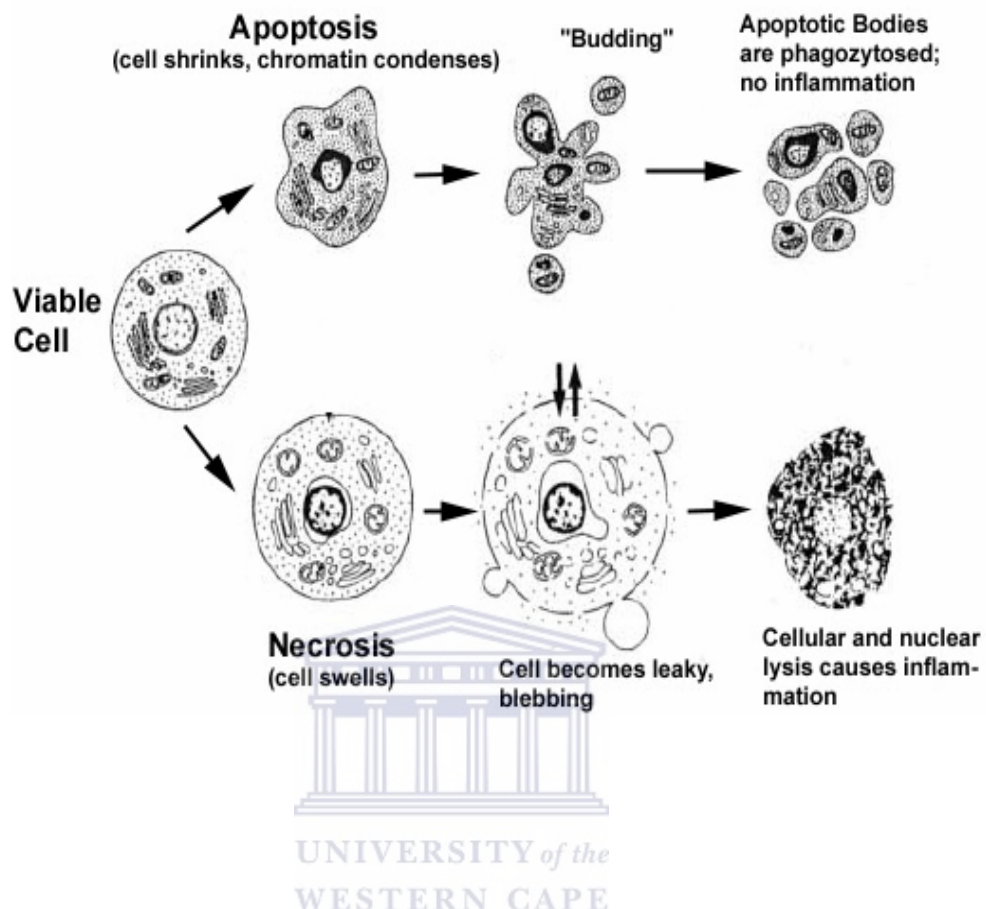


Figure 1.2. Sketch representation hallmarks of the apoptotic and necrotic cell

death:

Apoptosis includes cellular shrinking, chromatin condensation and margination at the nuclear periphery which ultimately results in membrane-bound apoptotic bodies / vesicles that are phagocytosed without triggering inflammatory responses. The necrotic cell swells, disrupts and releases its contents into the surrounding tissue causing inflammation (Van Cruchten and Van Den Broeck, 2002).

1.2.3) Physiological significance of apoptosis

The development and maintenance of biological systems depends on the refined interaction between cells. Throughout development many cells undergo apoptosis which contributes to the sculpturing of the organs and tissues (illustrated in figure 1.3) (Meier *et al.*, 2000). As an example, half of the neurons that are initially created during brain formation will die in the later stages of adult brain development (Hutchins and Barger, 1998). Also, adult organs maintain homeostasis by constantly undergoing physiological cell death which is balanced with proliferation. As an example, developing lymphocytes die in the formation of the antigen receptor, thereby controlling and maintaining relatively constant numbers of immune cells (Rathmell and Thompson, 2002). Holistically, the apoptotic processes are of widespread biological significance playing vital roles in development, differentiation, homeostasis, regulation and functioning of the immune system, as well as the removal of defective or harmful cells.

Consequently, the abnormal or excessive up-regulation and down-regulation of apoptosis is implicated in a variety of pathological conditions. The abnormal or excessive down-regulation and/or the termination of apoptosis result in the formation of malignant tumors and other diseases such as Autoimmune Lymphoproliferative Syndrome (ALPS) (Sneller *et al.*, 1997). Conversely abnormal or excessive up-regulation of apoptosis leads to other disease states such as Alzheimer's disease (Jellinger, 2001) and Parkinson's disease (Merad-Boudia *et al.*, 1998). Apoptotic cell death is a common discernible occurrence in all kinds of protozoans (Solomon *et al.*, 1999) and eukaryotes (Ameisen, 2002; Frohlich and Madeo, 2000). Insight into the

Fetal development



Figure 1.3. During limb formation separate digits evolve by death of interdigital mesenchymal tissue (BabyCenter, 2007).

origin and evolution of apoptosis has been made possible by the identification of crucial apoptosis components in the nematode worm, *Caenorhabditis elegans* (Hengartner and Horvitz, 1994).

1.2.4) Molecular mechanisms of apoptosis signaling pathways

1.2.4.1) Various death signals activate common signaling

Apoptosis is a tightly regulated cell death program which requires the interplay of a multitude of genes. The components of the apoptotic signaling network are genetically encoded in a nucleated cell equipped to be activated by a death-inducing stimulus (Ishizaki *et al.*, 1995; Weil *et al.*, 1996). The death inducing stimuli are of diverse origin but appear to activate common cell death machinery leading to the

characteristic features of apoptotic cell death. In mammalian pathways it is known that the B cell leukaemia-2 (Bcl-2) family of proteins plays a central role in the decision step of apoptosis whereas the cysteine aspartic-specific proteases (caspase) family is essential in the execution of cell death (Alnemri *et al.*, 1996; Chao and Korsmeyer, 1998).

The fact that the physiological process of apoptosis has been conserved through evolution has contributed immensely to our understanding of apoptosis (Raff *et al.*, 1993). Genetic analysis of the apoptosis process in *C. elegans* is a milestone in defining key components in mammalian apoptosis pathways (Hengartner and Horvitz, 1994). It has been established in *C. elegans* that the cell death defective-9 (ced-9) protein binds to the ced-4 protein preventing the onset of apoptosis (Chinnaiyan *et al.*, 1997). However, external germinal layer-1 (egl-1) negatively regulates ced-9 by binding to and directly inhibiting the activity of ced-9, that is, ced-4 is released from the ced-9/ced-4 protein complex (Conradt and Horvitz, 1998). The released ced-4 is now free to initiate apoptosis by activating ced-3 (Chinnaiyan *et al.*, 1997b). Due to the structural and functional similarity of these proteins to their mammalian homologues, researchers were able to delineate apoptotic pathways in mammals. The ced-9 protein is structurally and functionally similar to the mammalian Bcl-2-like survival factors. Likewise, the egl-1 protein is structurally and functionally similar to the mammalian Bax-like death factors (illustrated in figure 1.4.) (Hengartner and Horvitz, 1994). The ced-4 protein is homologues to the pro-apoptotic protease-activating factor (Apaf-1) (Yuan and Horvitz, 1992; Zou *et al.*, 1997). The ced-3 protein is homologues to the mammalian protein interleukin-1 beta converting

enzyme (ICE), also known as caspase-1 (Yuan *et al.*, 1993). ICE is an aspartate-specific cysteine protease and is classified as an effector caspase (Alnemri *et al.*, 1996).

To date 12 human caspase have been identified, along with the murine caspase (caspase-11), the bovine caspase (caspase-13) and a caspase found in most mammals (caspase-15) (Eckhart *et al.*, 2005; Koenig *et al.*, 2001; Lamkanfi *et al.*, 2002).

1.2.4.2) Key regulatory componenets in apoptosis signaling

1.2.4.2.1) The Caspase family: central initiators and executioners of apoptosis

The caspase family of proteases may be divided into initiator caspases that are activated through regulated protein-protein interactions and effector caspases that are activated proteolytically by an upstream / initiator caspase (figure 1.4.) (Hengartner, 2000).

Caspases are synthesized as enzymatically inert zymogens that consist of three domains namely, an *N*-terminal prodomain, a p20 domain and a p10 domain. Caspases are usually activated by proteolytic cleavage between these domains. They also bind to and associate with upstream regulators due to a protein-protein interaction module contained in the prodomain (Chang and Yang, 2000). Caspase-8 and caspase-10 have a death-effector domain (DED), whereas caspase-9 and caspase-2 contain caspase activation and recruitment domains (CARD) (Boldin *et al.*, 1996;

Li *et al.*, 1997). The death adapter domain mediates intra-family interactions i.e. DED/DED or CARD/CARD, but also interact as integration platforms binding to different proteins that could modulate their dimerization and hence, caspase activity (Chou *et al.*, 1998; Colussi *et al.*, 1998).

HUMAN CASPASES	ORIGINAL NAMES	FUNCTION	
		Apoptosis	Other
Caspase 1	ICE		Inflammation
Caspase 4	ICE II, TX, ICH-2		Inflammation
Caspase 5	ICE III, TY		Inflammation
Caspase 11	?		?
Caspase 12	?		?
Caspase 13	ERICE		Inflammation
Caspase 14	?		Inflammation
Caspase 3	CPP32, Yama, apopain	effector	
Caspase 6	Mch 2	effector	
Caspase 7	Mch 2, ICE-LAP3, CMH-1	effector	
Caspase 2	ICH-1	initiator/effector?	
Caspase 8	MACH, FLICE, Mch5	initiator	
Caspase 9	Mch 6, ICE-LAP6	initiator	
Caspase 10	Mch 4	initiator/?	
Caspase 15	?	initiator	

Figure 1.4. Current nomenclature for human caspases and their corresponding sub-family groups based on phylogenetic analysis (Lamkanfi *et al.*, 2002; Nicholson and Anderson, 2002).

1.2.4.2.2) *The Bcl-2 family*

The Bcl-2 family of proteins is divided into three groups based on structural similarity and functional criteria. Group I possesses anti-apoptotic activity, whilst Group II and III promote cell death (illustrated in [figure 1.5.](#)). The Bcl-2 family controls cell death by forming heterodimers (interaction between pro-apoptotic and anti-apoptotic Bcl-2 family members) that mutually neutralize pro-apoptotic and anti-

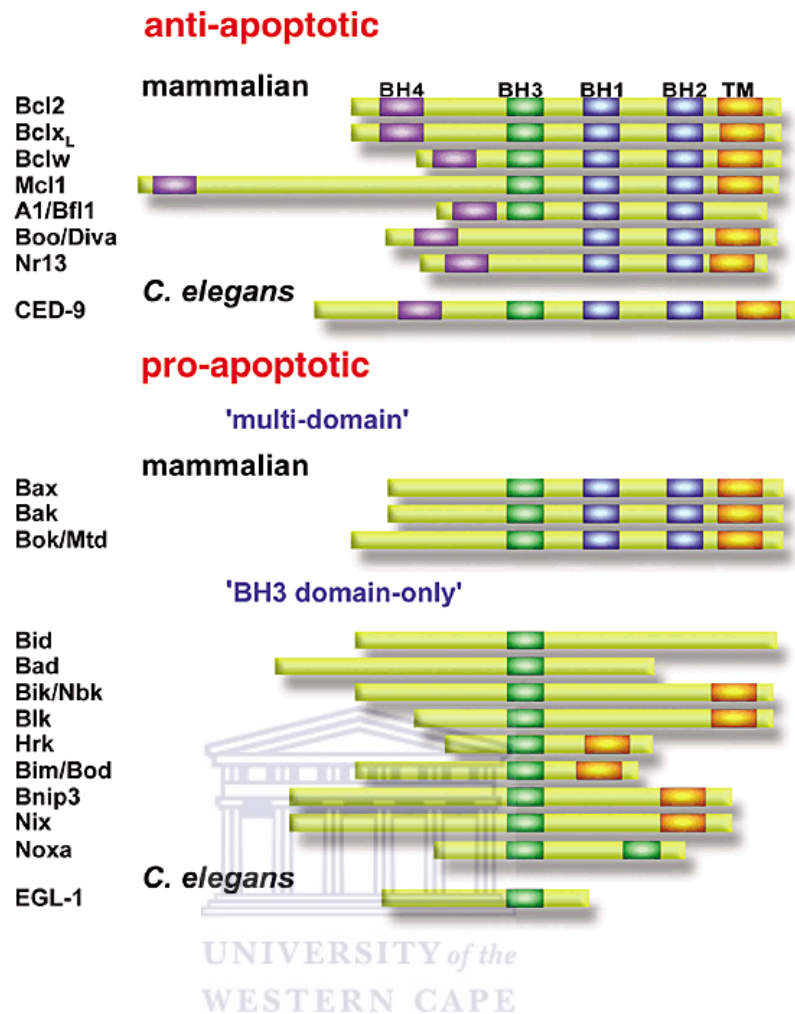


Figure 1.5: Bcl2 family members possess up to four Bcl-2 homology domains (BH1-4) corresponding to α -helical segments (denoted by coloured boxes). Some members also possess a carboxy-terminal hydrophobic trans-membrane (TM) domain (denoted by a orange box). The Bcl2 family includes both pro- and anti-apoptotic members. In general, anti-apoptotic Bcl2 family members display sequence conservation in all four BH domains. Pro-apoptotic members can be assigned to two subsets based on sequence conservation: the more fully conserved 'multi-domain' members and a divergent subset of 'BH3-domain only' members (Ranger *et al.*, 2001).

apoptotic proteins. Thus, the levels of pro-apoptotic and anti-apoptotic Bcl-2 family members determine how sensitive the cell is to cell death (Conradt and Horvitz, 1998; Ranger *et al.*, 2001). The Bcl-2 family members also protect against cell death directly by binding to Apaf-1 and indirectly by regulating the release of pro-apoptotic factors from the mitochondrial inter-membrane compartment into the cytosol (Wu *et al.*, 1997).

1.2.4.2.3) Regulation of apoptosis by inhibitors of apoptosis proteins (IAP's)

The transcription factor NF- κ B up-regulates the expression of pro-survival Bcl-2 members (Heckman *et al.*, 2002; Karin and Lin, 2002) and transactivates a number of other anti-apoptotic genes, such as the inhibitors of apoptosis proteins (IAP's). IAP's are a family of anti-apoptotic proteins that contain baculovirus IAP repeat (BIR) domains and 70 amino acid motifs. The human IAP homologues; XIAP, c-IAP1 and c-IAP2 are thought to directly inhibit caspase-3, -7, and -9 (Salvesen and Duckett, 2002; Takahashi *et al.*, 1998). The BIR3 domain of XIAP binds directly to the small subunit of caspase-9, whereas it is the BIR2 domain that interacts with the active-site substrate binding pocket of caspase-3 and -7 (Huang *et al.*, 2001; Srinivasula *et al.*, 2001). The c-IAP1, c-IAP2, and XIAP also contain a highly conserved RING domain at their C-terminal end which possesses E3 ubiquitin ligase activity enabling them to catalyze their own ubiquitination, thereby targeting them for degradation by the proteasome (Yang *et al.*, 2000), along with the bound proteins such as caspase-3 and -7 (Huang *et al.*, 2000; Suzuki *et al.*, 2001). Crucially, the inhibitory activity of the IAP's are counteracted when the negative regulator of IAP's, Smac/Diablo, is released from the mitochondrial inter-membrane space during

mitochondrial apoptotic events. Smac/Diablo binds to the IAP by displacing the caspase bound to it, thus enabling the caspase activation (Du *et al.*, 2000).

1.2.4.2.4) Regulation of apoptosis by heat shock proteins (Hsp)

Cells react to chemical and physiological stresses such as heat shock (Hahn and Li, 1982; Li and Hahn, 1990), chemotherapeutic agents, nutrient withdrawal (Mailhos *et al.*, 1993), ultraviolet (UV) irradiation (Simon *et al.*, 1995), polyglutamine repeat expansion (Warrick *et al.*, 1999) and TNF (Van Molle *et al.*, 2002), by synthesizing heat shock or stress proteins (Hsp). Hsp proteins are broadly categorized according to their size (Nollen and Morimoto, 2002). Despite the diversity in the sequence of Hsp proteins and the oligomeric assemblies, Hsp proteins have conserved structural organization: an N-terminal region that is highly variable in sequence and length, followed by a conserved α -crystallin domain and a C-terminal domain (Candido, 2002; Haslbeck *et al.*, 2004). To date, Hsp proteins that have been implicated in apoptosis include Hsp27, Hsp70, Hsp60, $\alpha\beta$ -crystallin, and Hsp90. These Hsp proteins have displayed the ability to regulate apoptosis as both pro-apoptotic and anti-apoptotic inducers.

1.2.4.3) The most extensively researched apoptosis pathways

The most extensively studied apoptosis pathways are the death receptor pathway, the mitochondrial pathway and the ER stress signaling pathway.

1.2.4.3.1) The death receptor or "extrinsic" apoptosis pathway of type I and type II

Extrinsic apoptosis signaling is mediated by the activation of cell surface receptors (death receptors) that transmit apoptotic signals after ligation with specific ligands. Death receptors belong to the tumour necrosis factor receptor (TNFR) gene superfamily and contain cysteine rich extra cellular sub-domains which allow them to recognize their ligands with specificity. Some members of the TNFR family and their specific ligands are; CD95/Fas (CD95L/FasL) (Peter and Krammer, 2003), TNFR1 (TNF) (Nagata, 1997; Smith *et al.*, 1994), DR3 (Apo3L) (Singh *et al.*, 1998), DR4 (TRAIL-R1) (Merino *et al.*, 2006; Pan *et al.*, 1997), DR5 (TRAIL-R2) (Merino *et al.*, 2006) and CAR1 (Brojatsch *et al.*, 1996). CD95/Fas signaling is mediated by the death receptor inside the cell cytoplasm that contains the conserved sequence termed the death domain (DD). Adapter molecules like Fas-associated death domain (FADD) or TNFR-associated death domain (TRADD) possess their own DD and DED, consequently they are recruited to the DD of the activated death receptor to form the death inducing signaling complex (DISC). The conserved DED sequence on the adapter molecule forms a homotypic DED/DED interaction by sequestering pro-caspase-8 to the DISC resulting in high local concentrations of zymogen. Under this condition, the low intrinsic protease activity of pro-caspase-8 is sufficient to allow various proenzyme molecules to mutually cleave and activate each other (induced proximity model) resulting in active caspase-8 (Bodmer *et al.*, 2000). Caspase-8 activation is regulated by caspase homologue c-FLIP, due to the fact that c-FLIP is able to bind to CD95 and TNFR1 preventing the activation of pro-caspase-8 (Chang *et al.*, 1999; Chinnaiyan *et al.*, 1995; Salvesen and Dixit, 1999; Srinivasula *et al.*, 1997). Active caspase-8 then directly activates downstream effector caspase-3

resulting in cell death. Cells harboring the capacity to induce cell death directly without the assistance of the mitochondrial released proteins, is classified as being type I cells (illustrated in [figure 1.6.](#)) (Scaffidi *et al.*, 1998).

In type II cells, the caspase signaling cascade does not generate a signal strong enough for the execution of cell death. Thus, the signal requires amplification by the simultaneous activation of the mitochondria-dependent apoptotic pathway. The mitochondria-dependent apoptotic pathway is activated when caspase-8 cleaves Bid to form truncated Bid (tBID) that translocates to the mitochondria (Luo *et al.*, 1998). The mitochondrial death decision is centered on two processes, the mitochondrial outer membrane permeabilization, in which the pro-apoptotic proteins such as tBID plays an active roles and inner membrane permeabilization that is promoted by the mitochondrial permeability transition pore formed across inner membranes when Ca^{2+} reaches a critical threshold (Belizario *et al.*, 2007). This membrane permeabilization leads to the release of cytochrome *c* (Kluck *et al.*, 1997) along with the apoptosis inducing factor (AIF) (Susin *et al.*, 1999), Smac/Diablo (Du *et al.*, 2000), EndoG (Li *et al.*, 2001) and HtrA2/Omi (Suzuki *et al.*, 2001a). The tBid also activates the AIF that is responsible for the externalization of the negatively charged phosphatidylserine on the cell membrane (Wang *et al.*, 2002).

The cytochrome *c* released from the mitochondria disrupts the binding between Bcl-2 and pro-apoptotic protease activating factor (Apaf-1). Apaf-1/caspase-9 complex forms active caspase-9 that together with ATP and cytochrome *c* form the apoptosome (Acehan *et al.*, 2002; Adams and Cory, 2002).

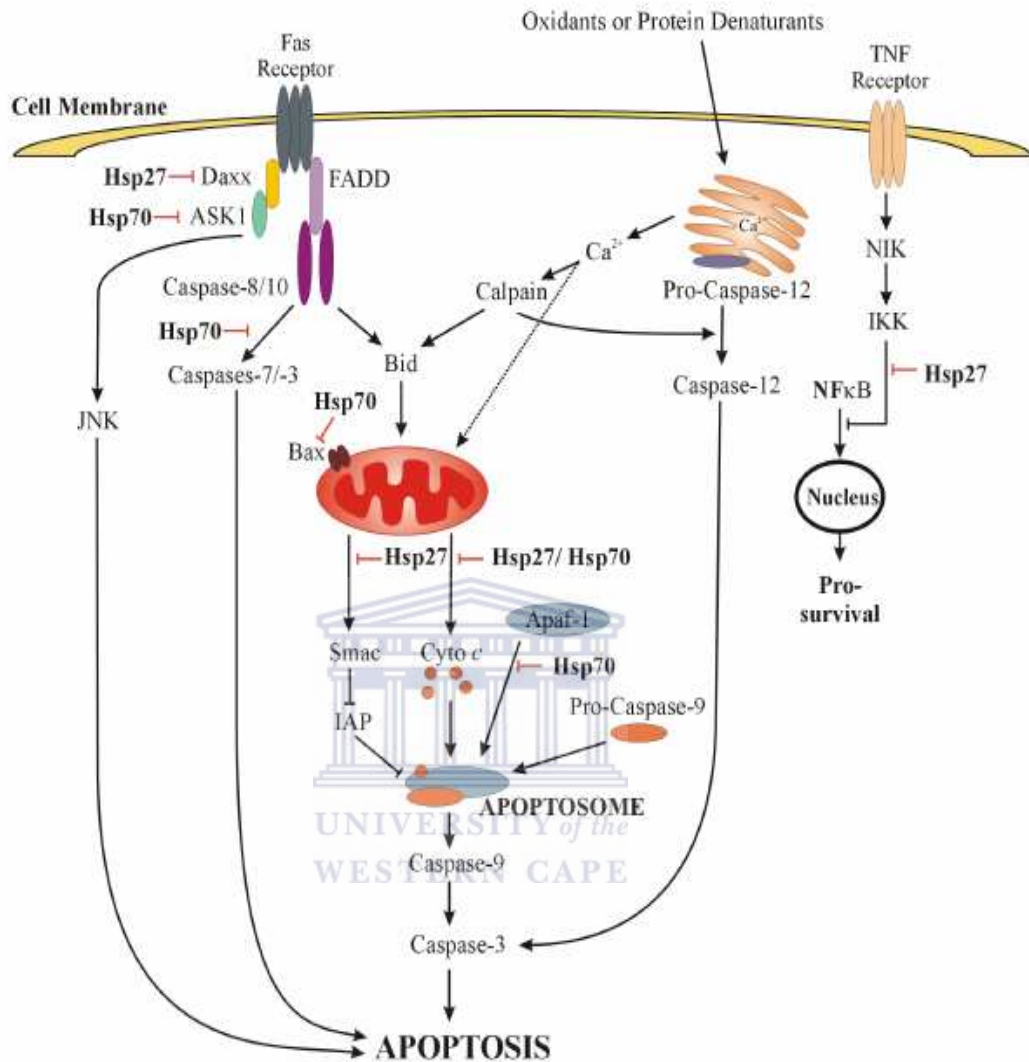


Figure 1.6 There is three major delineated pathways namely; the death receptor pathway, the mitochondrial pathway and the ER stress pathway. All three pathways lead to the activation of caspase-3 (Gill *et al.*, 2006).

The activated caspase-9 successively recruits and cleaves pro-caspase-3 to form active caspase-3 (Cain *et al.*, 1999). Active caspase-3 mediated cleavage of inhibitor caspase-activated deoxyribonuclease IFN (ICAD) resulting in the release and activation of the catalytic subunit CAD which is responsible for the fragmentation of the DNA into approximately 200bp fragments (Sakahira *et al.*, 1998; Zhao *et al.*, 2001). Simultaneously, caspase-3 also mediates cleavage of poly (ADP-ribose) polymerase (PARP) (Boulares *et al.*, 1999; Kaufmann *et al.*, 1993) and caspase-6 (Cecconi *et al.*, 1998; Kothakota *et al.*, 1997; Takahashi *et al.*, 1996); thus impeding the DNA repair mechanism, and bringing forth lamin protein degradation along with the disturbance of the fodrin and gelsolin matrix respectively. As a consequence of the above sequence of events, apoptotic cells display characteristic morphology changes that are distinct from than seen in necrotic cells.

CD95/Fas induced apoptosis typically involves ligation with adaptor molecule FADD. However, an alternative pathway involves the recruitment of an alternative adaptor molecule, Daxx that leads to activation of the MAPK apoptosis-signal-regulated kinase (ASK-1) to induce the activation of MAPK/JNK, leading to apoptosis (Chang *et al.*, 1998; Yang *et al.*, 1997). Hsp27 and Hsp70 appear to suppress Fas-induced apoptosis by binding to Daxx and ASK-1, respectively. (Charette *et al.*, 2000; Park *et al.*, 2002). Hsp70 suppresses caspase-dependent apoptotic signaling by binding to pro-caspase-3 and pro-caspase-7 and preventing their activation in U-937 cells. Hsp70 was however, unable to directly bind to activated caspase-3 and -7 (Komarova *et al.*, 2004). Hsp27 also binds to pro-caspase-3 to prevent its cleavage and activation (Pandey *et al.*, 2000a). Dissimilarly, the small Hsp

$\alpha\beta$ -crystallin can suppress caspase-8 and cytochrome *c* mediated activation of caspase-3 via a direct interaction with caspase-3 to prevent apoptosis. (Kamradt *et al.*, 2001). Hsp70 and Hsp27 are also reported to mediate Bid translocation to the mitochondria in response to TNF-induced apoptosis (Gabai *et al.*, 2002; Paul *et al.*, 2002). The interaction between Hsp27 and IKK β is enhanced by TNF-induced, MAP-kinase-dependent phosphorylation of Hsp27, which leads to an enhanced inhibition of IKK activity and consequent suppression of NF- κ B activity (Park *et al.*, 2003). Gotoh *et al.* have also implicated Hsp70 and its co-chaperones Hsp40 (Hdj-1) or HSDJ (Hdj-2) in the inhibition of Bax translocation to the mitochondria to prevent nitric-oxide-induced apoptosis (Gotoh *et al.*, 2004). Hsp70 also inhibits apoptosome formation by directly associating with Apaf-1 to prevent activation of pro-caspase-9 (Beere *et al.*, 2000; Saleh *et al.*, 2000). Hsp90 and Hsp27 are also reported to prevent Apaf-1 oligomerization by directly associating with Apaf-1 (Pandey *et al.*, 2000b) and cytochrome *c*, respectively (Bruey *et al.*, 2000).

Contrary to the above mentioned Hsp, Hsp60 enhances apoptosis by forming a multi-protein complex containing pro-caspase-3 and -6 or caspase-8, thus enhancing pro-caspase-3 activation by caspase-6/-8 in an ATP-dependent manner (Xanthoudakis *et al.*, 1999). Hsp60 can also form a complex with Hsp10 and pro-caspase-3 in the mitochondria to promote the cytochrome *c*/ATP-dependent activation of pro-caspase-3 (Samali *et al.*, 1999).

1.2.4.3.2) The mitochondrial or "intrinsic" apoptosis pathway

Above and beyond amplifying and mediating extrinsic apoptotic pathways, the mitochondria also play a central role in the integration and propagation of death signals originating intrinsically. Intrinsic death signals include; DNA damage, oxidative stress, starvation, and the activity of chemotherapeutic drugs (Kaufmann and Earnshaw, 2000; Wang, 2001).

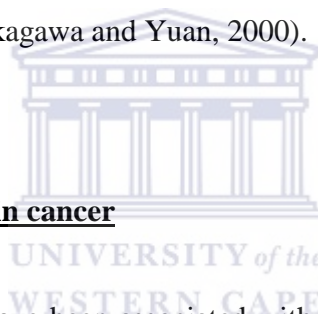
Intrinsic death signals activate the TNF ligand to binds to the TNF receptor thereby stimulating the accumulation of p53. The p53 protein then initiated the expression of the WAF gene producing p21 that binds to the cyclin / kinase complex giving rise to a cell cycle restriction site in which an attempt is made to repair the DNA. Simultaneously, p53 transcribes the GADD45 gene producing the transcription products GADD+PCNA that attempts to repair the DNA damage. If the DNA damage is irreparable p53 further initiated the expression of the Bax gene (Vogelstein *et al.*, 2000). This produces an excess of Bax that gives rise to the Bax/Bax complexes (pro-apoptotic complex) that displace the Bcl-2/Bax complexes (anti-apoptotic complex) because the two complexes compete for the same receptor site on the mitochondrial membrane (principle explained above under the Bcl-2 family segment in 1.2.4.3.1) (Cheng *et al.*, 1997). The attachment of Bax-Bax complex to the mitochondrial membrane brings forth the release of apoptogenic factors (Belizario *et al.*, 2007; Vogelstein *et al.*, 2000)

1.2.4.3.3) *The ER stress signaling pathway*

ER death signals include disturbance in calcium homeostasis or an accumulation of unfolded/misfolded proteins. These death signals can be triggered by various pathophysiological conditions such as Alzheimer's disease (AD), Parkinson's diseases and heart disease. However, the cell has protective strategies, commonly referred to as the Unfolded Protein Response (UPR), that induce signaling pathways that promote the survival of the stressed cell (Chan *et al.*, 2002; Keller *et al.*, 2005). If these signaling pathways fail to restore homeostasis then the cell initiates apoptosis via the ER stress signaling pathway.

In the ER stress signaling pathway, stress/disturbance of the endoplasmic reticulum (ER) homeostasis results in the cleavage of murine pro-caspase-12 that is predominantly localized in the ER to form active caspase-12. The ER-resident active caspase-12 directly cleaves other caspases resulting in apoptosis (Shiraishi *et al.*, 2006). However, the role of caspase-12 in the ER stress pathway is controversial as the human genome sequence homologous to the murine genomic sequence for pro-caspase-12 has been identified at the caspase-1/interleukin-1 β converting enzyme (ICE) loci on chromosome 11q22.3 (Fischer *et al.*, 2002), but the gene encoding human pro-caspase-12 is interrupted by frame shift and a premature stop codon, and has amino acid substitutions in the critical site for caspase activity (Fischer *et al.*, 2002). This finding is supported by the fact that human caspase-12 has been lost in most of the human race except some African descendants (Saleh *et al.*, 2004). Taking into account Darwin's concept of the survival of the fittest the question thus arises, which caspase in humans has functionally substituted for caspase-12 in mouse.

Fascinatingly, the human caspase-4 is located in the same locus and is localized in the ER membrane; with only 48 % homology to caspase-12 demonstrates the ability to increase ER stress-induced apoptosis and amyloid- β -induced cell death (Hitomi *et al.*, 2004). Also, overexpression of Bcl-2 does not affect the cleavage of caspase-4 suggesting it is primarily activated in ER stress induced apoptosis (Hitomi *et al.*, 2004). ER stress also induces a disruption of calcium homeostasis as cytosolic calcium levels increase. Calcium homeostasis is regulated by the interaction of Bcl-2 family members with the inositol 1,4,5-triphosphate receptor (InsP3R) ER calcium release channel. A significant increase in the calcium level activates calpain. Activated calpain cleaves tBid, which translocates to the mitochondria and activates the intrinsic pathway (Nakagawa and Yuan, 2000).



1.2.5) Genes implicated in cancer

Numerous cancer types have been associated with gene mutations in multiple genes, as opposed to a disease such as cystic fibrosis that is characterized by a single gene mutation. As an example multiple genes are implicated in non-syndromic pheochromocytoma namely, the proto-oncogene RET (associated with multiple endocrine neoplasia type 2 [MEN-2]), the tumor-suppressor gene VHL (associated with von Hippel-Lindau disease), succinate dehydrogenase subunit D (SDHD) and succinate dehydrogenase subunit B (SDHB) (associated with paraganglioma); which predispose carriers to pheochromocytomas and glomus tumors (Neumann *et al.*, 2002). These genes are recognized cancer pre-disposition genes (listed in [table 1.2.](#)).

Table1.2. Cancer Pre-disposition genes

Gene (synonym(s)) ^a	Syndrome	Hereditary pattern	Second hit	Pathway ^b	Major heredity tumor types ^c
Tumor-suppressor genes					
<i>APC</i>	FAP	Dominant	Inactivation of WT allele	APC	Colon, thyroid, stomach, intestine
<i>AXIN2</i>	Attenuated polyposis	Dominant	Inactivation of WT allele	APC	Colon
<i>CDH1</i> (E-cadherin)	Familial gastric carcinoma	Dominant	Inactivation of WT allele	APC	Stomach
<i>GPC3</i>	Simpson-Golabi-Behmel syndrome	X-linked	?	APC	Embryonal
<i>CYLD</i>	Familial cylindromatosis	Dominant	Inactivation of WT allele	APOP	Pilo-trichomas
<i>EXT1,2</i>	Hereditary multiple exostoses	Dominant	Inactivation of WT allele	GLI	Bone
<i>PTCH</i>	Gorlin syndrome	Dominant	Inactivation of WT allele	GLI	Skin, medulloblastoma
<i>SUFU</i>	Medulloblastoma predisposition	Dominant	Inactivation of WT allele	GLI	Skin, medulloblastoma
<i>FH</i>	Hereditary leiomyomatosis	Dominant	Inactivation of WT allele	HIF1	Leiomyomas
<i>SDHB, C, D</i>	Familial paraganglioma	Dominant	Inactivation of WT allele	HIF1	Paragangliomas, pheochromocytomas
<i>VHL</i>	Von Hippel-Lindau syndrome	Dominant	Inactivation of WT allele	HIF1	Kidney
<i>TP53</i> (p53)	Li-Fraumeni syndrome	Dominant	Inactivation of WT allele	p53	Breast, sarcoma, adrenal, brain...
<i>WT1</i>	Familial Wilms tumor	Dominant	Inactivation of WT allele	p53	Wilms'
<i>STK11</i> (<i>LKB1</i>)	Peutz-Jeghers syndrome	Dominant	Inactivation of WT allele	PI3K	Intestinal, ovarian, pancreatic
<i>PTEN</i>	Cowden syndrome	Dominant	Inactivation of WT allele	PI3K	Hamartoma, glioma, uterus
<i>TSC1, TSC2</i>	Tuberous sclerosis	Dominant	Inactivation of WT allele	PI3K	Hamartoma, kidney
<i>CDKN2A</i> (p16 ^{INK4A} , p14 ^{ARF})	Familial malignant melanoma	Dominant	Inactivation of WT allele	RB	Melanoma, pancreas
<i>CDK4</i>	Familial malignant melanoma	Dominant	?	RB	Melanoma
<i>RB1</i>	Hereditary retinoblastoma	Dominant	Inactivation of WT allele	RB	Eye
<i>NF1</i>	Neurofibromatosis type 1	Dominant	Inactivation of WT allele	RTK	Neurofibroma
<i>BMPRIA</i>	Juvenile polyposis	Dominant	Inactivation of WT allele	SMAD	Gastrointestinal
<i>MEN1</i>	Multiple endocrine neoplasia type I	Dominant	Inactivation of WT allele	SMAD	Parathyroid, pituitary, islet cell, carcinoid
<i>SMAD4</i> (<i>DPC4</i>)	Juvenile polyposis	Dominant	Inactivation of WT allele	SMAD	Gastrointestinal
<i>BHD</i>	Birt-Hogg-Dube syndrome	Dominant	Inactivation of WT allele	?	Renal, hair follicle
<i>HRPT2</i>	Hyperparathyroidism, Jaw-tumor syndrome.	Dominant	Inactivation of WT allele	?	Parathyroid, jaw fibroma
<i>NF2</i>	Neurofibromatosis type 2	Dominant	Inactivation of WT allele	?	Meningioma, acoustic neuroma
Stability genes					
<i>MUTYH</i>	Attenuated polyposis	Recessive	?	BER	Colon
<i>ATM</i>	Ataxia telangiectasia	Recessive	?	CIN	Leukemias, lymphomas, brain
<i>BLM</i>	Bloom syndrome	Recessive	?	CIN	Leukemias, lymphomas, skin
<i>BRCA1, BRCA2</i>	Hereditary breast cancer	Dominant	Inactivation of WT allele	CIN	Breast, ovary
<i>FANCA, C, D2, E, F, G</i>	Fanconi anemia	Recessive	?	CIN	Leukemias
<i>NBS1</i>	Nijmegen breakage syndrome	Recessive	?	CIN	Lymphomas, brain
<i>RECQL4</i>	Rothmund-Thomson syndrome	Recessive	?	CIN	Bone, skin
<i>WRN</i>	Werner syndrome	Recessive	?	CIN	Bone, brain
<i>MSH2, MLH1, MSH6, PMS2</i>	HNPCC	Dominant	Inactivation of WT allele	MMR	Colon, uterus
<i>XPA, C; ERCC2-5; DDB2</i>	Xeroderma pigmentosum	Recessive	?	NER	Skin
Oncogenes					
<i>KIT</i>	Familial gastrointestinal stromal tumors	Dominant	?	RTK	Gastrointestinal stromal tumors
<i>MET</i>	Hereditary papillary renal cell carcinoma	Dominant	Mutant allele duplication	RTK	Kidney
<i>PDGFRA</i>	Familial gastrointestinal stromal tumors	Dominant	?	RTK	Gastrointestinal stromal tumors
<i>RET</i>	Multiple endocrine neoplasia type II	Dominant	Mutant allele duplication	RTK	Thyroid, parathyroid, adrenal

(Vogelstein and Kinzler, 2004).

Mutated p53 has been linked to more than 50 % of human cancers (Harris and Hollstein, 1993; Vogelstein *et al.*, 2000). Also, virtually all DNA tumour viruses encode proteins that inactivate both Rb and p53 (Klein, 2002; zur Hausen, 2001). p53, also referred to as the "guardian of the genome", induces cell cycle arrest to facilitate the cells integrated DNA repair mechanism. Once the itinerary has been exhausted; that is, the DNA damage is irreparable; p53 will induce apoptosis to eliminate the cancer cell. This apoptosis pathway is commonly referred to as the mitochondrial or intrinsic pathway. This pathway along with other pathways, require members of the Bcl-2 gene family and the caspase gene family to secure the execution of the apoptotic pathway. Mutated p53 has been implicated in Li-Fraumeni syndrome, this cancer is the malignant breast, brain, adrenal etc. tumour (Savage *et al.*, 2007). In colon cancer, germ-line mutations have been identified in the p53 gene and the RB gene. These mutations are also accompanied by mutations in the FAP gene that leads to the syndrome of familial adenomatous polyposis coli (Cetta *et al.*, 2000). Under normal apoptotic conditions p53 initiates the expression of the Bax gene, a member of the Bcl-2 gene family. The Bax gene has been characterized with somatic frameshift mutations of the microsatellite mutator phenotype in colon cancer (Rampino *et al.*, 1997). The Bax initiated the release of cytochrome *c* from the mitochondria required for the activation of caspase-9 and -3 respectively. Caspase-3 mutation has been reported in the MCF-7 breast cancer cell line (Kurokawa *et al.*, 1999). Similarly, in the extrinsic pathway, Fas gene mutations have been implicated in non-small cell lung cancer, caspase-8 gene mutations have been implicated in gastric carcinomas and caspase-10 gene mutations have been implicated in non-Hodgkin lymphomas (Shin *et al.*, 2002; Soung *et al.*, 2005). Researchers are

exploiting the biochemical knowledge of the genes associated with cancer, the pathways the genes induce and the differences associated with diverse cancer cell types, coupled with the action of current anti-cancer drugs, to develop specific non-toxic drugs.

1.3) Plants as sources of anti-cancer drugs

Plants are photosynthetic, eukaryotic, multicellular organisms of the Kingdom Plantae that are believed to have evolved from green algae. They range in size and complexity from simple mosses to trees. The main plant groups are Phylum Bryophyta, Phylum Filicophyta, Phylum Sphenophyta, Phylum Coniferophyta, Phylum Cycadophyta and Phylum Angiospermophyta (McWhirter *et al.*, 1996). Plants are known to contain many nutritional substances required for the maintenance of mammalian cells (McWhirter *et al.*, 1996). Most notably, plants remain the major source of carbohydrates making them indispensable to our subsistence (Matthews and Van Holde, 1990). Plants perform refined defense mechanisms such as the poisoning of the soil with terpenes to inhibit competitors and producing alkaloids which make them unpalatable to insects and predators. This fact that plant biology performs tasks similar to higher organisms indicates that they may contain secondary metabolites compatible to higher organisms (Van Wyk *et al.*, 2000). This fact has already been proven as plant secondary metabolites are the biggest source of pharmaceutical drugs and they serve as templates for many medicinal derivatives (listed in [table 1.3.](#)).

Table 1.3 Plant derived pharmaceutical drugs

Plant	Medicinal value
Opium poppy (<i>Papaver somniferum</i>)	Morphine, a powerful analgesic alkaloid has been isolated from the opium poppy. Morphine and its derivative codeine is used to treat severe pain and headaches respectively (Page, 2005).
Quinine (<i>Cinchona</i> spp.)	Quinine is an alkaloid originally extracted from the bark of the quinine tree and is cultivated in South America, India, Java and Tropical Africa (Eisenhut <i>et al.</i> , 2005).
Amara (<i>Quassia amara</i>)	Amara contains bitter terpenoids known as quassinoids used as a bitter tonic to improve appetite and to treat minor stomach ailments (Barbetti <i>et al.</i> , 1987).
Pacific Yew (<i>Taxus</i> spp.)	Taxol (<i>Taxus</i> spp.) is a diterpenoid originally extracted from the bark of the Pacific yew. Taxol is a highly effective drug against breast cancer and ovarian cancer (Lanni <i>et al.</i> , 1997).

The discovery of plant derived drugs epitomizes the importance of using natural products and their derivatives to provide new target molecules for drug development (Taniguchi *et al.*, 2002; Thatte *et al.*, 2000). Systemic drug discovery and development have led to functional chemotherapeutic agents (see section 1.3.2). These chemotherapeutic agents have been derived from numerous sources, namely viruses, bacteria, plants etc. Plant derived apoptosis inducers or anti-cancer drugs include; paclitaxel (Taxol), docetaxel (Taxotere), camptothecin, betulinic acid, colchicine, podophyllotoxin and vinblastine, vincristine. These drugs act as DNA damaging agents that induce cellular stress by various mean.

1.3.1) Cell cycle regulation

Most somatic cells are continually dividing via a highly ordered and regulated process called the cell cycle (illustrated in figure 1.7). Cell cycle progression through these replication events is regulated at the G1/S checkpoint, the intra-S-phase checkpoint or the G2/M checkpoint, if DNA damage activates the DNA repair mechanism.

The DNA repair mechanisms include direct repair base excision repair, nucleotide excision repair, double-strand break repair and cross-link repair (Sancar *et al.*, 2004; Taniguchi *et al.*, 2002). These DNA repair mechanisms are activated by damage sensor proteins such as ATR, ATM, 9-1-1 complex and the Rad17-RFC complex. The damage sensor proteins initiate transducers, such as Chk1 and Chk2 Ser/Thr kinases and Cdc25 phosphatase that activate p53 and inactivate cyclin dependent kinases to inhibit cell cycle progression (illustrated in figure 1.8).

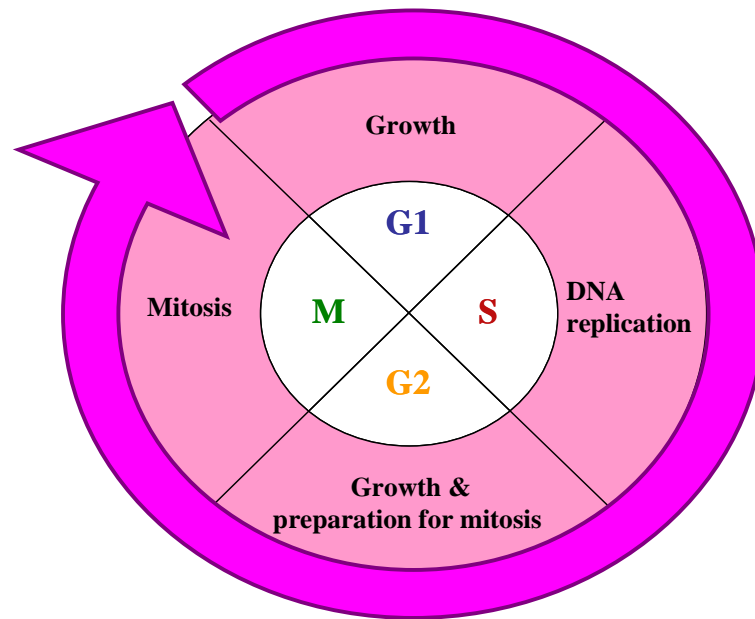
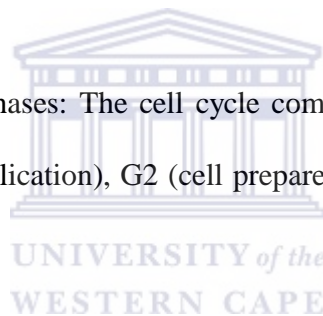


Figure 1.7. Cell cycle phases: The cell cycle comprises of four phases namely; G1 (cell grows), S (DNA replication), G2 (cell prepares to divide) and the M phase (cell division)



The G1/S checkpoint prevents cells from entering the S phase in the presence of stress thus inhibiting replication. Replication is inhibited as a result of the dephosphorylation of CDK2 by the non-phosphorylated Cdc25A proteins, as the CDK2 is required for the phosphorylation of Cdc45 that is involved in the initiation of replication (Falck *et al.*, 2001; Walter and Newport, 2000). The exact pathway of cell cycle arrest depends on the kind of stress induced. DNA double-strand breaks leads to the phosphorylation of the damage sensor protein ATM that initiates Chk2 (Falck *et al.*, 2001). Alternatively, single-stranded breaks result in the activation of

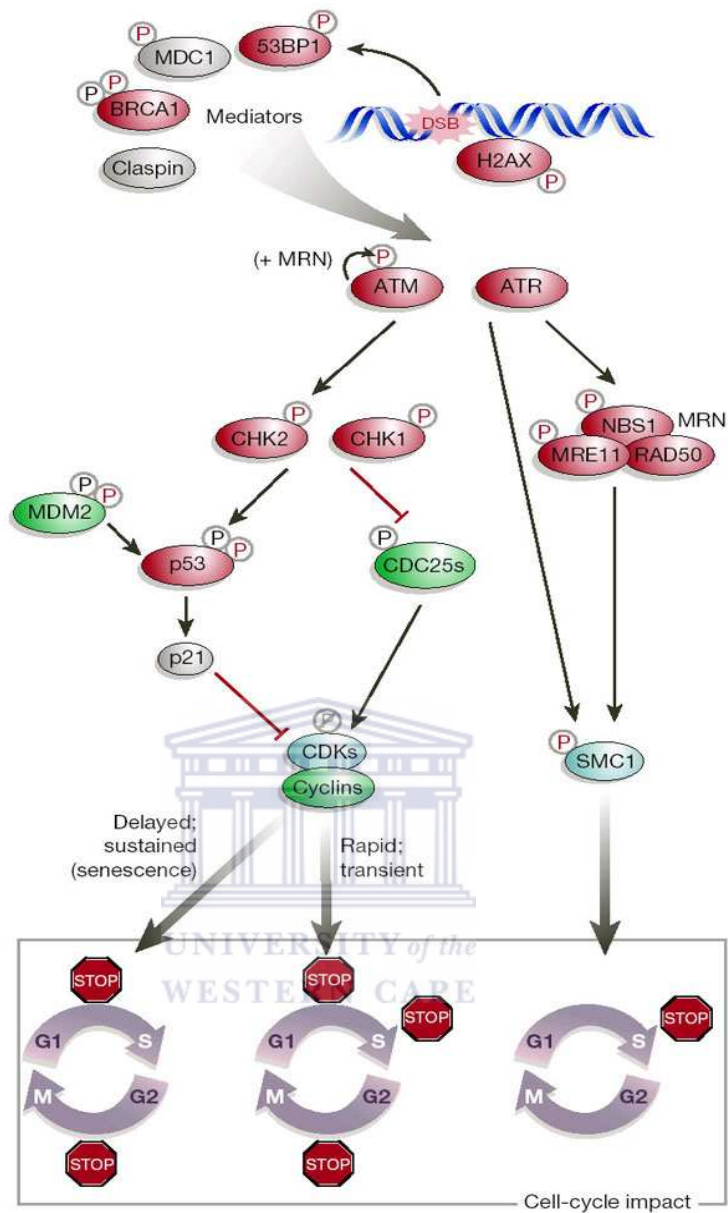
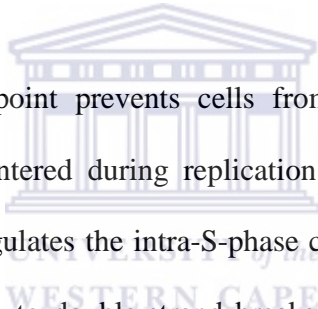


Figure 1.8 DNA repair: mechanisms regulating the cell cycle checkpoints G1/S, intra-S-phase and G2/M (Kastan and Bartek, 2004; Taniguchi et al., 2002).

the damage sensor proteins; Rad17-RFC, 9-1-1 complex and ATR that initiates Chk1 (Roos-Mattjus *et al.*, 2003; Weiss *et al.*, 2002). Ensuing phosphorylation of Cdc25A by Chk1 and Chk2 leads to G1 arrest. ATM and ATR also phosphorylate p53 (Banin *et al.*, 1998). p53 initiates expression of the WAF gene, GADD45 gene and the Bax gene. The WAF gene produces p21 that binds to the CDK2 complex giving rise to a restriction site (Panno *et al.*, 2006). Transcription of the GADD45 gene produces the transcription products GADD+PCNA that attempt to repair the DNA damage (Panno *et al.*, 2006). If the DNA damage is irreparable p53 further initiates the expression of the Bax gene that represents the onset of apoptosis (Taniguchi *et al.*, 2002; Vogelstein *et al.*, 2000).



The intra-S-phase checkpoint prevents cells from entering the G2 phase in the presence of stress encountered during replication or stress that escaped the G1/S checkpoint. The ATM regulates the intra-S-phase checkpoint that is characterized by two pathways in response to double-strand breaks induced by radiation. In the first pathway, ATM phosphorylates Chk2 on Thr68 through the intermediaries MDC1, H2AX and 53BP1 (Burma *et al.*, 2001; Goldberg *et al.*, 2003; Wang *et al.*, 2002). Once again, replication is inhibited as a result of the dephosphorylation of CDK2 by the non-phosphorylated Cdc25A proteins, as the CDK2 is required for the phosphorylation of Cdc45 that is involved in the initiation of replication. In the second pathway, ATM initiates phosphorylation of NBS1 of the M/R/N complex, SMC1, BRCA1 and FANCD2 (Kitagawa *et al.*, 2004; Taniguchi *et al.*, 2002).

The G2/M checkpoint prevents cells from entering the M phase (mitosis) in the presence of stress. This checkpoint is very similar to the G1/S checkpoint as the pathway activated depends on the stress induced namely, DNA double-strand breaks activates the ATM-Chk2-Cdc25 pathway and DNA lesions such as UV light activate the ATR-Chk1-Cdc25 pathway (Adamson *et al.*, 2005; Yamane *et al.*, 2004). At this checkpoint, down-regulated Cdc25A, Chk1, Chk2 and WEE1 regulates Cdk2 activity and consequently G2 arrest, alongside p53/p21 which is distinct from the G1/M checkpoint activities (Matsuda *et al.*, 2006). A second pathway can be initiated at the G2/M checkpoint (intra-S-phase checkpoint) namely, ATM initiates phosphorylation of NBS1 of the M/R/N complex, SMC1, BRCA1 and FANCD2 (Freie *et al.*, 2004).

1.3.2) Current plant-derived anti-cancer drugs

1.3.2.1) Paclitaxel and docetaxel

Paclitaxel (Taxol) and docetaxel (Taxotere) are diterpenoids originally extracted from the bark of the *Taxus brevifolius* (Taxaceae). Paclitaxel binds to the microtubules and inhibits their depolymerization (molecular disassembly) into tubulin (Schiff and Horwitz, 1980). This inhibiting the cells ability to break down the mitotic spindle during mitosis and consequently cells cannot divide into two daughter cells causing G₂-M arrest (Schiff *et al.*, 1979; Schiff and Horwitz, 1981). Paclitaxel is also associated with down-regulation of CDK4 (Yoo *et al.*, 1998) with concomitant G₁-S arrest. However, the primary effect of paclitaxel is to interfere with the assembly of the mitotic spindle, resulting in the failure of chromosomes to segregate (Long and

Fairchild, 1994). Paclitaxel is an intravenous drug that is most effective against ovarian carcinomas and advanced breast carcinomas. Adverse reactions include major breathing problems, edema, abnormally low neutrophil, abnormally low platelet counts and anaemia.

Docetaxel also prevents the mitotic spindle from being broken down by stabilizing the microtubule bundles, but clinical trials indicate it is two times more effective than paclitaxel in this process (Vacca *et al.*, 2002). Docetaxel, is also an intravenous drug, that is being tested on carcinomas of the bladder, cervix, lung, and ovaries. Thus far, side effects of docetaxel therapy include oedema, abnormally low neutrophil counts, and peripheral nervous system disorders.

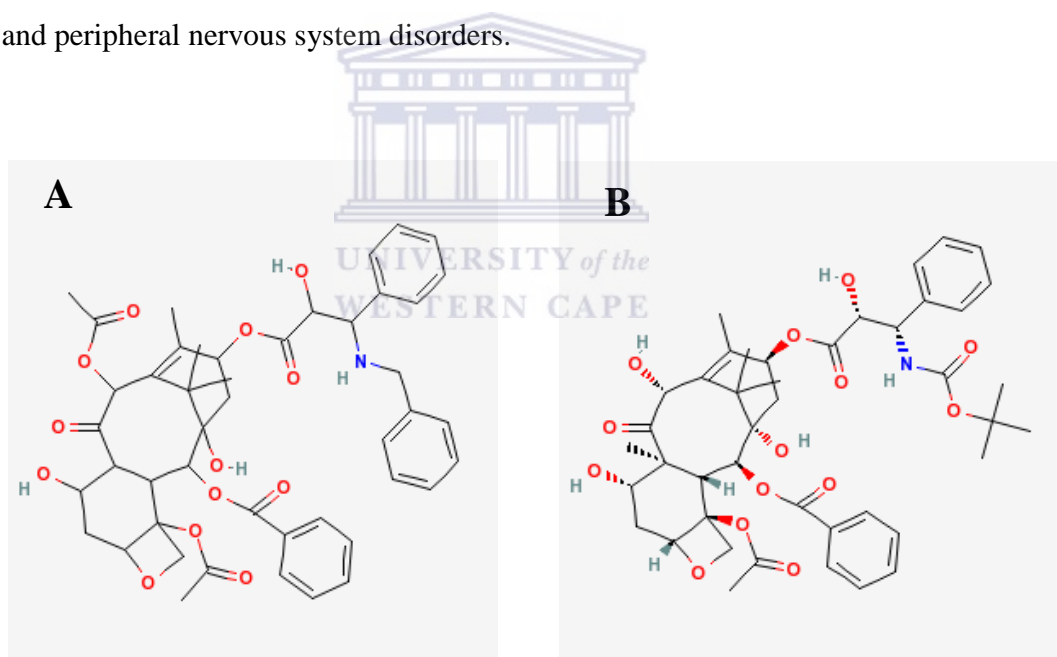


Figure 1.9. The chemical structure of (A) paclitaxel and (B) docetaxel

1.3.1.2) Camptothecin and topotecan

Camptothecin is a quinoline-based alkaloid isolated from the bark of the *Camptotheca acuminata* (Nyssaceae). Camptothecin and its close chemical relatives aminocamptothecin, CPT-11 [irinotecan], DX-8951f, and topotecan are S-phase-specific anticancer agents that inhibit the activity of the enzyme DNA topoisomerase-I (Morris and Geller, 1996).

In 1996, the FDA approved topotecan (manufactured by SmithKline Beecham Pharmaceuticals and sold under the trade name Hycamtin) as a treatment for advanced ovarian cancers, and irinotecan HCl (manufactured by Pharmacia & Upjohn and sold under the trade name Camptosar) as a treatment for metastatic cancer of the colon or rectum. Thus far, the major side effects of camptothecin drugs are potentially severe diarrhea, nausea, and lowered white blood cell counts.

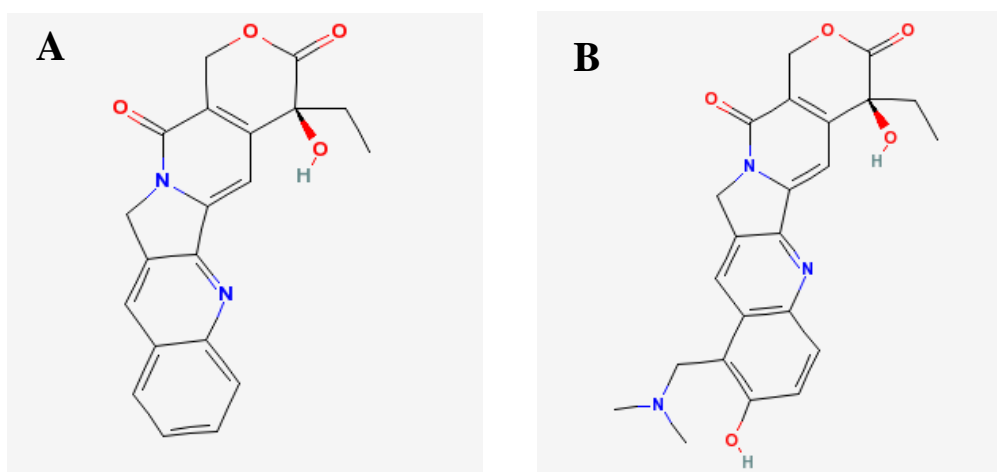


Figure 1.10. The chemical structure of (A) Camptothecin and (B) Topotecan.

1.3.1.3) Colchicine

Colchicine, a water-soluble alkaloid, was isolated from the *Colchicum autumnale* (Liliaceae). It suppresses cell division by inhibiting mitosis by binds to the tubulin molecule, thereby inhibiting its assembly into microtubules and consequently it inhibits the development of spindles as the nuclei are dividing. Cancer cells divide more rapidly than normal cells, thus cancer cells are more susceptible to being

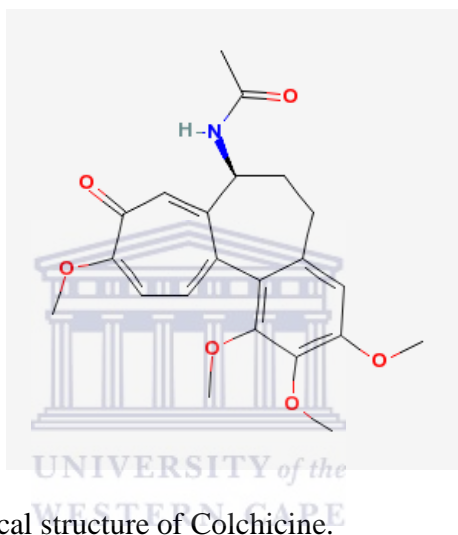


Figure 1.11. The chemical structure of Colchicine.

poisoned by mitotic inhibitors such as colchicine, paclitaxel, and the Vinca alkaloids (Jordan and Wilson, 1998). However, colchicine has proven to have a fairly narrow range of effectiveness as a chemotherapy agent, so its only FDA-approved use is to treat gout (trade name ColBenemid, an anti-gout drug marketed by Merck & Co.). However, it is used in veterinary medicine to treat animal cancers. It is also used as an anti-mitotic agent in cancer research involving cell cultures. Thus far, the major side effect of colchicine is abnormally low leukocyte levels that can rebound to an abnormally high level.

1.3.1.4) Podofilox and etoposide

Podofilox was extracted from the *Podophyllum peltatum* (Berberidaceae). Podophyllotoxin (podofilox) and its derivatives, etoposide and teniposide, are all cytostatic (antimitotic) glucosides. Etoposide and teniposide both block the cell cycle in two specific places i.e. the G1 phase and the S phase and act by causing breaks in DNA via an interaction with DNA topoisomerase II. (Clarke *et al.*, 1993). Podophyllotoxin (podofilox) is used in creams such as Oclassen's Condylox for the treatment of genital warts that are caused by the human papillomavirus (HPV). Human papillomavirus (HPV) has been associated with cancers of the genitals (squamous cell carcinomas) (Edwards *et al.*, 1988). Etoposide (manufactured by Bristol-Myers Squibb and sold under the trade name VePesid) is used mainly to treat testicular cancer that has failed to respond to other treatments and is also a first-line treatment for small-cell lung cancers, chorionic carcinomas, Kaposi's sarcoma, lymphomas and malignant melanomas (Henwood and Brogden, 1990).

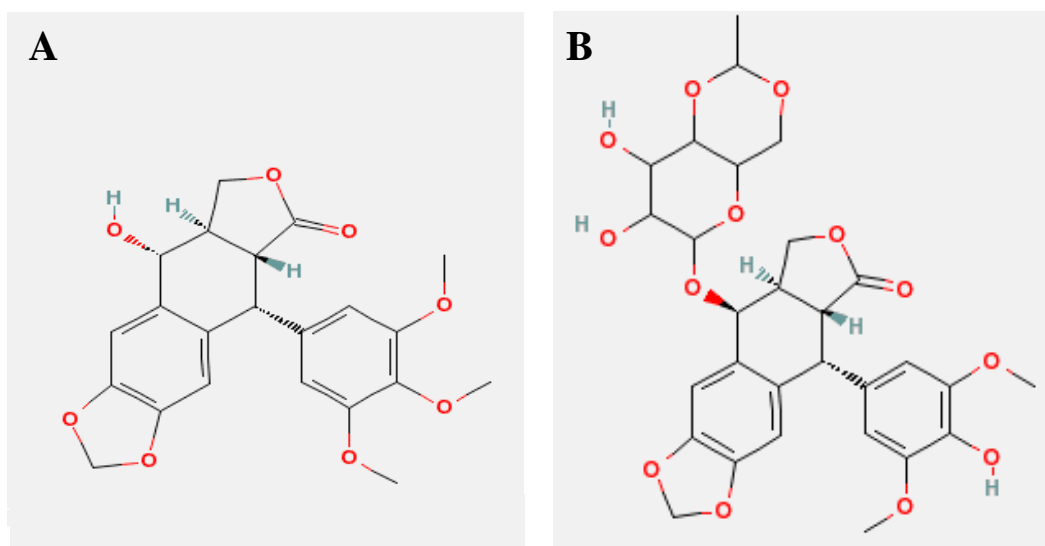


Figure 1.12. The chemical structure of (A) Podophyllotoxin and (B) Etoposide.

Major side effects include hair loss, nausea, anorexia, diarrhea, and low leukocyte and platelet counts. It can also cause genetic damage and may increase a patient's risk of developing leukemia. The less popular teniposide have similar side effects to etoposide, but is mainly used to treat lymphomas.

1.3.1.5) Vinblastine, vincristine, vindesine and vinorelbine

Vinblastine and vincristine are alkaloids found in *Catharanthus roseus* (formerly classified as *Vinca rosea*). These vinca alkaloids, vindesine, vinorelbine and the semi-synthetic derivatives of vinblastine, all work by inhibiting mitosis (cell division) in metaphase. These alkaloids bind to tubulin, thus preventing the cell from making the spindles it needs to be able to move its chromosomes around as it divides (this is similar to the action of colchicine) (Ngan *et al.*, 2001). Although these intravenous drugs are very similar in structure and have the same basic action, they have distinctly different effects on the body.

Vinblastine (marketed as Velban by Eli Lilly) is mainly useful for treating Hodgkin's disease, lymphocytic lymphoma, histiocytic lymphoma, advanced testicular cancer, advanced breast cancer, Kaposi's sarcoma, and leukemia (Bleyer *et al.*, 1991; Groninger *et al.*, 2005; Stokoe *et al.*, 2001). It also seems to fight cancer by interfering with glutamic acid metabolism. Side effects include hair loss, nausea, lowered blood cell counts, headache, stomach pain, numbness, constipation and mouth sores. Bone marrow damage is the typical dose-limiting factor (Uchida *et al.*, 1997). Vincristine (marketed as Oncovin by Eli Lilly) is used mainly to treat acute leukemia, rhabdomyosarcoma, neuroblastoma, Hodgkin's disease and other

lymphomas (Engert *et al.*, 2007; Kang *et al.*, 2007). The typical dose is 1.4 milligrams per square meter of body surface once a week, and neurotoxicity is the dose-limiting factor (it can cause damage to the peripheral nervous system). Side effects include those found with vinblastine, plus nervous system problems such as sensory impairment; some people may also develop breathing problems or lung spasms shortly after the drug is administered (Brockmann *et al.*, 1991; Carpentieri and Lockhart, 1978).

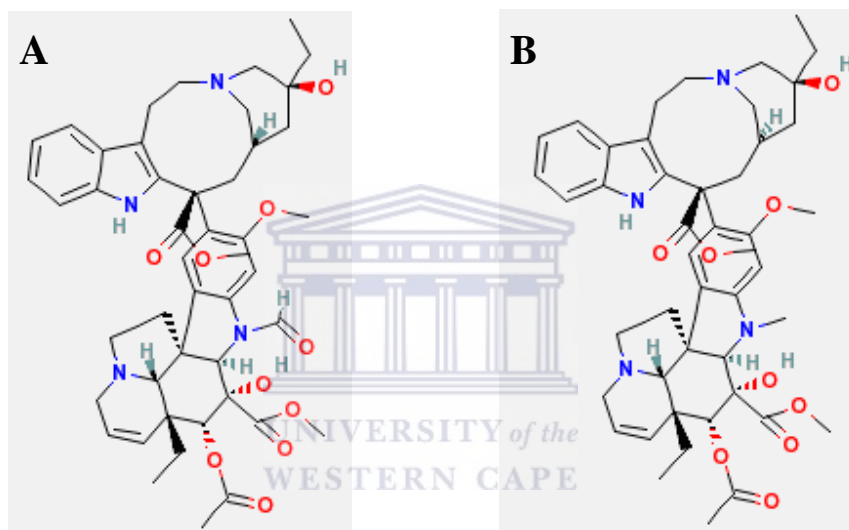


Figure 1.13. The chemical structure of (A) Vinblastine and (B) Vincristine

Vindesine (marketed under the names Eldisine and Fildesin) is used mainly to treat melanoma and lung cancers (carcinomas) and, together with other drugs, to treat uterine cancers (van Luijk *et al.*, 2007). Its toxicity and side effects are similar to those of vinblastine. Vinorelbine (marketed as Navelbine by Glaxo Wellcome, Inc.) is currently in Phase II clinical trials as a treatment for ovarian cancer (Rothenberg *et al.*, 2004). It however seems to have a wider range of antitumor activity than the other vinca alkaloids. In preclinical trials, it showed promise in treating patients with

epithelial ovarian cancers and, in combination with the chemotherapy drug cisplatin, in treating patients with non-small-cell lung cancers (Julien *et al.*, 1999). The side effects of this drug include diarrhea, nausea, and hair loss; it seems to be less of a nerve poison than vindesine.

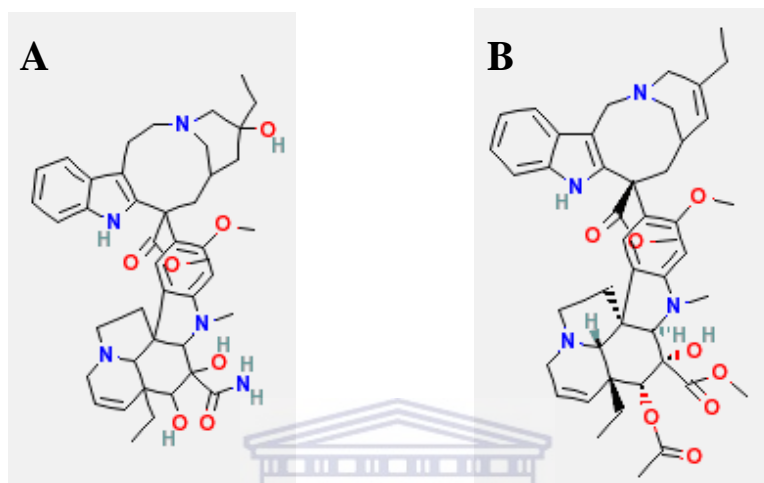


Figure 1.14. The chemical structure of (A) Vinorelbine and (B) Vindesine.

Current plant derived anti-cancer drugs primarily target cell division components, resultantly; their toxicity is not restricted to cancer cells. Clinical application of these drugs has been partially successful as they have been administered in phases and in combination with other anti-cancer agents. Phase administered drugs allow the patients body to recuperate between doses. This dose dependent administering of conventional drugs is however, acutely life threatening to patients. Many conventional drugs also induce genetic damage that can itself be carcinogenic. A segment of the research community is thus focusing on identifying novel chemotherapeutic agents in plants, that do not induce the destructive effects of conventional cytotoxic therapeutic agents.

CHAPTER 2: MATERIALS AND METHODS

2.1) General chemicals and assay kits

Active Caspase – 3 FITC Mab Apoptosis Kit	BD Biosciences
Agarose	Promega
Ampicillin	Roche
Annexin V- PE Apoptosis Detection Kit 1	Pharmingen
APOPercentage™ apoptosis assay	Biocolor Ltd
Bacteriological agar	Merck
Boric acid	Merck
Bromophenol blue	Sigma
Chloroform	BDH
Crystal Violet	Sigma
Dichloromethane	BDH
DAPI (4', 6'-diamidino-2-phenylindole)	Sigma
DMSO (Dimethyl sulphoxide)	Sigma
EDTA (Ethylene diamine tetra acetic acid)	Merck
Ethanol	BDH
Ethidium Bromide	Promega
Ethyl acetate	BDH
Gel Band Purification Kit	Amersham Biosciences
Glacial acetic acid	BDH
Glycerol	Merck



Hydrochloric acid	BDH
Illustra GFX™ PCR DNA	Amersham Biosciences
Methanol	BDH
N-Butanol	BDH
Paraformaldehyde	Sigma
pGEM®-T Easy Vector System	Promega
Propan-2-ol	BDH
Proteinase K	Roche
Silica gel 60 F ₂₅₄	Merck
Sodium chloride	Merck
Tris (Tris [hydroxymethyl] aminoethane)	BDH
Triton X-100 (iso-octylphenoxypolyethoxyethanol)	Roche
Tryptone	Merck
Xylene cyanol	BDH
Yeast extract	Merck



2.2) Stock solutions and buffers

10xTBE: 0.9 M Tris, 0.89 M boric acid and 25 mM EDTA, pH 8.3.

10xTE: 0.1 M Tris-HCl, and 0.01 M EDTA, pH 7.4.

Chloroform:isoamyl alcohol: 24 parts chloroform and 1 part isoamyl alcohol

LB agar: 10g/l Tryptone, 5g/l Yeast extract, 5g/l NaCl and 14g/l Bacteriological agar

L Broth: 10g/l Tryptone, 5g/l Yeast extract, 5g/l NaCl

Loading Buffer: 0.25 % Bromophenol blue, 0.25 % Xylene cyanol in 50 % glycerol

NR desorb: 1 % Glacial acetic acid, 50 % ethanol and 49 % dH₂O

PI Master Mix: PI (40µg/µl) and RNase A stock (100µg/µl) in PBS.

RNase A (DNase free): A 20 mg/ml stock solution was prepared in a buffer containing 0.1 M sodium acetate and 0.3 mM EDTA(pH 4.8, with acetic acid). This stock solution was boiled for 15 min. and cooled in ice water, dispensed into aliquots and stored at -20°C.

TTE: 1xTE, pH7.4, with 0.2 % Triton X-100

Turks reagent: 0.02 g of crystal violet and 7.2 % glacial acetic acid in dH₂O

2x CTAB buffer (1.4M): 1.4 M NaCl, 100 mM Tris-Cl pH8.0, 20 mM EDTA, 20g/l CTAB, 10g/l PVP40.



2.3) Tissue culture media and cell lines

Invitrogen supplied tissue culture media:

Dulbecco's modified eagle medium (DMEM) with 4.5g/L glucose, GlutamaxTM

Ham's F12 media with L-glutamine

RPMI 1640 medium with L-glutamine

PBS with CaCl₂ and MgCl₂

100x penicillin streptomycin

Foetal calf serum (FCS)

Complete Ham's F12 = Ham's F12 + 0.2 % penicillin streptomycin + 5 % FCS

Complete DMEM = DMEM + 0.2 % penicillin streptomycin + 10 % FCS

Complete RPMI = RPMI + 0.2 % penicillin streptomycin + 10 % FCS

Table 2.1. The cell lines used:

Species	Cell lines	Medium	Serum
Hamster	CHO 22	Hams F12	5 % FCS
Human	HeLa	DMEM	10 % FCS
Human	MCF7	RPMI 1640	10 % FCS

2.4) Culturing of cells

2.4.1) Thawing of cells

The vials of frozen cells were removed from storage at -150°C and immediately thawed in a 37°C water bath. The contents of the vials were then transferred into a 15 ml tube containing 5 ml Hams F12 media. The 15 ml tube was centrifuge for 2min. at 300 xg. The supernatant was discarded whilst the pellet was resuspended in 5 ml Hams F12 media and transferred to a 25cm^2 tissue culture flask for incubation. All the cell lines used were adherent and were incubated at 37°C in an atmosphere of 5 % CO_2 .

2.4.2) Trypsinization of cells

The cells were trypsinized once cells reached confluency. The Hams F12 media in the flask was discarded. Cells were washed with trypsin, then allowed to trypsinize with 3 ml of 0.0625 % Trypsin at 37°C . Cells completely trypsinized in 3 min. 12 ml of Hams F12 media were then added to stop trypsinization. The cells were split into three 25cm^2 tissue culture flasks for incubation in Hams F12 media.

2.4.3) Freezing of cells

To store cells, cells were trypsinized and centrifuged after which the cell pellet was re-dissolved in a 10 % DMSO and 90 % Hams F12 media mixture. The suspensions were aliquoted into 2 ml cryo-vials, then stored at -150°C.

2.4.4) Seeding of cells

Once cells were thawed and incubated in a 25cm² tissue culture flask, cells were incubated at 37°C for 48 h to 72 h to grow to confluency, Cells are then trypsinized, centrifuged to remove supernatant and re-suspended in 5 ml of Hams F12 media. Cells were counted using a Hausser Scientific Fuchs Rosenthal Ultra Plane Hemocytometer and seeded at a concentration of 2.5×10^4 cells per well. When 6, 24 or 96 well plates were used 2 ml, 500 ul or 100 ul of cells were seeded respectively. Cells were incubated overnight at 37°C and were ready for testing.

2.5) Tests authenticating the induction of apoptosis

2.5.1) Cytotoxicity assay

CHO (Chinese Hamster Ovary) cells were seeded in 96 well tissue culture plates and tested for 24 h with varying concentrations in triplicate. The supernatant was removed from the wells, cells were washed with 2 ml PBS and 100 µl of neutral red (NR) solution (100 µg/ ml, in serum free media) was added to each well. The plates were incubated for 2 h at 37°C. Wells were washed rapidly with 100 ul, 1 %

paraformaldehyde. The NR dye was extracted from the cells by adding 100 ul of NR desorb to each well, plates were incubated for 15 min., then placed on a shaker for an additional 30 min. before determining the optical density at 540 nm (OD₅₄₀) on a multiwell spectrophotometer. Cytotoxicity is calculated as follows:

$$\% \text{ cytotoxicity} = \frac{\text{Abs of negative control} - \text{Abs of treated cells}}{\text{Abs of negative control}}$$

2.5.2) APOPercentage™ assay

The APOPercentage™ dye was prepared by adding 15.9 ml F12 (Hams) media to 0.1 ml APOPercentage™ dye. Cells were seeded in 24 well tissue culture plates and tested for 24 h with varying concentrations of plant extract in triplicate. After the cells were treated with the plant extract, the extracts were transferred to 15 ml tubes. Cells were washed with 1 ml PBS and trypsinized with 300 ul trypsin that were both added to the removed extract. Cells were centrifuged at 500 xg for 5 min. Cells were re-suspended in 200 ul of the prepared APOPercentage™ dye, followed by incubation for 30 min. at 37°C. The cells were washed with 2 ml PBS to remove excess dye. The cells were analyzed by flow cytometry.

2.5.3) Annexin V- PE Apoptosis Detection assay

The assay was performed using the Annexin V-PE Apoptosis Detection Kit (BD Biosciences). The manufacturers' protocol was followed. CHO cells were seeded in

24 well tissue culture plates and cells were induced with extract for 6 h. After the cells were treated with the plant extract, the cells were washed with cold PBS. The cells were then trypsinized and re-suspended in 500 μ l 1 x binding buffer. To each suspension 5 μ l of Annexin V-PE and 5 μ l of 7-AAD was added. Suspensions were then gently vortexed and incubated for 15 min. at room temperature in the dark. The cells were analyzed by flow cytometry.

2.5.4) Active Caspase 3 - PE Mab Apoptosis

The assay was performed using the Active caspase 3-PE Apoptosis Kit (BD Biosciences). The manufacturers' protocol was followed. CHO cells were seeded in 24 well tissue culture plates and cells were induced with extract for 6 h. After the cells were treated with the plant extract, wells were washed with PBS; cells were trypsinized and re-suspended in 0.5 ml Cytotfix/Cytoperm, then incubated on ice for 20 min. The cells were centrifuged at 500 xg for 5 min. The cell pellets were washed twice with 0.5 ml Perm/Wash buffer followed by centrifugation. Each sample was re-suspended in 100 μ l of Perm/Wash buffer and 20 μ l of antibody. The samples were then incubated for 30 min. at room temperature. The samples were washed with 1 ml Perm/Wash buffer, and re-suspended in 0.5 ml Perm/Wash buffer. The cells were analyzed by flow cytometry.

2.5.5) APO-DIRECT™ Kit

The assay was performed using the APO-DIRECT™ Kit (BD Biosciences). The manufacturers' protocol was followed. CHO cells were seeded in 6 well tissue culture plates and cells were induced with 5 mg/ml plant extract for 48 h. After treatment with the plant extract, cells were trypsinized and re-suspended in 5 ml of 1 % (w/v) paraformaldehyde in PBS and placed on ice for 15 min. The cells were centrifuged at 500 xg for 5 min. and the supernatant was discarded. Cells were washed in 5 ml of PBS followed by centrifugation at 500 xg for 5 min. The wash step was repeated. The cells were re-suspended in 0.5 ml of PBS, to which 5 ml. of ice-cold 70 % (v/v) ethanol was added. Cells were stored at -20°C for 48 h. The cells were centrifuged at 500 xg for 5 min. and the supernatant was discarded. Each cell pellet was re-suspended in 1 ml of wash buffer. Samples were centrifuged as before and the supernatant was removed by aspiration. The wash step was repeated. The cells were re-suspended in 50 ml of the staining solution and incubated for 60 min at 37°C. 1 ml of Rinse Buffer was added to each tube and centrifuged as before. The supernatant was removed by aspiration. The cell rinsing step was repeated. The cells were resuspended in 0.5 ml of the Propidium Iodide/RNase A solution and incubation in the dark for 30 min. at room temperature. The cells were analyzed in Propidium Iodide/RNase solution by flow cytometry.

Table 2.2 APO-DIRECT™ kit staining solution

Staining Solution	1 Assay (µl)	4 Assay (µl)
TdT reaction	10	40
TdT enzyme	0.75	3
Fluorescein-dUTP	8	32
dH₂O	32	128
Total volume	50.75	203

2.6) Phylogenetic studies

2.6.1) 2x CTAB DNA extraction

Liquid nitrogen was added to 50 mg of leaf material to facilitate the grinding of the leaf material to a fine powder. 1 ml of 2 x CTAB buffer preheated to 62°C was mixed with the fine powder to obtain a consistent slurry. This mixture was incubated at 62°C for 30 min., then allowed to cool for 10 min. at room temperature before 10 µl of 10 mg/ml Proteinase K was added. The samples were incubated at 37°C for 30 min. Equal volumes of CIA was added to each sample followed by gentle mixing. The sample was centrifuged at 10 000 xg for 10 min. The top aqueous layer was collected and 2/3 v/v ice-cold isopropanol was added to the collected aqueous layer. The samples were mixed by inversion, then samples were incubated at 4°C for 20 min. The samples were centrifuged at 10 000 xg for 10 min. then the supernatant was discarded. The cells were washed twice with 500 µl ice-cold 70 % EtOH. The cells were air-dried, re-suspended in 100 – 200 µl TE buffer containing RNase (0.0625 mg/ml final concentration) then incubated at 37°C for 30 min. The DNA was re-precipitated with 0.5 v/v 7.5M NH₄Ac and 2.5 v/v cold Abs EtOH was added. The

sample was incubated for 30 min. at -20°C. The samples were centrifuged at 10 000 xg for 10 min. The DNA was air-dried and re-suspended in TE buffer.

2.6.2) Polymerase Chain Reaction (PCR)

PCR reactions were performed in 10x reaction buffer. The enzyme *Taq* polymerase was used at 0.2 units per reaction. The primers were present at 1 pmol, MgCl₂ concentration was 1.5 mM and 10 ng of DNA template was used in each reaction. Table 2.3 describes the experimental set up of each PCR reaction.

Table 2.3. Experimental set up of the PCR reactions

	Final Concentrations
10x Reaction buffer	1x
dNTP's	100µM
Forward primer	1µM
Reverse primer	1µM
dH₂O	
Taq	0.2u
DNA template	~10ng
Total reaction volume	

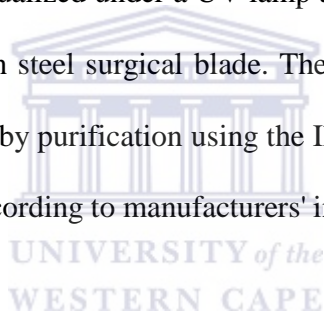
The PCR cycling conditions were as follows: 95°C for 10 min.; 95°C for 30 sec.; 56°C for 30 sec.; 72°C for 30 sec.; repeated for 30 cycles; followed by 72°C for 7 min. The successes of the PCR process were assessed by agarose gel electrophoresis.

2.6.3) Agarose gel electrophoresis of DNA

To 2 µl of the DNA sample prepared (as per method set out in 2.5.5.1), 2 µl of loading buffer was added. Samples were loaded alongside the molecular weight marker on a 1.5 % agarose gel containing 1 µl EtBr per 100 µl 1 x TBE buffer. The samples were electrophoresed at 10 V/cm in 1 x TBE buffer. DNA was visualized with a UVP transilluminator.

2.6.4) Purification of DNA fragments

The PCR product was visualized under a UV lamp and cut out of the agarose gel with a sterile single-use carbon steel surgical blade. The PCR product or DNA fragments were macerated followed by purification using the Illustra GFX™ PCR DNA and Gel Band Purification Kit (according to manufacturers' instruction).



2.6.5) Cloning PCR fragments into pGEM®-T Easy

PCR fragments were cloned using the pGEM®-T Easy Vector System (Promega). Table 2.4 describes how the ligation reactions were set up.

Table 2.4. Experimental set up of the ligation reaction

	Final concentrations
2x Rapid ligation buffer	1x
pGEM[®]-T Easy (1ng/ µl)	0.1ng
PCR product	0.05ng
Control insert	0.05ng
dH₂O	
T4 DNA ligase (1 unit/ µl)	1u
Total reaction volume	

The ligation reactions were briefly mixed and incubated overnight at 4°C. For the transformation process, 100 µl competent *E. coli* cells were added to the ligation reactions. The mixtures were incubated on ice for 20 min. The cells were then heat shocked at 42°C for 30 sec. followed by incubation on ice for 5 min. Each tube was filled up to 1 ml with pre-warmed L-Broth and incubated at 37°C with shaking. After 30 min., 100 µl of the transformed culture was plated on LA agar plates containing 100 µg/ ml ampicillin and incubated at 37°C overnight.

2.6.6) Colony PCR and sequence analysis

Following the transformation process, colonies to be screened were removed from the plate and re-suspended in 100 µl deionised water. *E. coli* colonies were screened for the presence of the insert by colony PCR. Table 2.5 describes the colony PCR reactions.

Table 2.5. Experimental set up of the colony PCR

	Final concentrations
10x Reaction buffer	1x
dNTP's	100 μ M
M13 Forward primer	1 μ M
M13 Reverse primer	1 μ M
dH₂O	
Taq	0.2u
Colony cell suspension	
Bacterial cell suspension	
Total reaction volume	

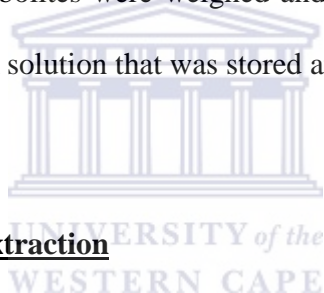
The PCR cycling conditions were as follows: 95°C for 10 min.; 95°C for 30 sec.; 95°C for 30 sec.; 58°C for 30 sec.; 72°C for 30 sec.; repeated for 35 cycles; followed by 72°C for 7 min. The successes of the colony PCR process were assessed by agarose gel electrophoresis.

.The colony PCR product were spread on L-agar plates and grown at 37°C. Positive clones were sent for sequencing at Inqaba Biotechnical Industries (Pty) Ltd, South Africa. Glycerol stocks were prepared of the positive clones, by dilution of the culture with an equal volume of 80% sterile glycerole. These were then stored at -80°C

2.7) Methods of fractionation

2.7.1) Aqueous extraction

The plant material was cut to increase the surface area, and then dried in an oven at 40°C overnight. The dried plant material was blended to a powder and 10g was weighed out and mixed with 500 ml distilled water. This mixture was then stirred for 16 h. The supernatant containing the extracted secondary metabolites was then removed and the extraction step was repeated twice on the same plant material. The extracted mixture was then filtered, frozen at -80°C and then freeze dried. The dried extracted secondary metabolites were weighed and re-dissolved in distilled water to produce a 40 mg/ml stock solution that was stored at -20°C.



2.7.2) Organic solvent extraction

The active aqueous extracts were individually fractionated by organic solvent extraction. The aqueous extract was mixed vigorously with acetone in a 1:4 ratio. The solvents were then placed in a separation funnel and allowed to phase separate. The acetone was removed; another 80 ml of acetone was added to the 20 ml aqueous extract in the separation funnel. The extraction step was repeated in triplicate on the same aqueous extract. The same extraction procedure was used for other solvents with increasing polarity (except that a 1:1 ratio was used). The other solvent used was n-butanol **3.9**, ethyl acetate **4.3**, chloroform **4.4**, petroleum ether **5** (polarity of solvents represented by bold numeric following the solvent name). The solvents were

then evaporated using a rotary evaporator and the concentrations of the extracts were established. The extracts were re-dissolved in ethyl acetate, as it had been determined that 1 % ethyl acetate is not toxic to the cells. Thus, for testing purposes 0.5 % ethyl acetate concentrations were used.

The stock solution was diluted with Hams F12 media to produce different concentrations of the extract for testing purposes. These different dilutions of plant extracts were filtered (through a 0.22 micro-pore cameo filter) before screening for induction of apoptosis.

2.7.3) Thin Layer Chromatography (TLC)

2.7.3.1) Determining the solvent system need to separate extract by TLC

Before performing TLC or LCC, the solvent system needed to separate the compounds was determined. TLC aluminium sheets (20 x 20 cm; silica gel 60 F₂₅₄) were cut into 10 cm x 1.5 cm rectangles. A light pencil line was drawn 1 cm from the bottom and top edge of the chromatographic plate. The sample was spotted on this line (<0.5 mm in diameter) and placed in a developing chamber. The solvent was allowed to migrate up the plate via capillary action until the pencil line drawn across the top edge was reached. The plates were then examined under ultraviolet (UV) light. A solvent that results in strong mobility of the extract and one in which the extract remains stationary are combined in different ratios. The ratio that best separates the extract into different layers is utilized as the solvent system for TLC and/or LCC.

2.7.3.2) Concentrated compound fractionation by TLC

A TLC glass plate (20 x 20 cm; silica gel 60 F₂₅₄) was used for the fractionation of compounds. A light pencil line was drawn 1cm from the bottom and top edge of the chromatographic plate. A capillary was used to streak the extract across the bottom edge as thinly as possible. A developing chamber was filled 0.5 cm with the solvent system established above. The solvent migrated up the plate via capillary action until it reaches the pencil line drawn across the top edge. The TLC plate was removed from the developing chamber, and allowed to air-dry. The plates were examined under ultraviolet (UV) light and the layers were outlined with a pencil. The R_f values for each layer were calculated (illustrated in figure 2.1), as unknowns can be identified using R_f values. Each layer of silica/ extract was scrapped off the TLC glass separately.

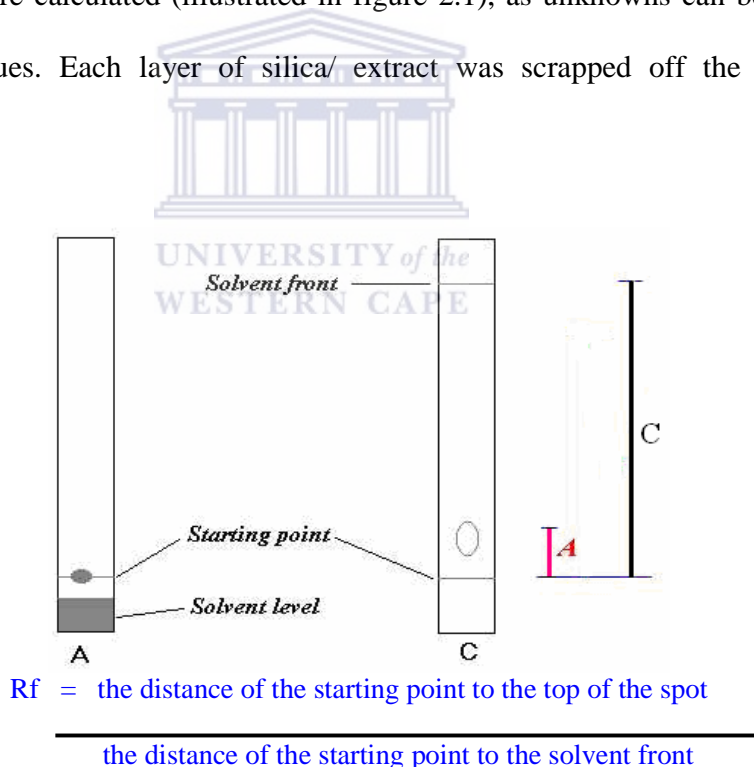


Figure 2.1. Illustration of how the R_f was calculated. The R_f equals the distance of the starting point to the top of the spot divided by the distance of the starting point to the solvent front.

To separate the silica from the extract, a cotton stopper was firmly placed in a column, followed by the silica/extract, and then 100 % of the solvent in the solvent system was poured into the column. The extract eluted in the solvent that is captured in a beaker placed beneath the tap of the column. Fractions were then dried by rotary evaporation and re-dissolved in ethyl acetate and tested for apoptosis activity.

2.7.4) Liquid Column Chromatography (LCC)

A chromatography column was set up and approximately 75% of the column was filled with silica. A 1-2 cm layer of silica was mixed with extract then the mixture was dried by rotary evaporation to bind the extract to the silica. The layer of extract bound silica was placed on the clean silica in the column. A cotton plug was placed on the silica to prevent the extract from re-dissolving into the solvent system. A small quantity of solvent system was added slowly to the column to settle the cotton plug. The column was filled with solvent and the solvent level was maintained. The eluting solvent was captured by a fraction collector. The fractions collected were spotted on TLC plates to establish distinction in fractions collected. Fractions were then dried by rotary evaporation, re-dissolved in ethyl acetate and tested for apoptosis activity.

2.7.5) Reverse-Phase High Performance Liquid Chromatography (RP-HPLC)

Samples were monitored and fractionated using the Beckman HPLC system in combination with the chromatography station with Windows, Clarity™ DataApex and collected using the FOXY JR 202F20077 fraction collector. The Beckman HPLC

system consisted of an autosampler 501, organizer 340, 2 x solvent delivery system module 110 and the Knauer variable wavelength monitor.

The chromatographic conditions for the analytical C-18 250 x 4.6mm Luna 5u (Phenomex): Mobile phase solvent A consisted of 1 % acetic acid in water (v/v) mobile phase solvent B consisted of 100 % methanol. The gradient was premeditated as follows: the column was equilibrated with 100 % solvent A and 0 % solvent B for 5 min. then solvent A was decreased to 60 % and solvent B was increased to 40 % for 10 min. Solvent A was then decreased to 40 % and solvent B was increased to 60 % in 2 min. This solvent system remained constant for 10 min. Solvent A was then further decreased to 20 % and solvent B was increased to 80 % in 2 min. This solvent system remained constant for 10min. Solvent A was decreased to 0 % and solvent B was increased to 100 % in 2 min. This solvent system remained constant for 10 min. Solvent A was decreased to 100 % and solvent B was increased to 0 % in 2 min. and remained constant for 5 min. to re-equilibrate the column in preparation for subsequent fractionations.

CHAPTER 3: SCREENING INDIGENOUS SOUTH AFRICAN PLANTS FOR PRO-APOPTOTIC ACTIVITY

3.1) Introduction

The use of traditional medicine has a long history and is still the major source of medicine in developing countries. Approximately 70 % of the South African population consults traditional healers, perpetuating the need for scientific appraisal of traditional medicine as a means to establish its efficiency and safety (Puckree *et al.*, 2002). Also, pharmacological and phytochemical insights into several plants have led either to the discovery of novel chemicals and therefore novel drugs, or to novel chemical structures that can serve as lead compounds/templates for the design of new drugs (section 1.3.1). Natural product research has thus been developed specifically for the isolation of secondary metabolites with a particular biological activity.

Plants contain two classes of compounds namely; primary metabolites that are required for the livelihood of the plant i.e. the plants machinery, and the secondary metabolites that are not a necessity for the plants survival. Some secondary metabolites protect plants against fungi, bacteria, insects, and viruses. Extracted secondary metabolites have been used as food flavourants, colour dyes, poisons, perfumes, industrial products (e.g. oil) and prescription drugs, however the functions of majority of the secondary metabolites are not known (Wink, 1999). Plant derived secondary metabolites and their derivatives have also been a major source of anti-cancer drugs.

The identification and purification of bioactive secondary metabolites from plant extracts can be a tedious and expensive operation. In an attempt to cut down on the cost of drug discovery and to increase the probability of identifying useful secondary metabolites, research methodology allows the screening of multiple natural products for prospective drug development. One approach is to screen plants with well-known ethno-medicinal value, although it has been established that the ethno-medicinal data obtained for a plant extract is not necessarily a reliable source (Cragg *et al.*, 1994). However, there also seem to be a greater possibility of finding biological activity among plants with ethno-medicinal value rather than from plants randomly selected (Chapuis *et al.*, 1988; Cordell *et al.*, 1991). The second approach is to use the rapid, inexpensive and highly automated screening methods. With respect to anti-cancer drug screening it is believed that cytotoxicity and cell viability assays provide important preliminary data to help select plant extracts with potential anti-cancer properties for future work (Cardellina *et al.*, 1993). This strategy is based on the fact that these assays measure cell death or inhibition of cell growth and that a potential anti-cancer drug will either inhibit cancer growth or kill cancerous cells. However, most of these assays do not discriminate between toxic cell death and cell death induced by apoptosis. Colorimetric bio-assays, such as the APOPercentageTM assay, specifically detect and quantify apoptosis, making them better high-throughput, inexpensive accurate preliminary screen of pro-apoptotic activity. However, accurate quantification of the pro-apoptotic activity is lacking. This dilemma has been solved by analyzing APOPercentageTM assay results by FACScan. The conventional APOPercentageTM assay requires 100 µl of 1/20 dilution of APOPercentageTM dye per reaction whereas, APOPercentageTM assay/FACScan only require 100 µl of 1/160

dilution of APOPercentage™ dye. The APOPercentage™ assay/FACScan results are thus more laborious to obtain but preferable as they are quantitative (Johnson *et al.*, 2003).

The objective of this section was to do comparative screening of poisonous native South African plants with and without ethno-medicinal value (listed in [table 3.1.](#)). Thus, the present enquiry reports on the cytotoxicity (using the neutral red colorimetric assay) and apoptosis activity (using the APOPercentage™ assay, Biocolor Ltd) of the aqueous extracts of nine native South African plants on three cell lines namely MCF7 (human breast adenocarcinoma), HeLa (human cervical carcinoma) and the 'normal' animal cell line, CHO (Chinese Hamster Ovaries). All experiments were repeated thrice to ensure that the results obtained were accurate and reproducible. The cytotoxic and apoptotic activity was used to identify the plant extract with the most significant anti-cancer activity. This plant pro-apoptotic activity was demonstrated with more specific markers of apoptosis namely the externalization of phosphatidylserine, caspase-3 activation and DNA fragmentation.

The nine plants screened were; the poisonous *Cotyledon orbiculata*, *Oxalis pes caprae*, *Echium plantagineum*, *Cissampelos capensis*, *Euphorbia mauritanica*, *Haemanthus pubescens*, *Cynanchum africanum* and the non-poisonous *Lessertia frutescens* and *Elytropappus rhinocerotis* (see the pictorial representation in [figure 3.1.](#)). Some of these plants are used as traditional remedies to treat cancer. Except for

Table3.1. Plants screened to treat conditions consistent with cancer symptomatology

Plant species (family)	Common name	Distribution	Traditional medicinal uses	Some reported pharmacological activities	References
<i>Cotyledon orbiculata</i> (Crassulaceae)	pigs ears	Southern Africa	boils, inflammation, earache, syphilis, ulcers	four bufadienolides; orbicucosides A, B, C and tyledoside C causes 'krimpsiekte' in stock	Steyn et al. 1986
<i>Oxalis pes caprae</i> (Oxalidaceae)	yellow sorrel	Western Cape	arthritis, asthma, boils, burns, cancer , tuberculosis, tumors	oxalates are poisonous to humans and animals	Bruneton. 1999
<i>Echium plantagineum</i> (Boraginaceae)		Western Cape Province	n/a	heliosupine, echimidine, echiumie etc.these toxins accumulatively cause liver damage in animal	Van Wyk et al. 2000
<i>Cissampelos capensis</i> (Menispermaceae)	dawidjies	Western parts of South Africa	diabetes, tuberculosis, urinary stones, stomach and skin cancer	n/a	
<i>Euphobia mauritanica</i>	melkbos	Southern Africa: western parts and dry interior	n/a	cause fatal nervous disorder in sheep characterized by muscle tremers, bloat, diarrhoea and fever	Kellerman et al. 1988
<i>Haemanthus coccineus</i>	April's fool		ulcers, anthrax, edema, diuretic, asthma	n/a	
<i>Cynanchum africanum</i> (Asclepiadaceae)	bobbejaantou	Cape Peninsula: Namaqualand to Port Elizabeth	n/a	cause cattle and sheep poisoning called cynanchosis	Kellerman et al. 1988
<i>Lessertia frutescens</i> (Fabaceae)	cancer bush	Southern Africa: Western Cape, Eastern Cape, Namibia, Karoo.	chickenpox, diabetes, hemorrhoids, rheumatism, cancer	L-canavanine has documented anti-cancer activity	Swaffer et al. 1995
<i>Elytropappus rhinocerotis</i> (Asteraceae)	renosterbos	Western Cape and Eastern Cape	'flu, indigestion, lack of appetite, ulcers and stomach cancer.	rhinocerotinoic acid, a diterpene with anti-inflammatory properties	Dekker et al. 1988

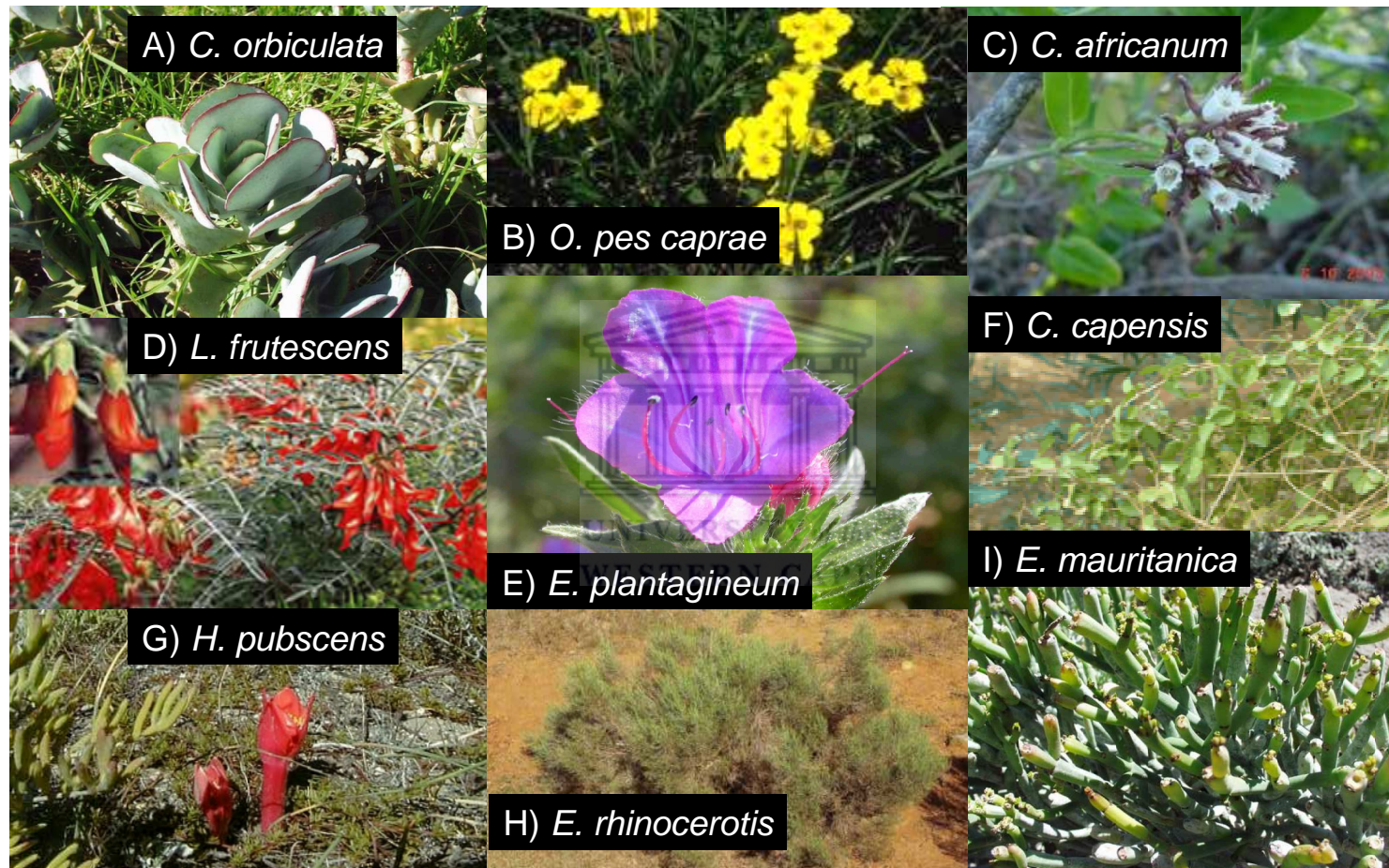


Figure 3.1. Pictorial representation of the nine indigenous South African plant screened for apoptosis activity. **A** represents *Cotyledon orbiculata*. **B** represents *Oxalis pes caprae*. **C** represents *Cynanchum africanum*. **D** represents cytotoxicity and apoptosis activity induced by *Lessertia frutescens*. **E** represents *Echium plantagineum*. **F** represents *Cissampelos capensis*. **G** represents *Haemanthus pubescens* **H** represents *Elytropappus rhinocerotis*. **I** represent *Euphorbia mauritanica*.

L. frutescens none of these plants have reported anti-cancer activity. An anti-cancer compound in *L. frutescens* has been identified as L-canavanine (Crooks and Rosenthal, 1994; Swaffar *et al.*, 1994). *L. frutescens* displays significant pro-apoptotic activity on numerous cell lines including; CHO, Jurkat (human T cell leukemia) and MCF7 (Chinkwo, 2005; Tai *et al.*, 2004). *Cotyledon orbiculata*, *Oxalis pes caprae*, *Echium plantagineum*, *Euphorbia mauritanica* and *Cynanchum africanum* has been documented to be poisonous to animals ([Table 3.1.](#)).

3.2) Aqueous extraction of plant secondary metabolites

Traditional remedies necessitate the extraction of plant secondary metabolites by boiling in water. This extraction method allows for the indiscriminate extraction of the secondary metabolites, a method perfectly apt for the screening of an unknown secondary metabolite. Efficiency of the aqueous extraction process was ensured by the effective drying, blending and grinding of the plant material, as this process assists with the penetration of the solvent to the plant cellular structure to dissolve the secondary metabolites i.e. it increased the yield of extraction by increasing the surface area (Cannell, 1998).

A 40 mg/ml stock solution of aqueous extracted plant extract was prepared using the method described in section 2.6.1 and was stored at -20°C. The aqueous extraction produced yields between 4 % and 10 % of dry plant product compared to the mass of the dry plant product used as the starting material in the extraction ([Table 3.2.](#)).

Table 3.2 Yields associated with the aqueous extraction of the dry plant material

Plant species	Time of collection	Area of collection	Dry weight (g)	Plant part	Yield (%)
<i>C. orbiculata</i>	May	Cape Flats	10	lf	5.8
<i>O. pes caprae</i>	May	Cape Flats	10	lf,st	4.2
<i>E. plantagineum</i>	May	Cape Flats	10	lf,st	6.4
<i>C. capensis</i>	July	Cape Flats	10	lf,st	4.2
<i>E. mauritanica</i>	July	Cape Flats	10	lf,st	6.1
<i>H. coccineus</i>	July	Cape Flats	10	lf	5.7
<i>L. frutescens</i>	July	Wellington	10	lf,st	6.0
<i>C. africanum</i>	July	Cape Flats	10	lf,st	5.4
<i>E. rhinocerotis</i>	July	Tulbagh	10	lf,st	8.2
<i>E. rhinocerotis</i>	September	Tygerberg	10	lf,st	7.3
<i>E. rhinocerotis</i>	September	Helderberg	10	lf,st	7.1
<i>E. rhinocerotis</i>	September	Blaauwberg	10	lf,st	7.6
<i>E. rhinocerotis</i>	September	Kirstenbosch	10	lf,st	7.3

*lf - leaf; st - stem

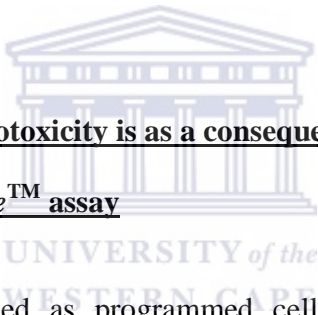
3.3) Analysis of the cytotoxic and pro-apoptotic effects of plant extracts

3.3.1) Screening cytotoxic effects of plant aqueous extracts using the neutral red (NR) assay

The neutral red (NR) cytotoxicity assay is a cell viability assay, based on the ability of viable cells to incorporate and bind the NR dye. NR is a weak cationic dye that penetrates cell membranes by non-ionic diffusion. It accumulates intracellular at the anionic sites in the lysosomal matrix. Alterations in the cell membrane or the sensitive lysosomal membrane leads to lysosomal fragility (Borenfreund and Puerner, 1985). As a consequence only cells that are intact / viable will bind NR dye i.e. the viable cells with an intact lysosomal membrane will be dye stained with the dye while the dead cells with lysosomal membrane damage will not be labelled. They dye trapped within live cells can be released, quantified and expressed as a function of cell death.

Cells were plated in 96 well tissue culture plates as described in section 2.5.1. The cells were treated with aqueous extract of all plants used for 24 h. The concentrations ranged between 0.625 mg/ml and 5 mg/ml. Cytotoxicity effect was measured by the colorimetric Neutral red assay. The cytotoxicity induced by individual plant extracts are presented on Figure 3.2, 3.3 and 3.4 (in blue) that represent the MCF7, HeLa, and CHO cell lines respectively.

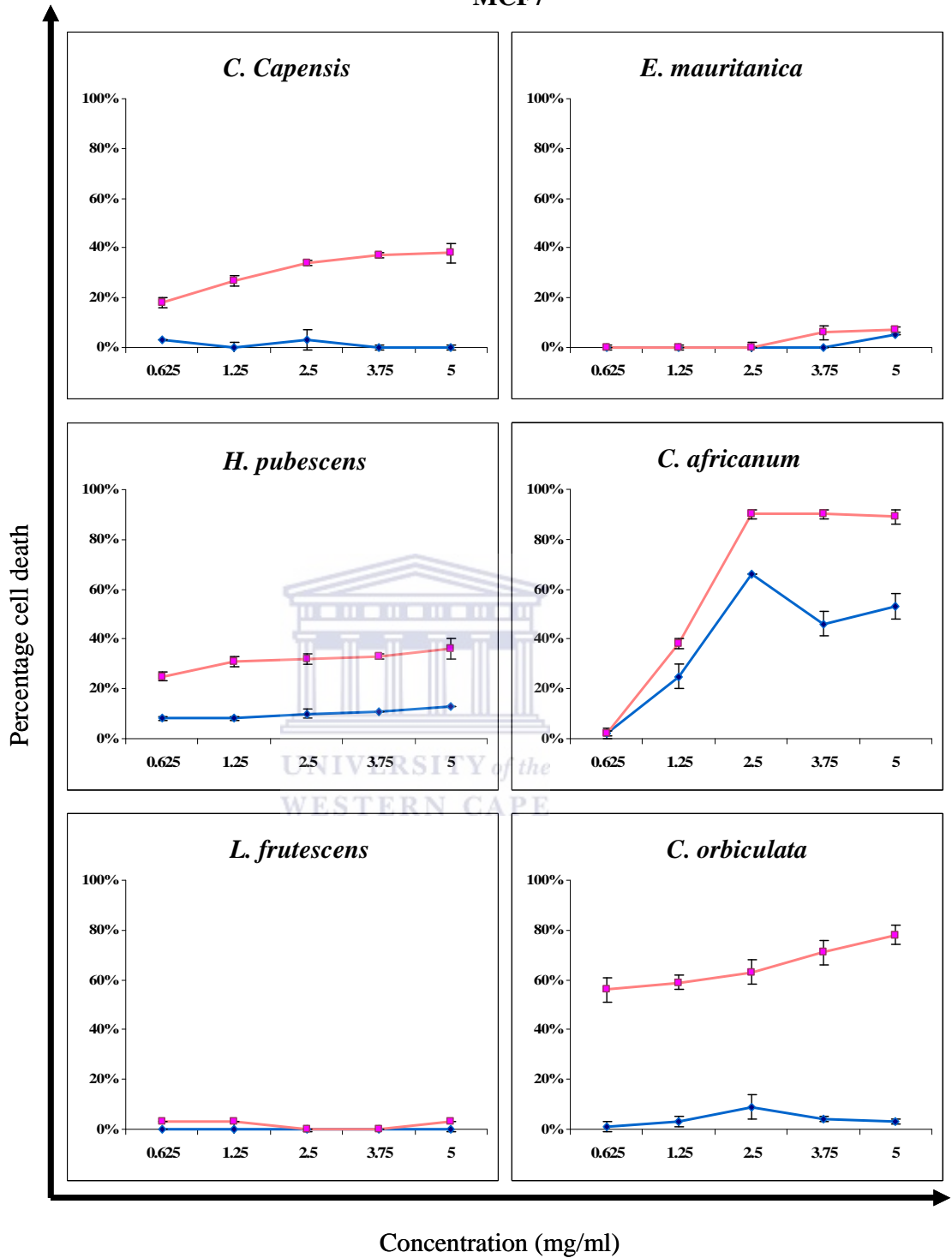
The aqueous extract of *C. orbiculata* is the only extract tested that displays induction of noteworthy cell death or high levels of cytotoxicity in the breast cancer cell line (MCF7) presented in figure 3.2, whereas *C. capensis*, *E. mauritanica*, *H. pubescens*, *C. africanum* and *C. orbiculata* display signs of considerable cell death or high levels of cytotoxicity in the cervical cancer cell line (HeLa) presented in figure 3.3. However, cytotoxicity is negligible (below 40 %) in the non-cancerous cell line (CHO) for all plant extracts tested. These results indicate that cytotoxicity induced were specific to the cells lines tested as cytotoxicity is not constantly induced in all the cell lines. The question now arises, is the cell death a consequence of pro-apoptotic activity or necrosis?



3.3.2) Ascertaining if cytotoxicity is as a consequence of apoptosis induction using the APOPercentage™ assay

Apoptosis may be defined as programmed cell death characterized by certain morphological features such as membrane asymmetry and attachment, condensation of the chromatin, and internucleosomal cleavage of DNA. In apoptotic cells, the membrane phospholipid phosphatidylserine (PS) is externalized to the outer-leaflet of the plasma membrane (Fadok *et al.*, 1992). The APOPercentage™ assay is a dye uptake assay which stains apoptotic cells with a red dye (Biocolor Ltd). The exposure of the PS allows the unidirectional uptake of the APOPercentage™ dye. As a consequence only those apoptotic cells that have undergone the externalization of phosphatidylserine will be dye labeled, whereas the normal and necrotic cells that are present remain unlabelled.

MCF7



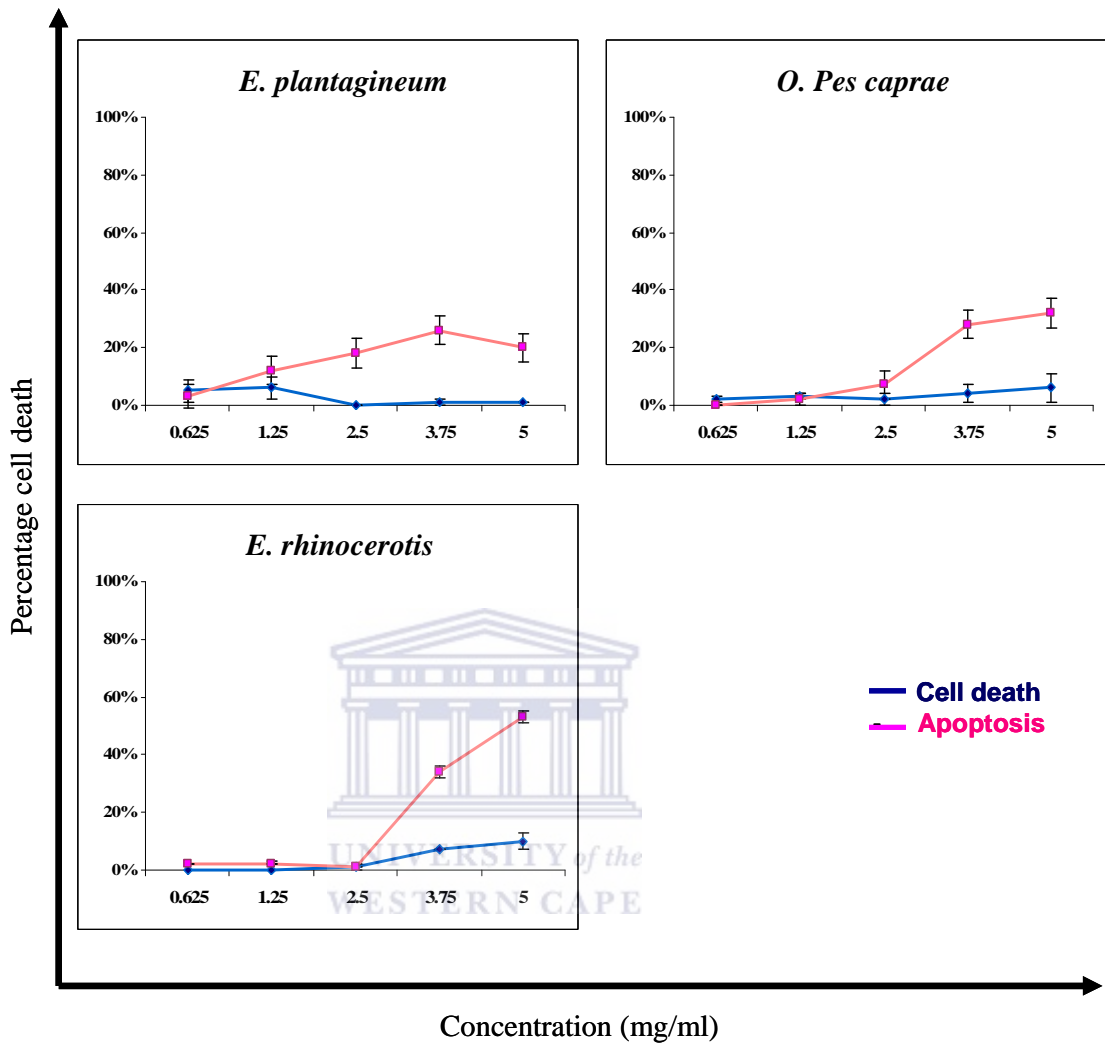
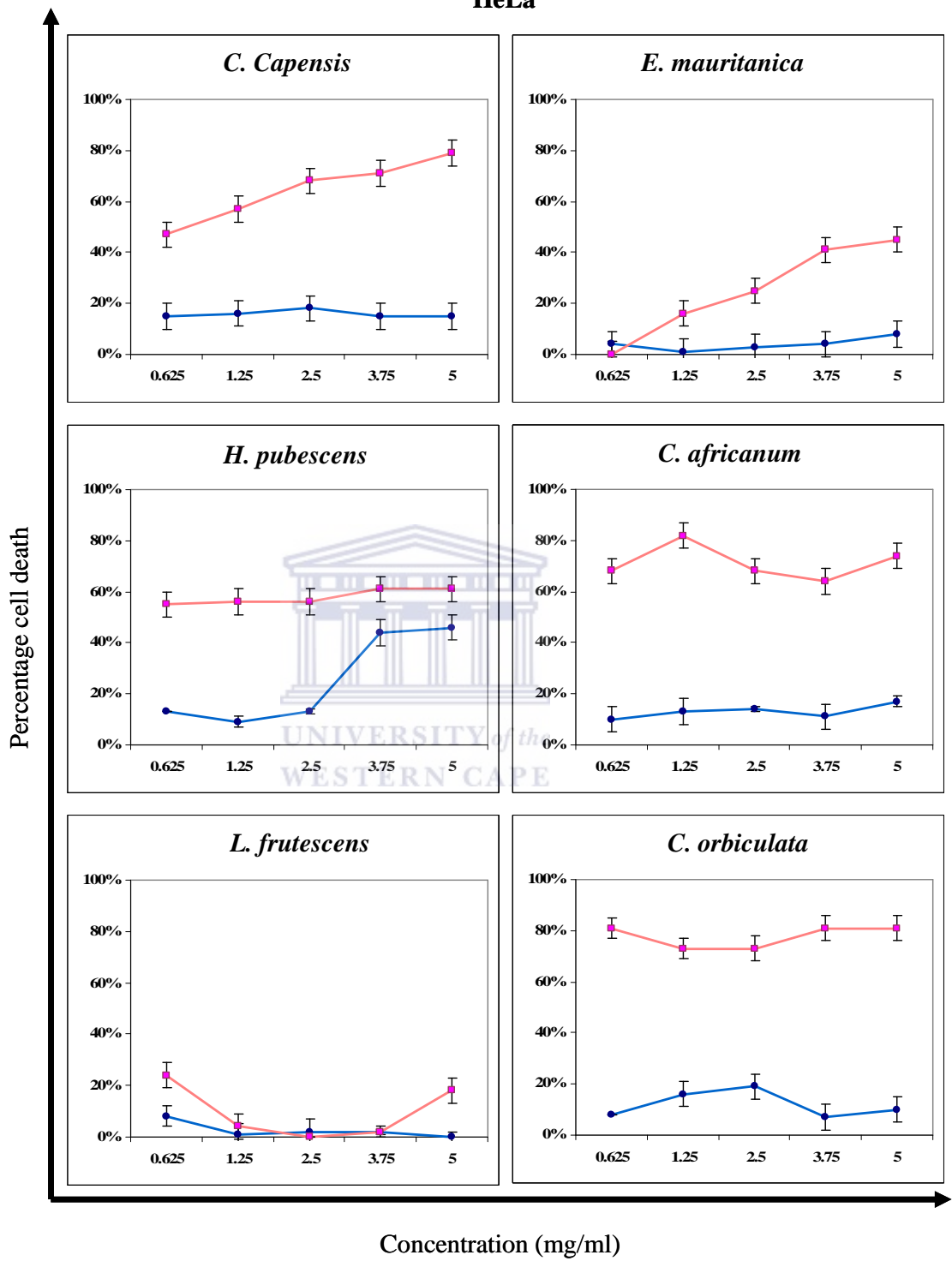


Figure 3.2. Neutral red assay demonstrating cytotoxicity (represented by the blue graphs) and the APOpercentage™ assay kit demonstrating apoptosis (represented by the pink graphs). Cells were treated for 24hrs with increasing concentrations (0.625, 1.25, 2.5, 3.75 and 5mg/ml) of plant aqueous extracts on the MCF7 cell line.

HeLa



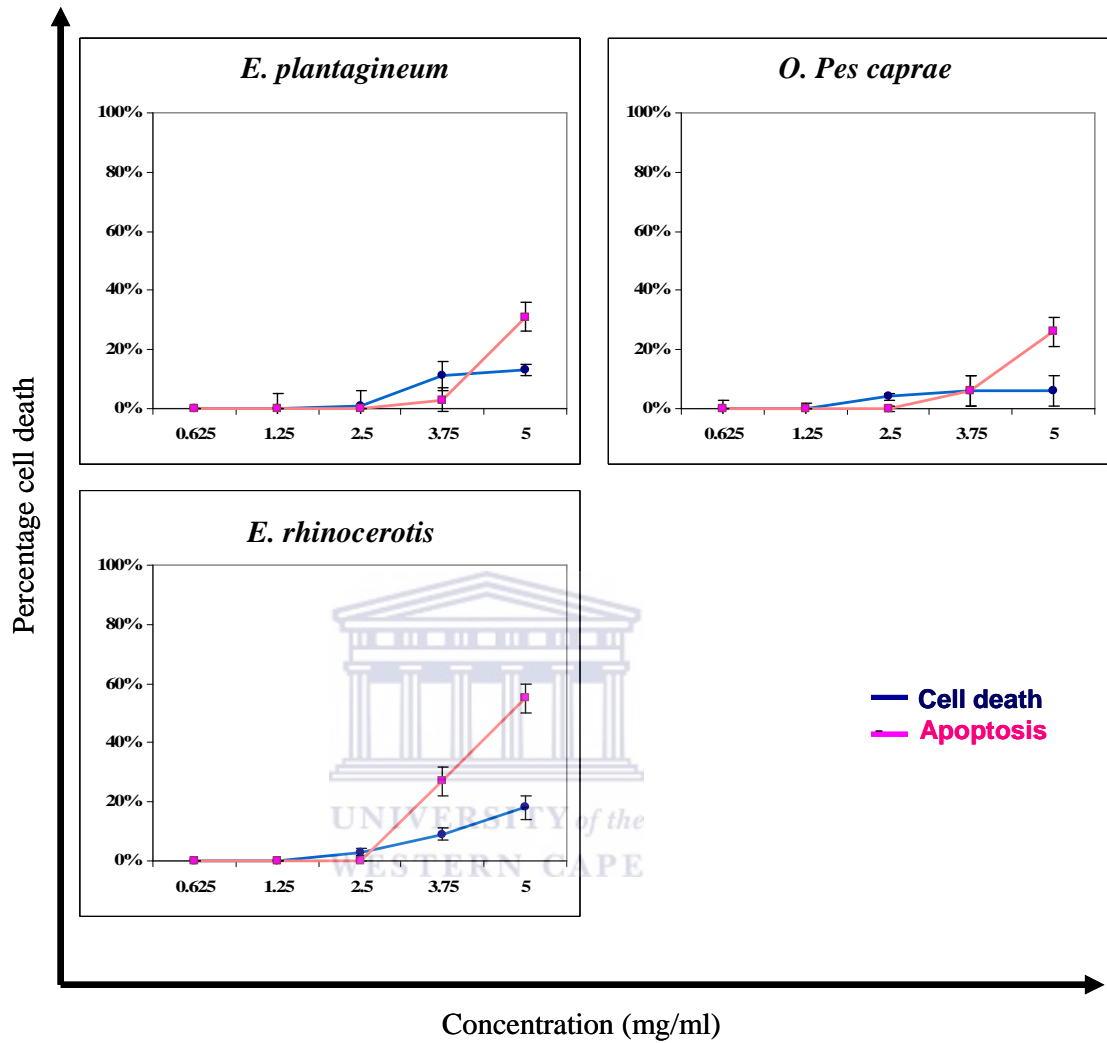
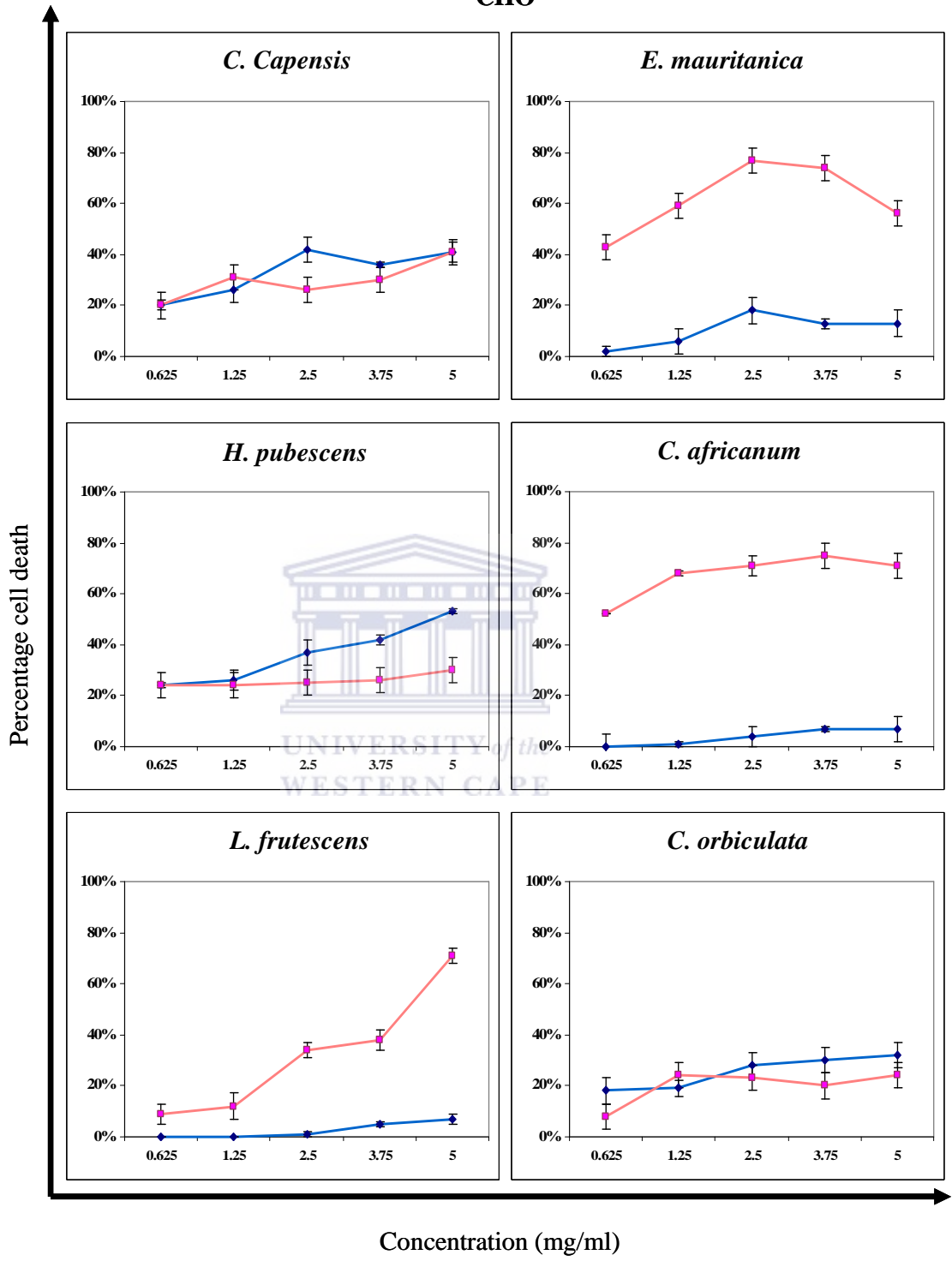


Figure 3.3. Neutral red assay demonstrating cytotoxicity (represented by the blue graphs) and the APOpercentage™ assay kit demonstrating apoptosis (represented by the pink graphs). Cells were treated for 24hrs with increasing concentrations (0.625, 1.25, 2.5, 3.75 and 5mg/ml) of plant aqueous extracts on the HeLa cell line.

CHO



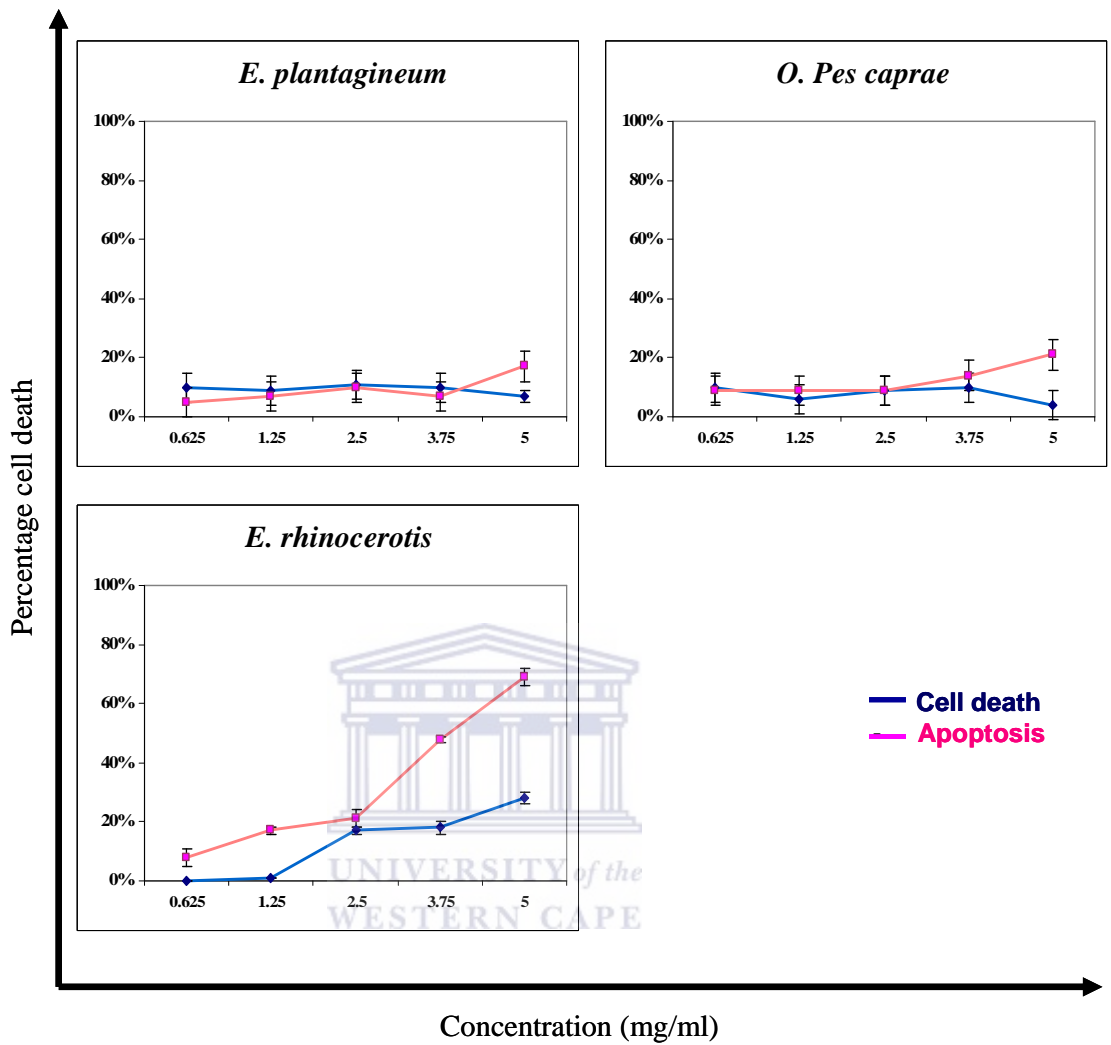


Figure 3.4. Neutral red assay demonstrating cytotoxicity (represented by the blue graphs) and the APOpercentage™ assay kit demonstrating apoptosis (represented by the pink graphs). Cells were treated for 24hrs with increasing concentrations (0.625, 1.25, 2.5, 3.75 and 5mg/ml) of plant aqueous extracts on the CHO cell line.

CHO cells were plated in 24 well tissue culture plates as described in section 2.5.2. The cells were treated with aqueous extract of all plants used for 24 h. The concentrations ranged between 0.625 mg/ml and 5 mg/ml. Cells were treated, permeabilized and stained with APOPercentageTM dye, the cells were analyzed on a FACScan instrument using CELLQuest PRO software (BD Biosciences). The cell fluorescence was measured by flow cytometry using the FL2 channel (565 to 605 nm) and a minimum of 10 000 events was acquired per sample. The pro-apoptotic activity induced by individual plant extracts are presented on Figure 3.2, 3.3 and 3.4 (in red) that represent the MCF7, HeLa, and CHO cell lines respectively.

The aqueous extract of *C. africanum* and *E. rhinocerotis* display noteworthy pro-apoptotic activity (above 40 %) in relation to the extracts of the other seven plants that display pro-apoptotic activity below 10% in the breast cancer cell line (MCF7) results presented in figure 3.2. The apoptosis induction by *C. orbiculata* were negligible, even at lower concentrations such as 312.5 µg/ml, 156.25 µg/ml and 78.13 µg/ml (results not shown), thus cell death may be an effect of necrosis. The aqueous extract of *H. pubescens* and *E. rhinocerotis* displayed the highest pro-apoptotic activity (above 40 %) in the cervical cancer cell line (HeLa) results presented in figure 3.3. Thus, *H. pubescens* is the only extract that induced cell death as a consequence of apoptosis in the HeLa cell line, as opposed to *C. capensis*, *E. mauritanica*, *C. africanum* and *C. orbiculata* that may be inducing cell death as a consequence of necrosis. *E. rhinocerotis* induced pro-apoptotic activity with negligible cytotoxicity. The aqueous extracts of *E. mauritanica*, *C. africanum*, *L. frutescens* and *E. rhinocerotis* displayed pro-apoptotic activity (above 40 %) in

relation to the extracts of the other five plants in the non-cancerous cell line (CHO) results presented in figure 3.4.

The results for the CHO cell line proved that the cytotoxicity test is not reliable as the extracts of *E. mauritanica*, *C. africanum*, *L. frutescens* and *E. rhinocerotis* displays considerable pro-apoptotic activity but negligible cytotoxicity indicating that these plants would have been unduly eliminated in the screening process. The pro-apoptotic activity of the nine plants at 5 mg/ml on all three cell lines were further tabulated to provide a concise visual representation of results for easy interpretation (see table 3.3). *C. africanum*, *L. frutescens* and *E. rhinocerotis* extracts induce the highest degree of apoptosis for the CHO cell line. Also, the CHO cell line displays the highest degree of susceptibility to the nine plant extracts, as opposed to MCF7 that displays the least sensitivity. This is to be expected as the CHO cell line is a so called 'normal' animal cell line that should not have mutations rendering it less resistant to apoptosis inducers. Also, MCF7 has been characterized with caspase-3 gene mutation (Kurokawa *et al.*, 1999). From the extensive coverage of the most common pathways in section 1.3.4 it can be inferred that most of the pathways commonly converge at caspase-3. This highlights the reason why the presence of caspase-3 is recognized as a hallmark of apoptosis and accounts for the high resistance to apoptosis inducers displayed by the MCF7 cell line. *C. africanum* and *E. rhinocerotis* extracts display the highest degree of activity in the MCF7 cell line. It can thus be deduced that the *C. africanum* and *E. rhinocerotis* extracts can induce an apoptosis pathway independent of caspase-3. *H. pubescens*, *L. frutescens* and *E. rhinocerotis* extracts are the most active apoptosis inducers for the HeLa cell line. The HeLa cell line may be more

resistant to apoptosis inducers as a consequence of being infected with the human papillomavirus (HPV) that synthesizes the protein products E6 and E7. The E6 and E7 proteins bind to and inhibit p53 and Rb, thus increasing the HeLa cell line resistance to apoptosis pathways involving these genes (Phelps *et al.*, 1991; Scheffner *et al.*, 1991).

Table 3.3. Apoptosis activity induced by the nine indigenous South African plants at 5 mg/ml.

Plants	Apoptosis (%)		
	CHO	MCF7	HeLa
<i>C. capensis</i>	42	6	37
<i>E. mauritanica</i>	53	10	31
<i>H. pubescens</i>	34	6	43
<i>C. africanum</i>	71	43	34
<i>L. frutescens</i>	71	8	41
<i>C. orbiculata</i>	34	7	34
<i>E. plantagineum</i>	24	6	30
<i>O. pes caprae</i>	31	6	31
<i>E. rhinocerotis</i>	71	50	43

The purpose of this section is to identify a lead compound that would be subjected to combinatorial chemistry techniques after characterization to develop a future site specific non-toxic anti-cancer drug. Thus, *E. rhinocerotis* aqueous extract that induced considerable pro-apoptotic activity across all the cell lines was tested for specific hallmarks of apoptosis and active compounds from it will be purified and characterized.

3.4) Screening *E. rhinocerotis* aqueous extract for the ability to induce specific markers of apoptosis

3.4.1) Externalization of phosphatidylserine (PS)

The characteristic externalization of the phosphatidylserine (PS) is a prominent marker of apoptosis. Annexin V-PE Apoptosis Detection assay allows for the detection and quantification of the externalized phosphatidylserine (PS) by FACS analysis. The Annexin V-PE Detection assay is based on the principle that annexin V, the 35-36 kDa Ca^{2+} dependent phospholipid binding protein, has a strong affinity for PS. Annexin V can also be conjugated to fluorochromes such as Phycoerythrin (PE) without affecting its affinity for PS, thus making annexin V-PE a sensitive probe for apoptosis detection. Externalized PS will thus be fluorescently labeled by annexin V-PE (Vermees *et al.*, 1995). Results can be acquired and analyzed in the form of a histogram or dot plot. For the results obtained in histogram form, normal cells will fluoresce in the first decade (10^1), whilst a fluorescent shift along the x-axis from the first decade (10^1) to the second decade (10^2) or third decade (10^3) is expected for apoptotic cells.

CHO cells were plated in 24 well tissue culture plates as described in section 2.5.3. The cells were treated with aqueous extracts from *E. rhinocerotis* and known apoptosis inducers *L. frutescens* and staurosporine, stained with annexin V-PE and analyzed on a FACScan instrument using CELLQuest PRO software (BD

Biosciences). The cell fluorescence was measured by flow cytometry using the FL2 channel (565 to 605 nm) and a minimum of 10 000 events was acquired per sample.

Less than 2 % of the cells were stained positive for externalized phosphatidylserine in the untreated control presented as figure 3.5A. However, as much as 78 % of the cells were stained positive for externalized phosphatidylserine in cell treated for 1 hour with 1.3 μ M staurosporine presented in figure 3.5B. This increase in externalized phosphatidylserine is denoted by the shift of the cell distribution to the right into the second decade (10^2), that is, an increase in the fluorescence of PE. The externalized phosphatidylserine was also demonstrated in figure 3.5C and 3.5D that represents cells that were treated for 6 h with 3.5 mg/ml of *E. rhinocerotis* and *L. frutescens*, respectively. Extracts of *E. rhinocerotis* and *L. frutescens* displayed that 71 % and 93 % of cells stained positive for externalized phosphatidylserine, respectively, compared to the negligible 2 % of the cells in the untreated control. Previous studies have shown that *L. frutescens* contains pro-apoptotic secondary metabolites (Chinkwo, 2005; Tai *et al.*, 2004). These results show that *E. rhinocerotis* also contain secondary metabolites with pro-apoptotic activity.

3.4.2) Caspase-3 activation

Another prominent hallmark of cells undergoing apoptosis is the activation of caspase-3 (reviewed in section 1.3.4). The active Caspase-3 PE Detection assay allows for the detection and quantification of active caspase-3 by FACS analysis (BD Bioscience). This assay is based on the principle that active caspase-3 is recognized

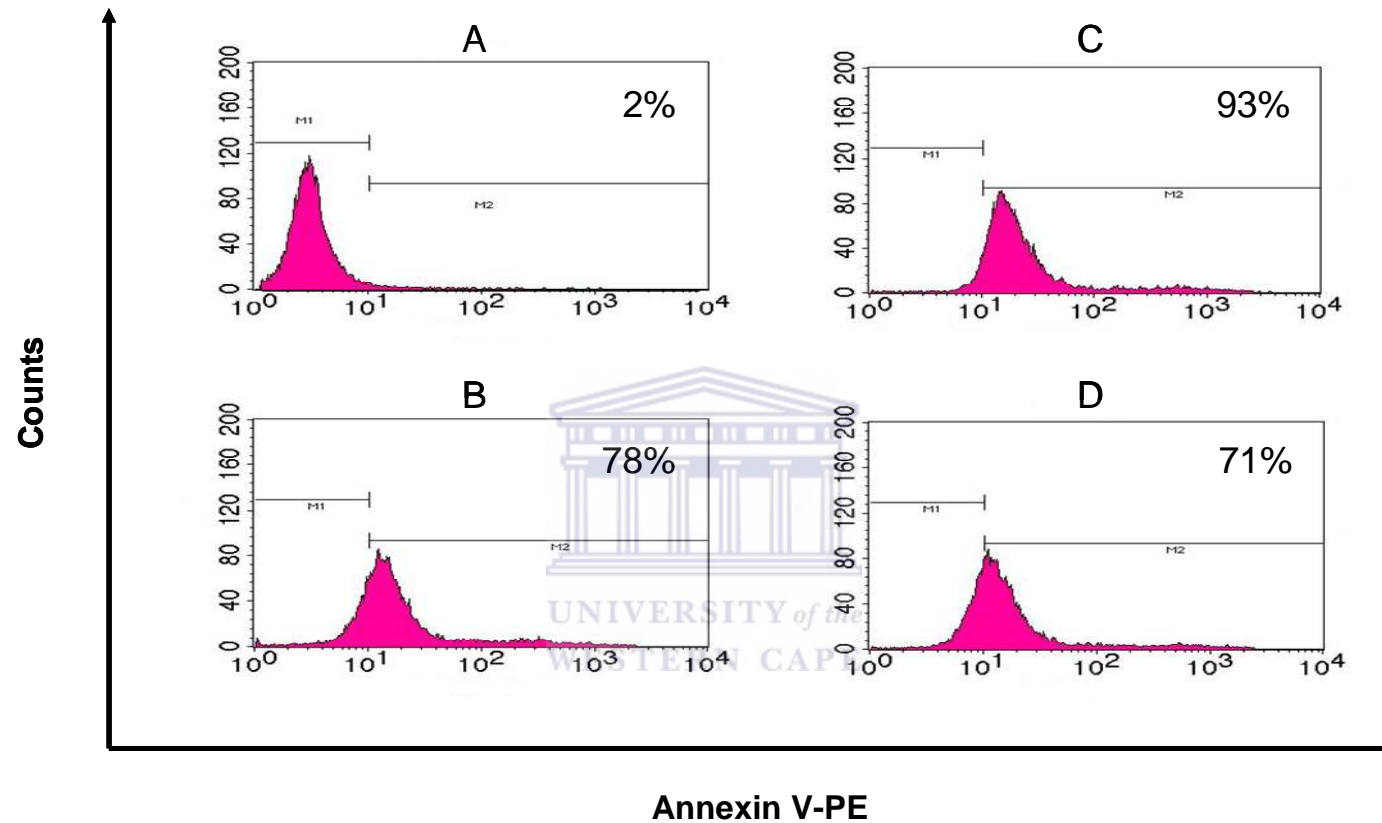


Figure 3.5. Flow cytometry analysis demonstrating the externalization of phosphatidylserine in CHO cells treated for 6 h with 3.5 mg/ml of plant aqueous extract. Experiments were repeated in triplicate. Annexin V- PE Apoptosis Detection assay results are resented in histogram form, denoting the percentage of cells staining positive (in the M2 region) for annexin V. **A** represents the untreated control. **B** represents the positive control (staurosporine). **C** represents the aqueous extract of *L. frutescens*. **D** represents the aqueous extract of *E. rhinocerotis*.

by monoclonal antibodies that were specifically made against the cleaved form of caspase-3. The monoclonal antibodies are conjugated with the fluorochrome PE (Belloc *et al.*, 2000). Consequently, the apoptotic cells that contain active caspase-3 will fluoresce.

Cells were plated in 24-well tissue culture plates as described in section 2.5.4. After cells were treated, permeabilized and stained with PE-conjugated polyclonal active caspase-3 antibody, the cells were analyzed on a FACScan instrument. Less than 2 % of the cells were stained positive for active caspase-3 in the untreated control presented as figure 3.6A. However, a noteworthy 49 % of the cells were stained positive for active caspase-3 in the cell treated for 1 h with 1.3 μ M staurosporine. This increase in active caspase-3 is denoted by the shift of the cell distribution to the right into the second decade (10^2), that is, an increase in the fluorescence of PE. The externalized phosphatidylserine was also demonstrated in figure 3.6C and 3.6D that represents cells treated for 6 h with 3.5 mg/ml of *E. rhinocerotis* and *L. frutescens*, respectively. *E. rhinocerotis* and *L. frutescens* displayed 50 % and 60 % of cells stained positive for active caspase-3, respectively, compared to 2 % of the cells in the untreated cells. These results clearly show that the secondary metabolites from *E. rhinocerotis* induce the activation of caspase-3. In section 3.3 it was demonstrated that *E. rhinocerotis* induces apoptosis activity in the MCF7 cell line that has been documented to have caspase-3 gene mutation (Kurokawa *et al.*, 1999), indicating that the secondary metabolites in this extract are inducing both caspase dependent and caspase independent pathways.

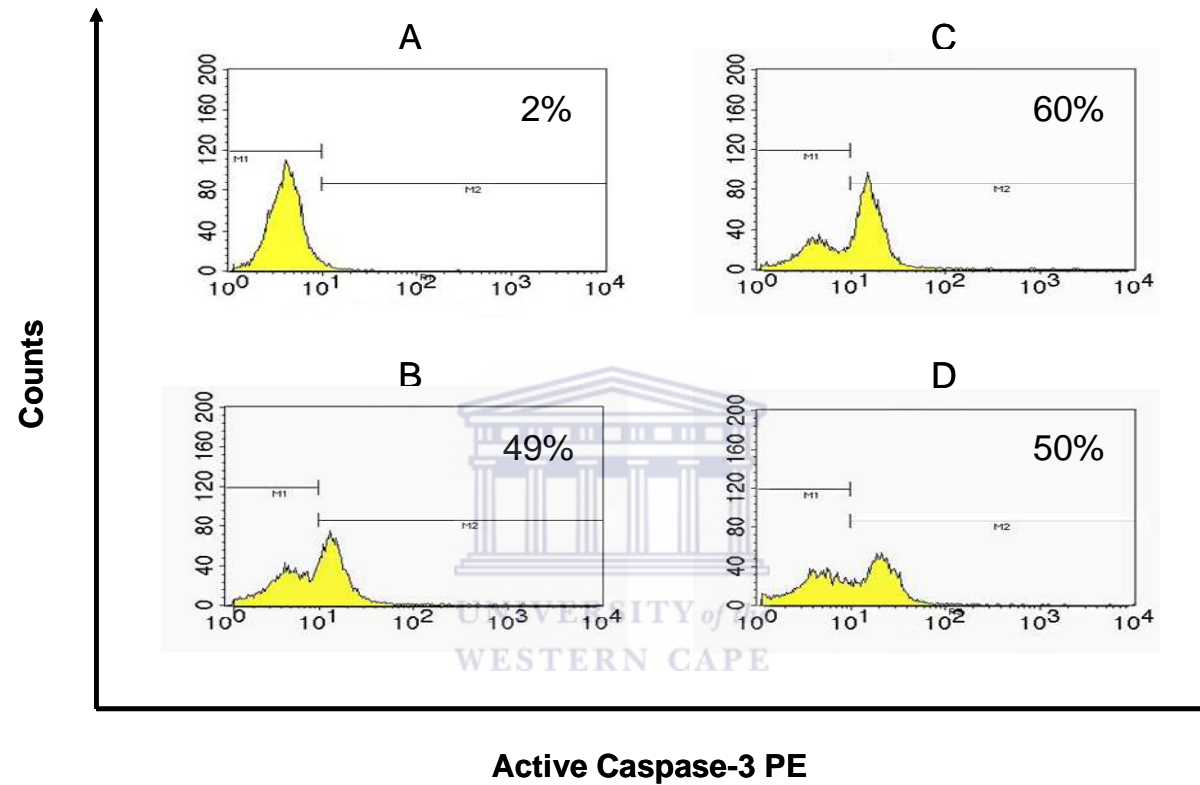


Figure 3.6. Flow cytometry analysis demonstrating the presence of active caspase-3 in CHO cells treated for 6 h with 3.5 mg/ml of plant aqueous extract. Experiments were repeated in triplicate. Active caspases-3 PE Detection assay results are presented in histogram form, denoting the percentage of cells staining positive (in the M2 region) for active caspases-3. **A** represents the untreated control. **B** represents the positive control (staurosporine). **C** represents the aqueous extract of *L. frutescens*. **D** represents the aqueous extract of *E. rhinocerotis*.

3.4.3) DNA fragmentation

The fragmentation of the genomic DNA is a late event during apoptosis. DNA fragmentation is a result of active caspase-3 mediated cleavage of ICAD to activate CAD which is responsible for the fragmentation of the DNA (Sakahira *et al.*, 1998; Zhao *et al.*, 2001). The APO-DIRECT™ Kit allows for the detection and quantification of DNA breaks by FACS analysis. The result of DNA fragmentation during apoptosis is the exposure of a multitude of 3'-hydroxyl termini. This characteristic can be used to differentiate apoptotic cells from viable cells by labeling the DNA breaks with fluorescein isothiocyanate-tagged deoxyuridine triphosphate nucleotides (FITC-dUTP). The enzyme terminal deoxynucleotidyl transferase (TdT) catalyzes a template-independent addition of deoxyribonucleoside triphosphates to the 3' hydroxyl ends of double- or single-stranded DNA (Eschenfeldt and Berger, 1987). Results has been acquired and analyzed in the form of a histogram or dot plot. For the results obtained in histogram format, viable cells fluoresce within the first decade (10^0 - 10^1), whilst apoptotic cells shifts beyond 10^1 . For the results obtained as a dot plot, the convention is to display DNA content (Linear Red Fluorescence) on the X-axis and the FITC-dUTP (Log Green Fluorescence) on the Y-axis. Acquisition of the DNA content parameter allows for discrimination between cells in G1 and G2 phase of the cell cycle, since cells in G2 phase will have double the DNA content of cells in G1 phase. When analyzing DNA content of cells it is important that only single cells and not cell doublets or cell clusters are evaluated. To achieve this dual parameter analysis (DNA area signal on the Y-axis and DNA width on the X-axis) is used to exclude DNA doublet events. Single cells will have a defined area and width, while cell doublets and cell clusters will have a much higher area and width. It is

therefore possible to identify the cell doublets and cell clusters and exclude them from the analysis. Once single cells have been identified and gated, these cells are evaluated for FITC-fluorescence. Since only the apoptotic cells are labeled with FITC-dUTP these cells will display increased FITC-fluorescence on the Y-axis.

Cells were plated in 6 well tissue culture plates as described in section 2.5.5. The cells were treated, permeabilized and labelled with F-dUTP using the APO-DIRECT™ staining kit. Cells were analyzed on a FACScan instrument using CELLQuest PRO software. Less than 2 % of the cells stained positive for F-dUTP in the untreated control presented as figure 3.7A. However, 43 % of the cells were stained positive for F-dUTP in the cell treated for 24 h with 1.3 µM staurosporine presented in figure 3.7B. DNA strand breaks were also demonstrated in figure 3.7C and 3.7D that represents cells treated for 48 h with 5 mg/ml of *L. frutescens* and *E. rhinocerotis*, respectively. Extracts of *L. frutescens* and *E. rhinocerotis* respectively induce DNA fragmentation in 86 % and 75 % of the cells, compared to the 2 % of the cells in the untreated cells.

3.3.4) Summary

The aim of this study was to identify plant aqueous extracts with pro-apoptotic activity and therefore also anti-cancer activity. These results demonstrate that not all plant extracts tested in this study have the potential to induce pro-apoptotic activity. Furthermore, it also shows that extracts that are cytotoxic are not necessarily pro-apoptotic, that is, cell death induced by these secondary metabolites may be a consequence of necrotic rather than apoptotic cell death.

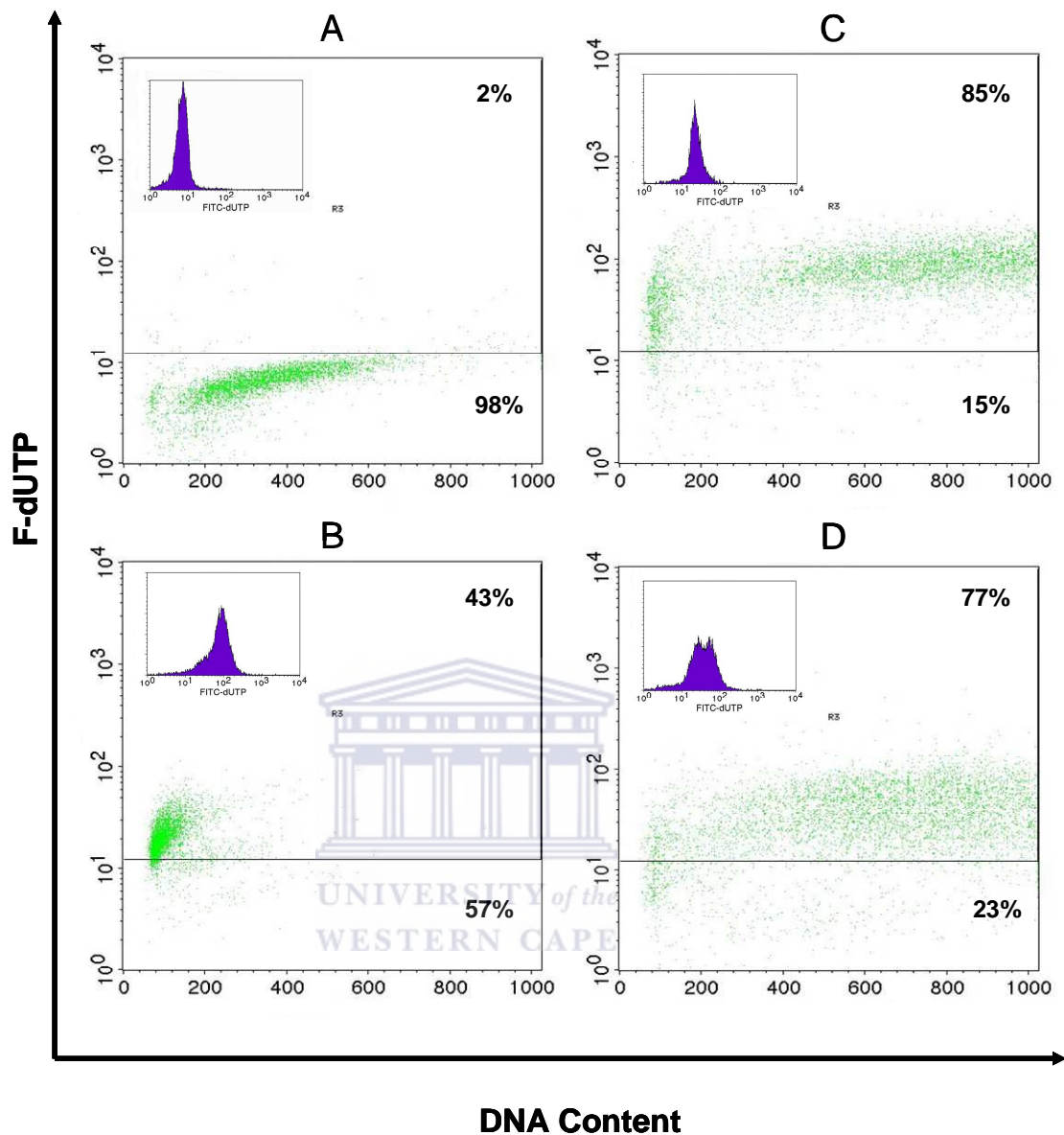


Figure 3.7. Flow cytometric analysis of DNA fragmentation. CHO cells were treated for 48 h with 5 mg/ml of plant aqueous extract. Experiments were repeated in triplicate. As a positive control cells were treated with 1.3 μ M staurosporine. DNA fragmentation results are presented as a dot plot and in histogram form. **A** represents the untreated control. **B** represents the positive control (staurosporine). **C** represents the aqueous extract of *L. frutescens*. **D** represents the aqueous extract of *E. rhinocerotis*.

Extracts from *C. africanum*, *H. pubescens*, *L. frutescens* and *E. rhinocerotis* demonstrated much higher pro-apoptotic activity than the other five plants. Also, the non-cancerous CHO cells were more sensitive to the effects of the plants extracts than the cancer cell lines. This is to be expected, since the CHO is not a transformed cell line, whereas the cancer cell lines have mutations which make these cells less sensitive to apoptosis inducers. *E. rhinocerotis* and *C. africanum* are the only plants that induce apoptosis in the MCF7 cell line that is characterized with caspase-3 gene mutation. This result is notable as most apoptosis inducers require caspase-3 activation. *E. rhinocerotis* extract also displays the ability to induce specific markers of apoptosis in CHO cells such as phosphatidylserine externalization, activation of caspase-3 and DNA fragmentation. This ability of the *E. rhinocerotis* extract to induce activation of caspase-3 in CHO cells and induce apoptosis in the MCF7 cell line that is characterized with caspase-3 gene mutation indicates that this extract has the ability to induce apoptosis via caspase-3 dependent and caspase-3 independent pathways respectively.

E. rhinocerotis was selected for further study as it was the only extract that displayed notable apoptosis activity across all three cell lines. It also induced specific markers of apoptosis and activated more than one apoptosis pathway. This ability to induce more than one apoptosis pathway may also suggest the presence of more than one apoptosis inducer in the crude *E. rhinocerotis* extract.

CHAPTER 4: INVESTIGATING WHETHER THE
VARIATION IN BIOACTIVITY WITHIN THE *E.*
RHINOCEROTIS SPECIES IS ASSOCIATED WITH
GENETIC VARIATION

4.1) Introduction

Previous studies demonstrated that the variation in bioactivity within the same plant species can be linked to seasonal and geographical variation (Yang and Loopstra, 2005). For example, it has been demonstrated that extracts for *L. frutescens* collected from different geographical locations display variation in pro-apoptotic activity (Chinkwo, 2005). The variation in the bioactivity of plant extracts within the same plant species from different geographical locations can be ascribed to the plant chemistry, that is, the difference in the composition of the secondary metabolites present. It is possible those environmental factors can influence plant chemistry or that genetic mutations in the plant can result in genetic variants with different plant chemistry.

Several plant extracts were screened for pro-apoptotic activity. It was concluded in chapter 3 that not all these plant extracts contain pro-apoptotic activity. Also, *E. rhinocerotis* exhibited the most significant apoptosis activity across all the cell lines screened. Therefore, the aim of this section was to compare the bioactivity of *E. rhinocerotis* samples collected from different geographical locations and to determine

if there is any genetic variance in this *E. rhinocerotis* samples collected from the different geographical locations that may account for the variation in pro-apoptotic activity.

The genetic variation between plants can be illustrated by the construction of phylogenetic tree based on the conservation or slow evolution of particular genes across species (Alvarez and Wendel, 2003). Phylogenetic relationships among congeneric species and closely related genera in Asteraceae have been elucidated by DNA sequence analysis of the internal transcribed spacer (ITS) of nuclear ribosomal DNA (nrDNA) (Samuel *et al.*, 2003). This study by demonstrates that the phylogenetic analysis based on the ITS regions provide higher resolution compared to the phylogenetic analysis based on the maternally inherited *trnL* intron, *trnL/F* spacer, and *matK* sequence (Samuel *et al.*, 2003). To date only the *trnL/F* spacer of *E. rhinocerotis* has been sequenced for phylogenetic studies; at the Australian National University, Division of Botany and Zoology (Bayer *et al.*, 2000).

The degree of pro-apoptotic activity present in *E. rhinocerotis* from different geographical locations was determined by the APOPercentageTM assay. The investigation into the presence of genetic variance was determined by the amplification of the ITS1 region using the universal primers ITS5 and ITS2 (White *et al.*, 1990).

4.2) Pro-apoptotic activity of *E. rhinocerotis* from different geographical location

E. rhinocerotis was collected from various places in the Western Cape, namely Blaauwberg, Helderberg, Tygerberg, Kirstenbosch and Tulbagh. Aqueous extractions of these plants were performed as described in section 2.7.1. CHO cells were plated in 24-well tissue culture plates as described in section 2.5.2. The cells were treated with 5 mg/ml aqueous extract for 24 h. After the cells were treated and stained with APOPercentage™ dye, the cells were analyzed on a FACScan instrument. The results were plotted as a bar graph with the apoptosis activity on the Y-axis and the fractions on the X-axis.

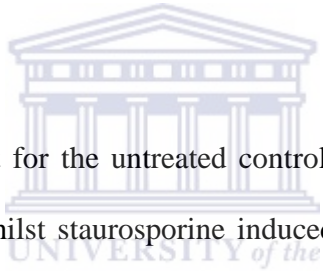


[Figure 4.1](#) illustrated that for the untreated control less than 2 % of the cells were positive for apoptosis, whilst staurosporine induced apoptosis in 78 % of the cells. The fractions from Blaauwberg, Helderberg, Tygerberg, Tulbagh and Kirstenbosch induced apoptosis in 42 %, 57 %, 51 %, 71 % and 7 % of the cells, respectively. This results show that there was a notable variance (7% to 71%) in the bioactivity of *E. rhinocerotis* collected from the different geographical locations. The extract from the plant material collected from Kirstenbosch showed the lowest activity, whilst the extract from the plant material collected from Tulbagh showed the highest pro-apoptotic activity.

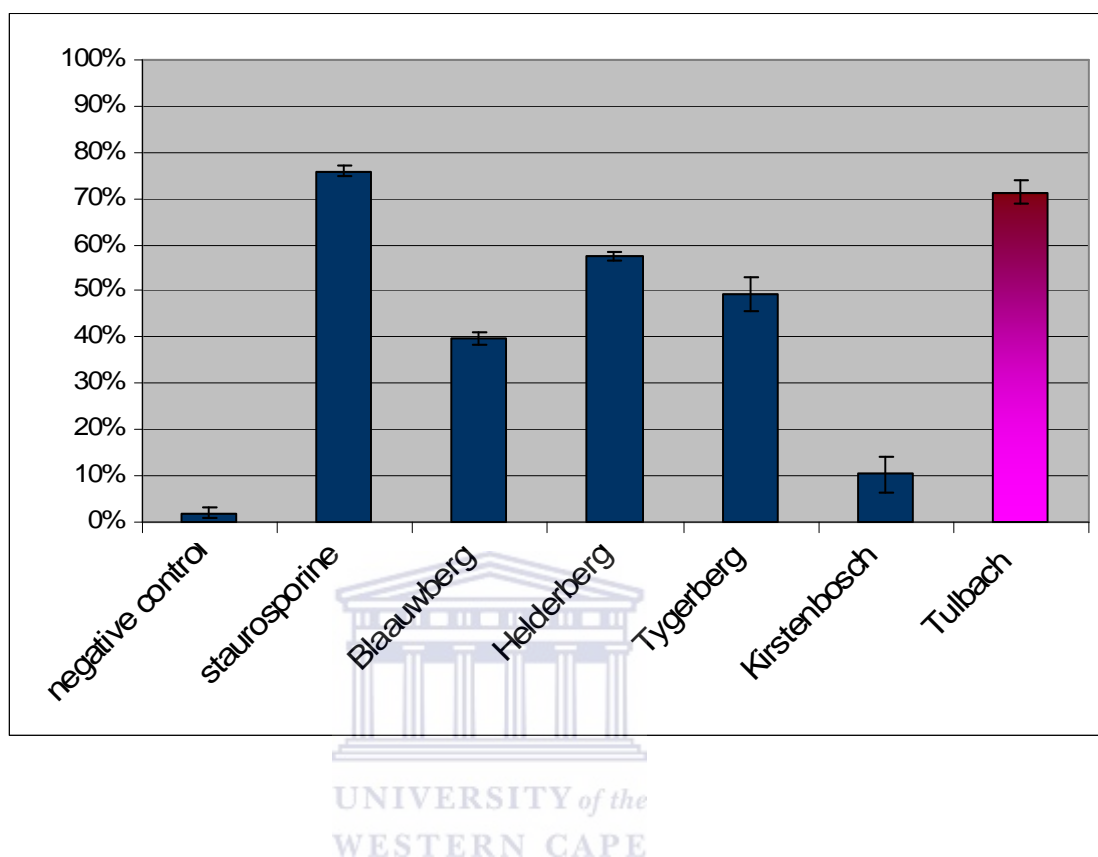


Figure 4.1 Flow cytometric analysis of the *E. rhinocerotis* extracts from different geographical locations by APOpercentageTM staining. CHO cells were treated for 24 h with 5 mg/ml of *E. rhinocerotis* collected from different geographical locations. Experiments were repeated in triplicate. As a positive control cells were treated with 1.3 μ M staurosporine. The results were plotted on a bar graph with apoptosis activity on the Y-axis and the *E. rhinocerotis* extracts on the X-axis. The reddish-pink bar indicates the fraction that displayed the highest pro-apoptotic activity.

4.3) Genetic study

4.3.1) Cloning ITS1 into pGEM[®]-T Easy vector

The gDNA of *E. rhinocerotis* collected from Blaauwberg, Helderberg, Tygerberg, Kirstenbosch and Tulbagh were extracted as described in section 2.6.1. The extracted gDNA was electrophoresed on an agarose gel to assess the quality of the DNA. [Figure 4.2](#) illustrated that all the samples had high molecular weight intact fragment.

ITS1 was amplified by PCR using the forward primer ITS5 and reverse primer ITS2 as described in section 2.6.2. The amplification of ITS1 was verified by agarose gel electrophoresis. [Figure 4.3](#) showed the PCR amplification of ITS1. The negative control displayed no traces of contaminating DNA. For each DNA sample (representing the different geographical locations) a single fragment of ± 370 bp was amplified.

The PCR products were purified as described in section 2.6.4. The purified ITS1 products were cloned into pGEM-T easy vector as described in section 2.6.5. The transformed colonies were screened for the presence of the insert as described in section 2.6.6. [Figure 4.4](#) showed the colony PCR screen for the presence of the ITS1 insert. The negative control displayed no traces of contaminating DNA. For each geographical location, four single colonies were screened. Figure 4.4 shows that all the colonies screened were positive for the presence of the ITS1 fragment. As expected the PCR products were bigger than the original ITS1 fragment, since M13

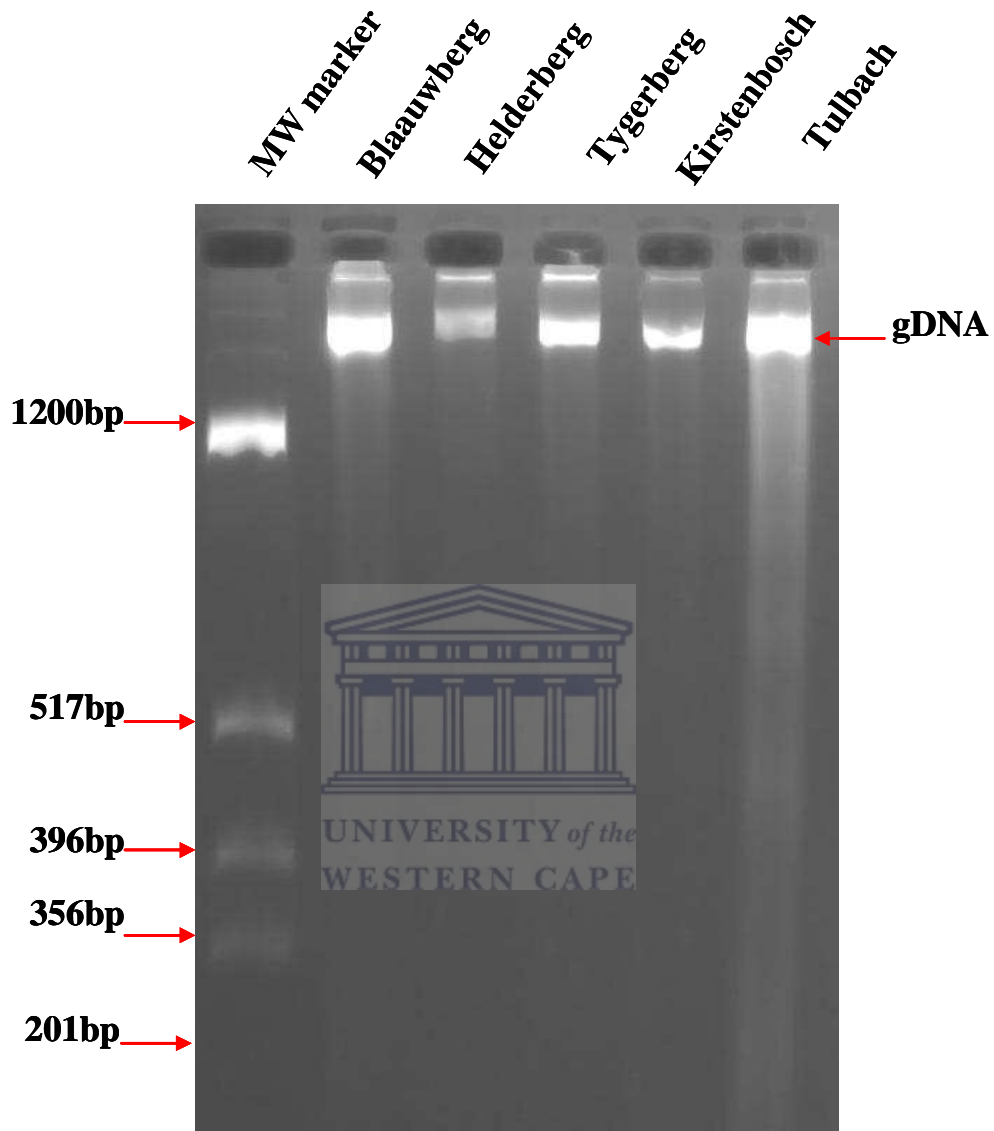


Figure 4.2 Agarose gel electrophoretic representation of the gDNA extracted from the *E. rhinocerotis* plants collected from different geographical locations. The gDNA extracted are indicated on the figure.

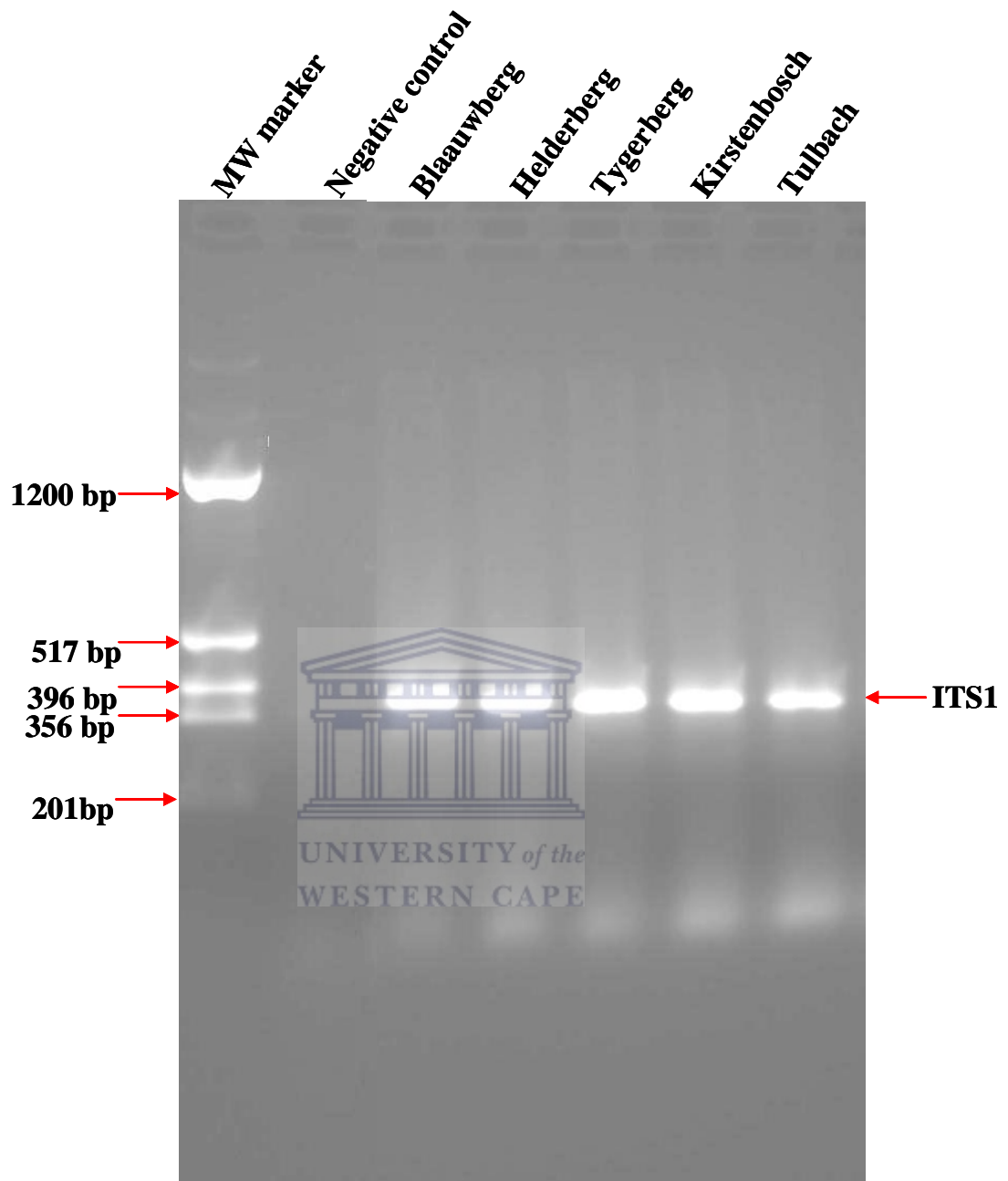


Figure 4.3 PCR screening for the presence of the ITS1 sequence of *E. rhinocerotis* plants collected from different geographical locations. The amplified ITS1 sequences are indicated on the figure.

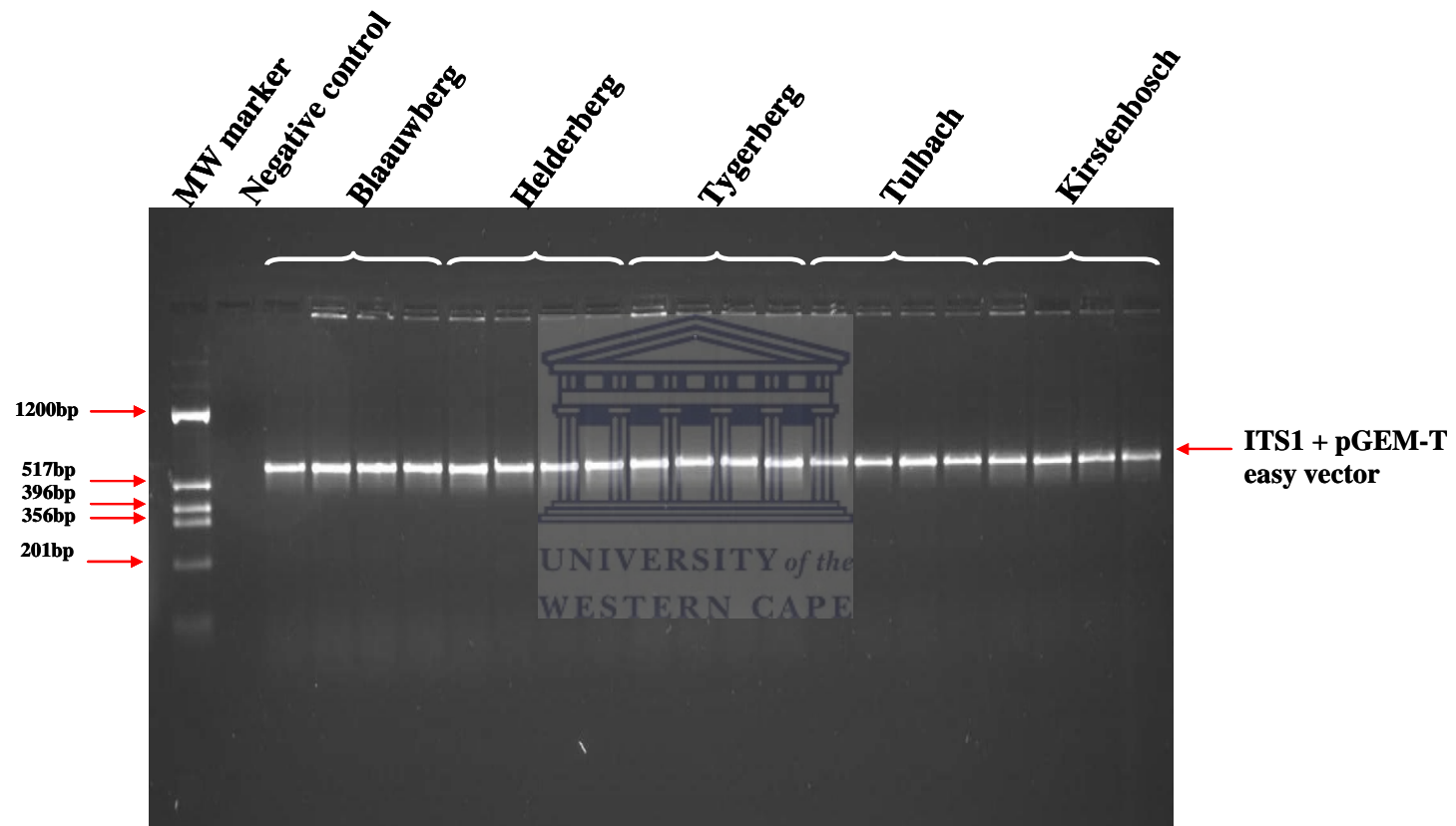


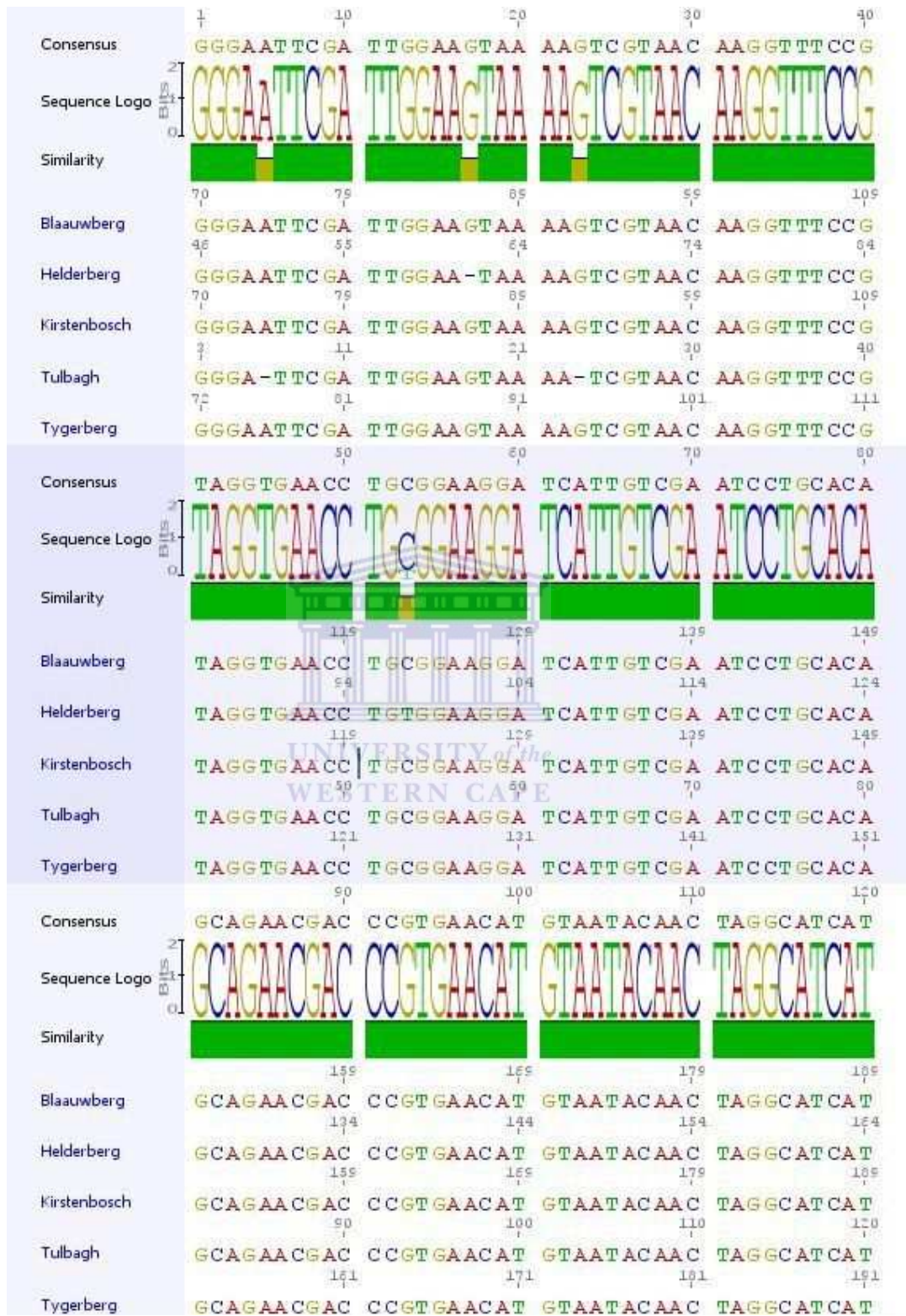
Figure 4.4 Colony PCR screening for the presence of the ITS1 sequence of *E. rhinocerotis* plants collected from different geographical locations. Four random colonies were screened from each geographical location. The different geographical locations are indicated on the figure.

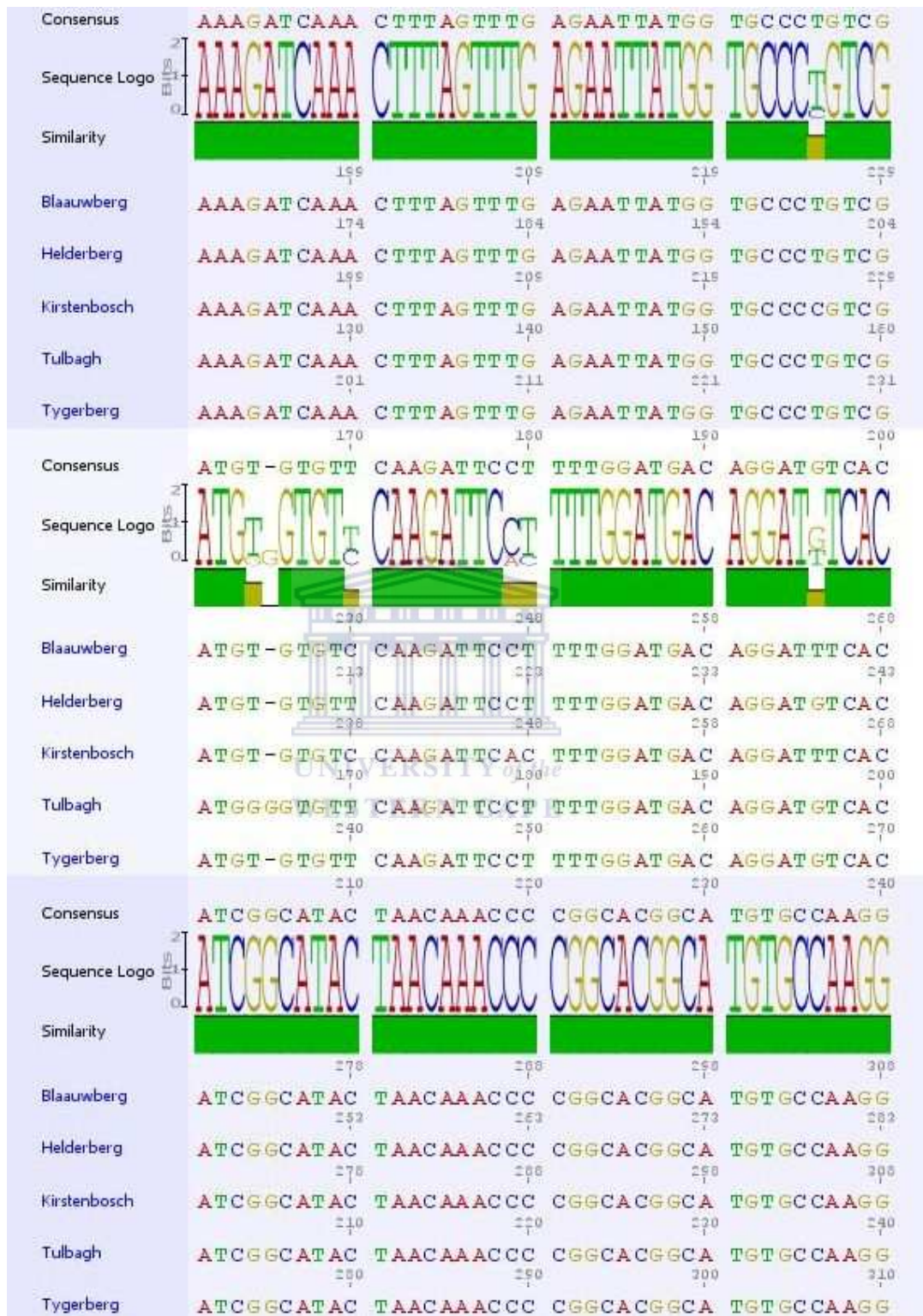
primers were used for the colony PCR screen. Glycerol stocks of the positive clones were prepared. These positive PCR clones were also sequenced by Inqaba Biotechnical Industries (Pty) Ltd. For each plant one colony was selected and sequenced in both the forward (5' to 3') and reverse (3' to 5') orientation.

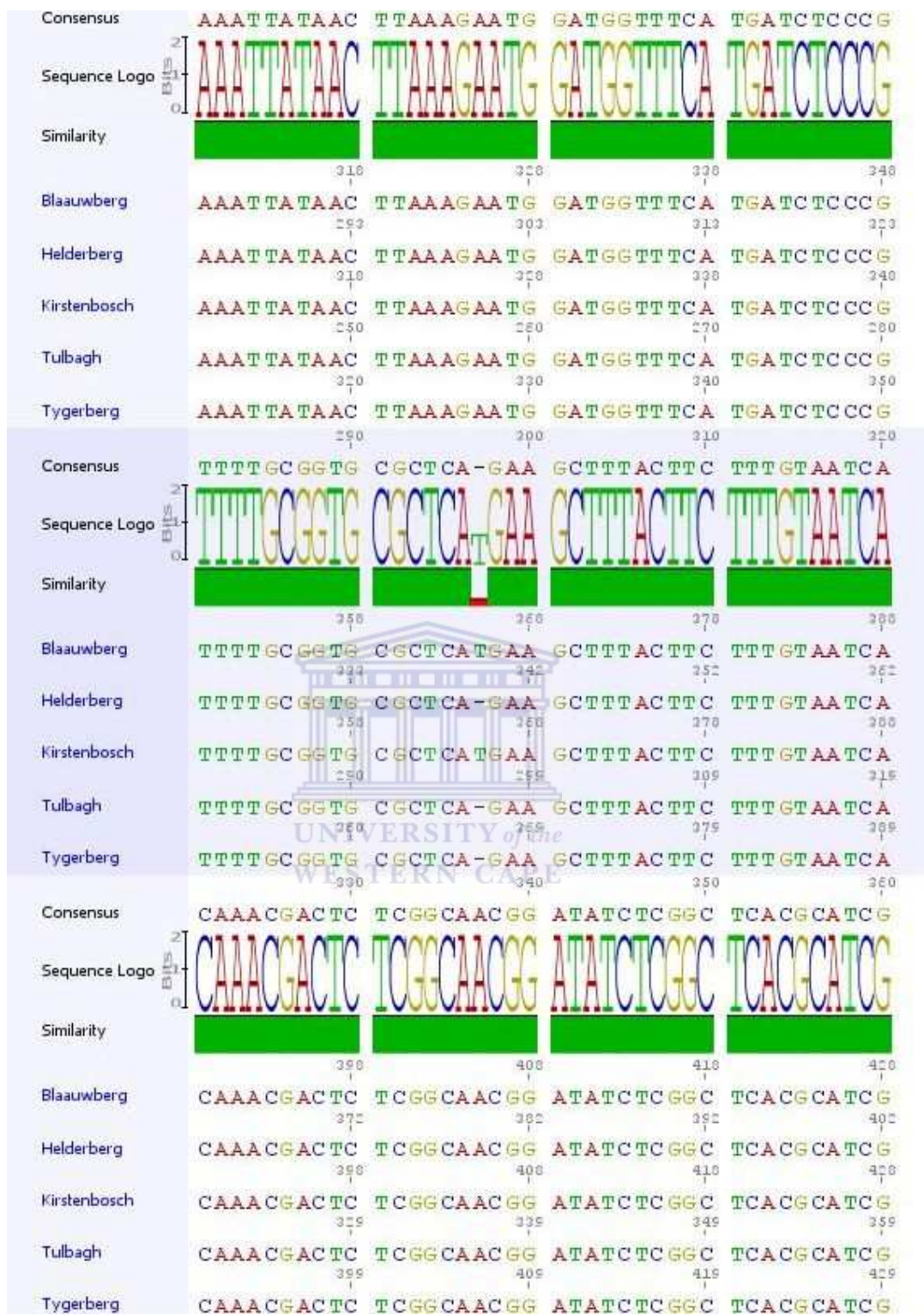
4.3.2) Phylogenetic analysis of ITS1

The ITS1 sequences were aligned with the sequencing alignment programme, ClustalX. [Figure 4.5](#) shows the aligned sequences from the different geographical locations. Alignment homology ranged between 100 % and 98 %. Single nucleotide polymorphisms (SNP) were found at position 156 (T/C), 179 (C/A), 180 (T/C), 196 (G/T) and 297 insT for the Kirstenbosch sequence. Also, a SNP was found at position 170 (T/C) and 297 insT for the Blaauwberg sequence and a SNP was found at position 52 (C/T) and a deletion was found at positions 17 delG and 390 delT for the Helderberg sequence. Deletions were also found at positions 5 delA, 23 delG, 390 delT.

Sequences that are homologous to the five ITS1 sequences were retrieved using BLAST. The homologous sequences retrieved were all members of the Asteraceae family. These homologous sequences and the five ITS1 sequences were re-aligned using Geneious software. A phylogenetic tree of the re-aligned data was constructed using Geneious software with 1000 bootstrapping and the Jukes Cantor genetic distance model by Neighbor-Joining method. [Figure 4.6](#) shows the phylogenetic tree of the re-aligned sequences. The phylogenetic tree indicates that there are basically 5







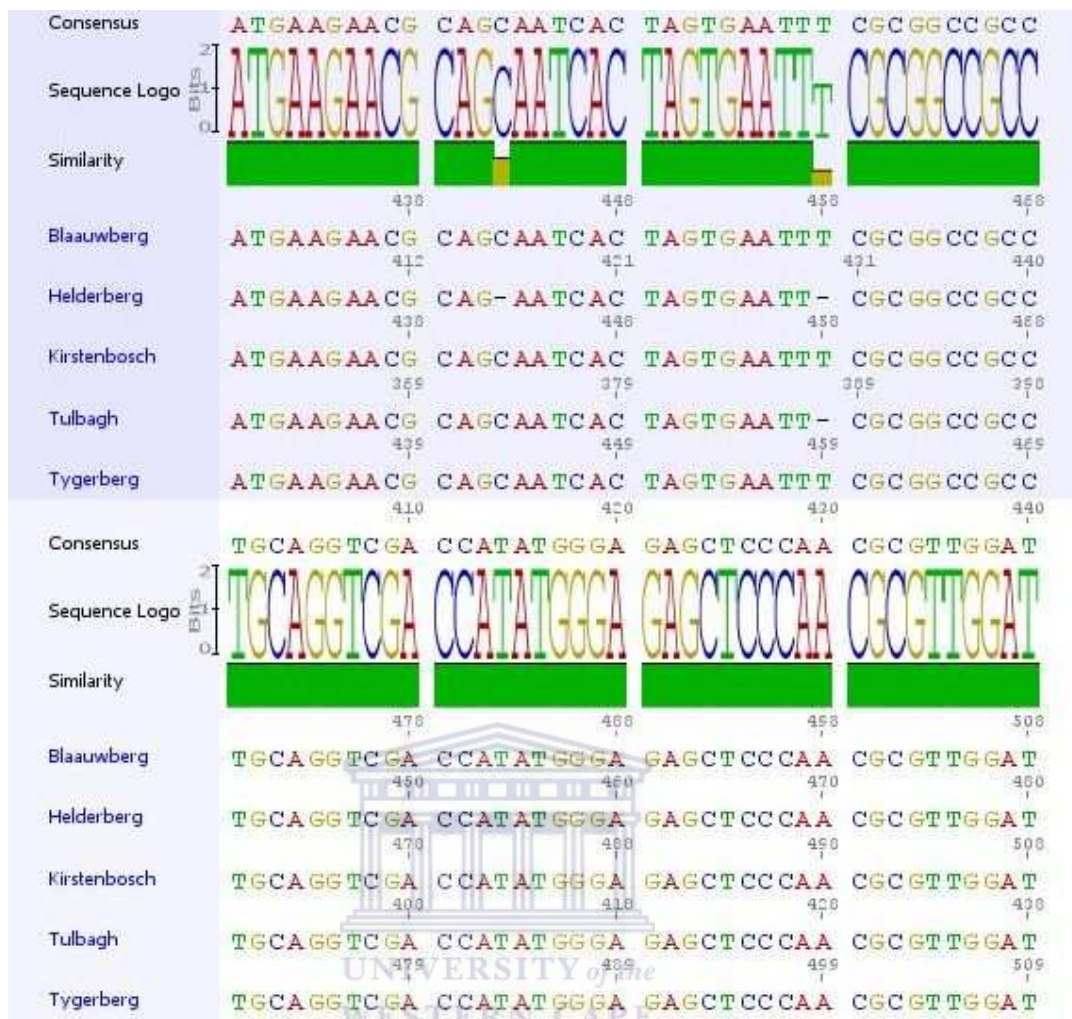


Figure 4.5 Sequence alignment of the ITS1 sequences of the *E. rhinocerotis* plants collected from different geographical locations. Dissimilarities are indicated by the colour () break in the green similarity sequence.

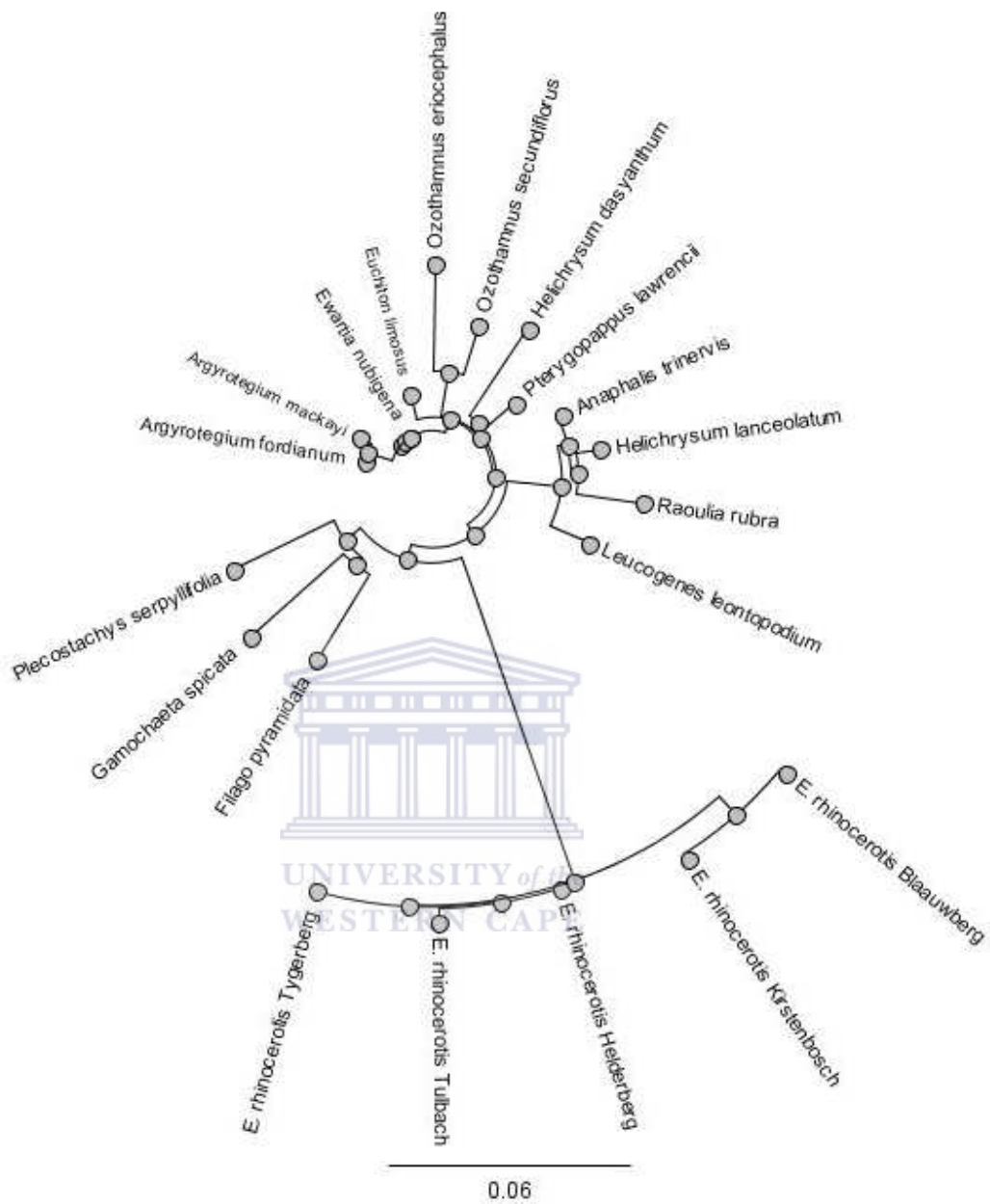
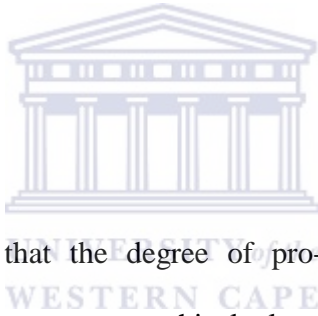


Figure 4.6 Phylogenetic tree of the aligned ITS1 sequences of the *E. rhinocerotis* plants collected from different geographical locations and homologous sequences that were retrieved using Blastn. The different geographical locations are Helderberg, Tygerberg, Blaauwberg, Kirstenbosch and Tulbagh.

groups emerging from the root. Of the homologous sequences generated by BLAST, *P. serpyllifolia* is most similar to the *E. rhinocerotis* consensus sequence.

Also, the *E. rhinocerotis* sequences representing the different geographical locations are diverging at different times, which highlighting their genetic variance. The Tulbagh sequence is most analogous to the root sequence, trailed by the Tygerberg sequence, the Helderberg and Blaauwberg sequence. The Blaauwberg sequence and the Kirstenbosch sequence diverge at the same time point. The variation in ITS1 sequences in the same species is very significant. Thus, this preliminary data suggest genetic variation.

4.4) Summary



It has been established that the degree of pro-apoptotic activity present in *E. rhinocerotis* from different geographical locations differ significantly. The Kirstenbosch extract displays the least activity (7%), whilst the Tulbagh extract displays the most activity (71%). If this variation in pro-apoptotic activity correlates to the genetic variation, it propagates that a link may exist as genetic variation is responsible for differences in plant chemistry.

The ITS1 sequence was successfully amplified with the universal primers ITS5 and ITS2; and cloned into the pGEM-T easy vector for sequencing. The sequence alignment displayed 100 % to 98 % homology, which denotes significant variation in the same species. When comparing the genetic variation of the ITS1 sequences with

their corresponding levels of apoptosis activity that is; Tulbagh (71%), Tygerberg (57%), Helderberg (51%), Blaauwberg (42%) and Kirstenbosch (7%); a pattern emerges; the degree of pro-apoptotic activity decreases, the more the sequence deviates from the root sequence. This preliminary data suggest a link between the genetic variation and pro-apoptotic activity. However, the difference in genetic variation highlights the possibility that the difference may be as a consequence of subspecies variation. Also, more than one colony should be sequenced from each colony PCR plate to ensure accuracy and a larger sample it required, along with other *Elytropappus* species to establish statistical significance.



CHAPTER 5: THE PARTIAL PURIFICATION OF THE
PRO-APOPTOTIC SECONDARY METABOLITE/S
ISOLATED FROM *E. RHINOCEROTIS*

5.1) Introduction

In chapter 4 it was concluded that the aqueous extract of *E. rhinocerotis* collected from Tulbagh contains a secondary metabolite(s) with pro-apoptotic activity. Therefore, the aim of this section was to isolate and characterize this compound(s). Bio-activity guided fractionation was used to trace the isolation of the pro-apoptotic metabolite(s). Fractionation involves the separation of a mixture of metabolites based on their molecular structures and intermolecular forces (Robards *et al.*, 2002). Examples of separation technology that use these principles to separate molecules are; organic extraction, Liquid Column Chromatography (LCC), Thin Layer Chromatography (TLC) and High Performance Liquid Chromatography (HPLC). At each fractionation step bio-assays were used to identify the fraction containing the highest activity and therefore the secondary metabolite(s) of interest (Sezik *et al.*, 2005; Wu *et al.*, 2003).

Purification of secondary metabolites from plant extracts can be an expensive and time consuming process that requires the consideration of many possible problem areas to ensure its success. For example; it is possible that the bio-activity observed in total extracts, is as a consequence of multiple metabolites acting in a synergistic

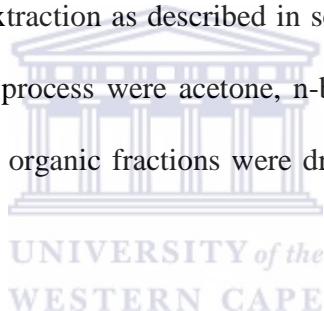
fashion. The separation of such secondary metabolites by fractionation will result in reduced or lost bio-activity. Furthermore it is expected, that a portion of the secondary metabolites of interest will be sacrificed during the fractionation process. To maintain a reasonable level of purity, only the fraction with the highest activity will be further processed. The less active fractions can be reprocessed to recover more active material, but these fractions, also contain other non-bioactive secondary metabolites/'impurities' that may be re-introduced into the more active fraction. The purity of the active, unknown secondary metabolite is of paramount importance as the 99 % pure product may not be responsible for the major activity but rather the 1 % of 'impurity'. This is highly probable especially if the 'impurity' is an analog of the major secondary metabolite. This dilemma may be bypassed by using synthetic chemistry to produce an array of analogs of the major secondary metabolite that can be screened comparatively for apoptosis activity and consequently the analog responsible for the major activity can be identified. It must also be noted that NMR and X-ray crystallography requires at least 95 % and 99 % purity, respectively (Cannell, 1998). NMR and X-ray crystallography also require a specific yield of 'pure' compound for structure determination. The yield obtained at the end of the fractionation process may be insufficient for NMR or X-Ray analysis. This problem can be circumnavigated by starting the isolation process with a higher yield of total extract.

5.2) Organic extraction used to fractionate the aqueous extract from *E.*

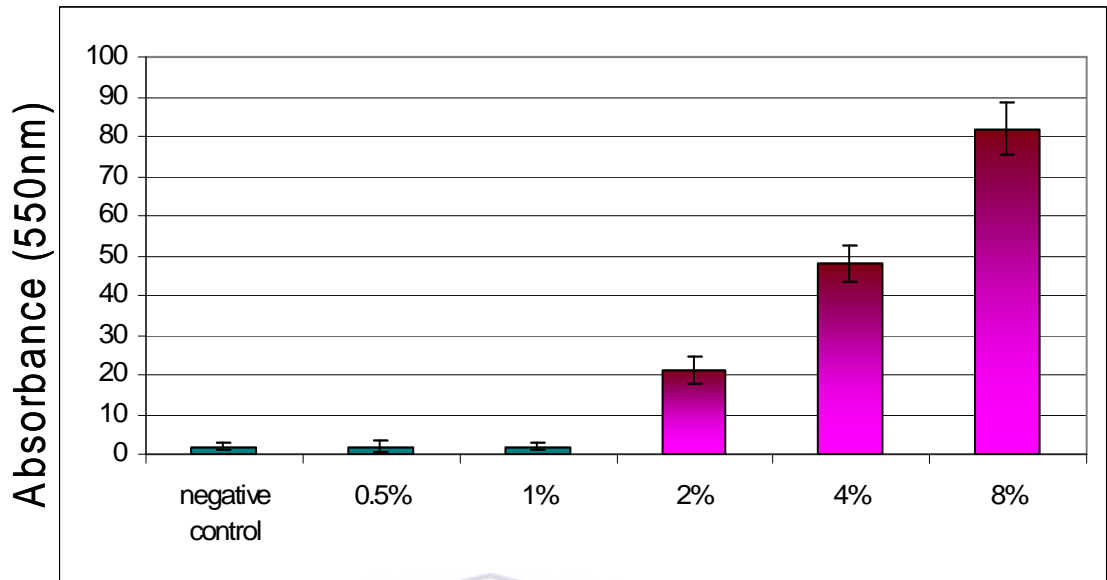
rhinocerotis

The wide array of secondary metabolites extracted by aqueous extraction, provide a platform from which the secondary metabolites can be fractionated or separated by organic extraction. In principle, organic extraction separate secondary metabolites based on increasing polarity (Ohno *et al.*, 2005).

An aqueous extract of 1 kg dried plant material was prepared. The aqueous extraction yielded 2 000 ml extract at 40 mg/ml. The 2 000 ml aqueous extract was fractionated by organic extraction as described in section 2.7.2. The solvents used in the organic fractionation process were acetone, n-butanol, ethyl acetate, chloroform and petroleum ether. The organic fractions were dried by rotary evaporation and re-dissolved in methanol.



Methanol is toxic to cells. Hence, a methanol dose response was used to determine the minimum methanol concentration that would not affect the cells. Cells were plated in 96-well tissue culture plates and exposed to methanol with concentrations ranging between 0.5 % and 8 % for 48 h. After the cells were treated and stained with APOPercentageTM dye, the trapped dye was released from the cells and quantified by colorimetric measurement. The results were plotted as a bar graph with absorbance at 550 nm on the Y-axis and the percentage methanol on the X-axis. [Figure 5.1](#) shows that methanol concentrations of up to 1 % did not induce apoptosis. At these concentrations no morphological changes were observed. Methanol concentrations



Percentage Methanol

Figure 5.1. Flow cytometric analysis of the effects of methanol using the APOPercentage™ assay. CHO cells were treated for 48 h with 0.5 %, 1 %, 2 %, 4 % and 8 % methanol. As a positive control, cells were treated with 1.3 μ M staurosporine. The experiment was repeated in triplicate. The results were plotted on a bar graph with apoptosis activity on the Y-axis and the concentration of methanol on the X-axis. The reddish-pink bar indicates the fractions that displayed the highest pro-apoptotic activity.

between 2 % and 8 % caused changes in cell shape and size which were accompanied by increased levels of apoptosis. This result shows that the methanol concentration of 0.5 % will not have any adverse affects on the cells. Hence, in subsequent experiments the final methanol concentrations were maintained below 0.5 %.

The organic extracts were prepared at 40 mg/ml dissolved in 10% methanol. Cells were plated in 24-well tissue culture plates as described in section 2.5.2 and treated with 2 mg/ml of each fraction for 24 h. As a positive control, cells were treated with 1.3 μ M staurosporine for 1 h. Following treatment, cells were stained with APOPercentageTM dye and analyzed on a FACScan instrument. The results were plotted as a bar graph with the apoptosis activity on the Y-axis and the fractions on the X-axis. [Figure 5.2](#) shows that no significant levels of apoptosis activity were detected for the untreated and methanol controls. However, 78 % of the cells treated with staurosporine stained positive for apoptosis, whilst the chloroform, *n*-butanol, ethyl acetate, petroleum ether, and the remaining aqueous fraction induced apoptosis in 52 %, 60 %, 11 %, 20 % and 12 % of the cells, respectively. The chloroform and *n*-butanol fractions demonstrated notable apoptosis activity. The *n*-butanol (nB) fraction was selected for further fractionation by LCC.

5.3) Chromatography

Chromatography comprises of two phases; the stationary phase and the mobile phase. The extract to be fractionated is bound to the stationary phase to which a continuous mobile phase is supplied. This allows for the separation of the extract into discrete

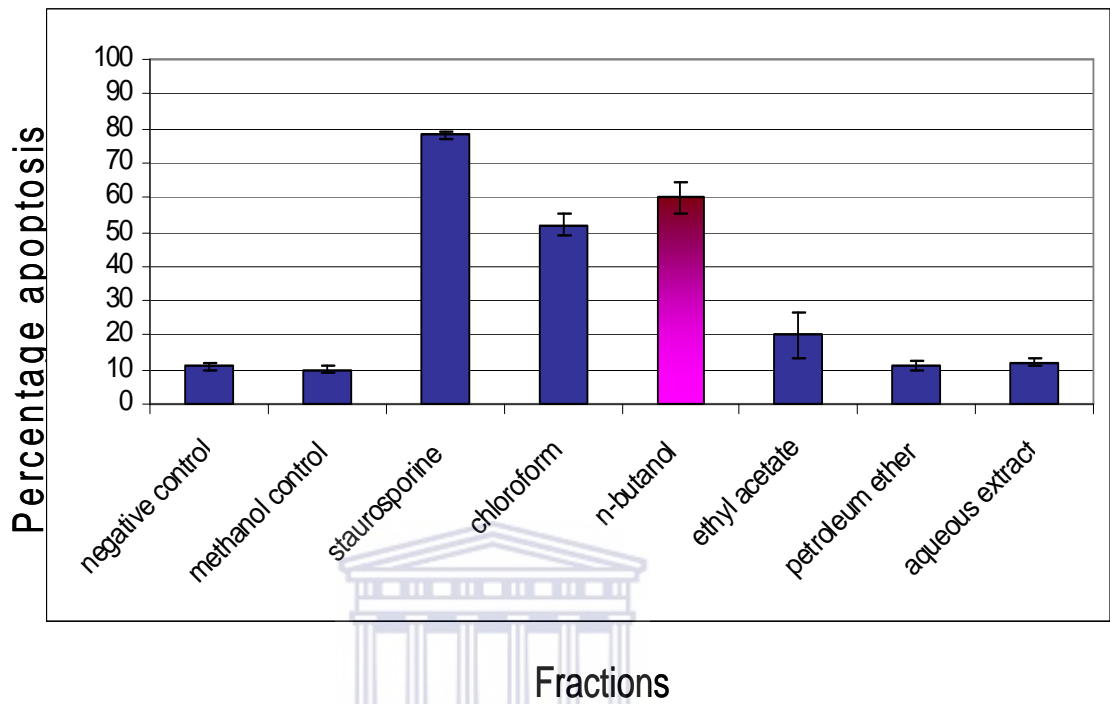


Figure 5.2. Flow cytometric analysis of the organic fractions by APOPercentage™ staining. CHO cells were treated for 24 h with 2 mg/ml of each organic fraction. As a positive control, cells were treated with 1.3 μM staurosporine. The experiment was repeated in triplicate. The results were plotted on a bar graph with apoptosis activity on the Y-axis and the fractions on the X-axis. The reddish-pink bar indicates the fraction that displayed the highest proapoptotic activity.

fractions through the stationary phase. The secondary metabolites distribute between the two phases which depend on their relative affinities for the phases, as determined by molecular structures and intermolecular forces (Robards *et al.*, 1994). Thus, the secondary metabolites with a lower affinity for the stationary phase will separate more rapidly. This differential migration rate of the secondary metabolites, results in their separation through the system. Separation would further be affected by; the nature of the two phases, the temperature and the velocity of the mobile phase. (Robards *et al.*, 1994).

5.3.1) Thin Layer Chromatography (TLC)

TLC is a simple and rapid separation technology which has modest demands on equipment resources and has the added advantage of being able to separate a larger sample capacity than HPLC. This technique only requires the TLC plate, solvent and a suitable container for development. Evaluation of the plate is feasible with the naked eye, spray reagents and ultra violet (UV) light at specific wavelengths. TLC separates the extract based on polarity and the liquid phase mobilizes as a result of capillary action. TLC is also used to determine the mobile phase required for product separation by LCC (Cannell, 1998).

5.3.2) Liquid Column Chromatography (LCC)

Although LCC is more complex and time consuming than TLC, it has the added advantage of being able to separate a larger sample capacity than TLC and has modest demands on equipment resources. The stationary phase in LCC may be

packed into a glass or metal column, to which a mobile phase is continuously supplied. The size of the column used depends on the volume of material separated and the degree of separation required. In column chromatography the liquid phase mobilizes as a result of gravity as apposed to TLC which makes use of capillary action. Detection methods that can be used include UV light, GC-MS, NMR and numerous bioactivity guided assays (Cannell, 1998).

TLC demonstrated that ethyl acetate:hexane (1:3) is the mobile phase required to separate the active nB fraction into discrete fractions (results not shown) (Miceli *et al.*, 2005; Sezik *et al.*, 2005). The active nB fraction was fractionated by LCC as described in section 2.7.4. The LCC fractions were dried by rotary evaporation and re-dissolved in methanol. Cells were plated in 24-well tissue culture plates as described in section 2.5.4 and treated with 0.50 mg/ml of each fraction for 24 h. After cells were treated and stained with APOPercentage™ dye, the cells were analyzed on a FACScan instrument. The results were plotted as a bar graph with the apoptosis activity on the Y-axis and the fractions on the X-axis. [Figure 5.3](#) shows that for the untreated control less than 2 % of the cells were positive for apoptosis, whilst staurosporine induced apoptosis in 88 % of the cells. The nB fraction was separated into 9 fractions by LCC. The following fractions: nB 1 and nB 2 were combined as the concentrations of these fractions were at least 10 times less than the concentrations obtained for the other fractions. The fractions nB 1+2, nB 3, nB 4, nB 5, nB 6, nB 7, nB 8 and nB 9 induced apoptosis in 2 %, 3 %, 5 %, 19 %, 72 %, 87 %, 35 % and 33 % of the cells, respectively. Fractions nB 6 and nB 7 demonstrated notable pro-apoptotic activity. These successive fractions were

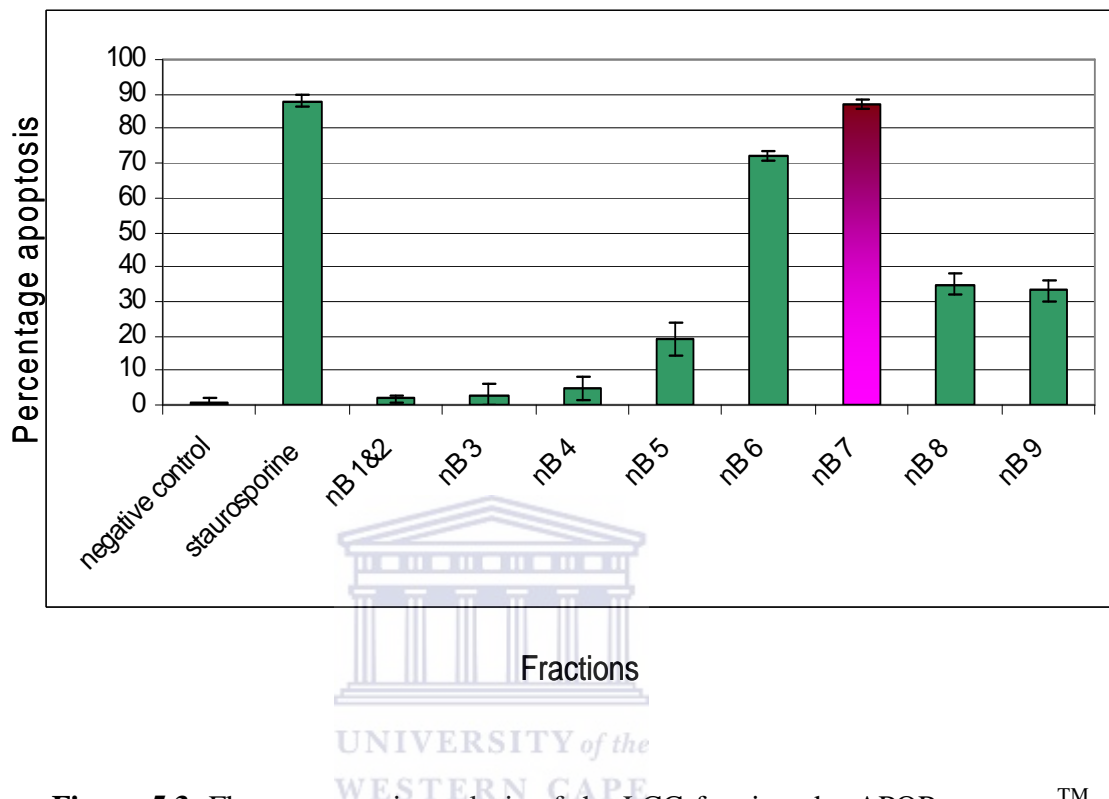


Figure 5.3. Flow cytometric analysis of the LCC fractions by APOPercentageTM staining. CHO cells were treated for 24 h with 0.50 mg/ml of each LCC fraction. As a positive control, cells were treated with 1.3 μ M staurosporine. Experiment was repeated in triplicate. The results were plotted on a bar graph with apoptosis activity on the Y-axis and the fractions on the X-axis. The reddish-pink bar indicates the fraction that displayed the highest pro-apoptotic activity.

combined to form fraction nB 67. The R_f of the active nB 67 fraction ranged between 0.1 and 0.44. The active nB 67 fraction was selected for further fractionation by TLC. The active nB 67 fraction was further fractionated on the glass TLC plates as described in section 2.7.3.2. The solvent system utilized was ethyl acetate : hexane in a 1 : 9 ratio. This solvent system was determined using TLC aluminium sheets as described in section 2.7.3.1. The TLC fractions were dried by rotary evaporation and re-dissolved in methanol. Cells were plated in 24-well tissue culture plates as described in section 2.5.4. The cells were treated with 0.25 mg/ml of each fraction for 24 h. After cells were treated and stained with APOPercentage™ dye, the cells were analyzed on a FACScan instrument. The results were plotted as a bar graph with the apoptosis activity on the Y-axis and the fractions on the X-axis. [Figure 5.4](#) shows the untreated and methanol controls induce apoptosis in less than 1 % of the cells and that staurosporine induces apoptosis in 74 % of the cells. The active nB 67 fraction was fractionated into 5 fractions by TLC. The fractions nB 67.1, nB 67.2, nB 67.3, nB 67.4 and nB 67.5 induced apoptosis in 5 %, 82 %, 5 %, 11 % and 5 % of the cells, respectively. Only fraction nB 67.2 demonstrate significant apoptosis activity. The R_f of the active nB 67.2 fraction ranged between 0.15 and 0.24. The active nB 67.2 fraction was selected for further fractionation by HPLC.

5.3.3) Reverse-Phase High Performance Liquid Chromatography

Compared to TLC and LCC; HPLC is more complex, time consuming, has a small sample capacity and requires more expensive equipment resources. HPLC is exceptional for quantification of compounds and resolution between similar

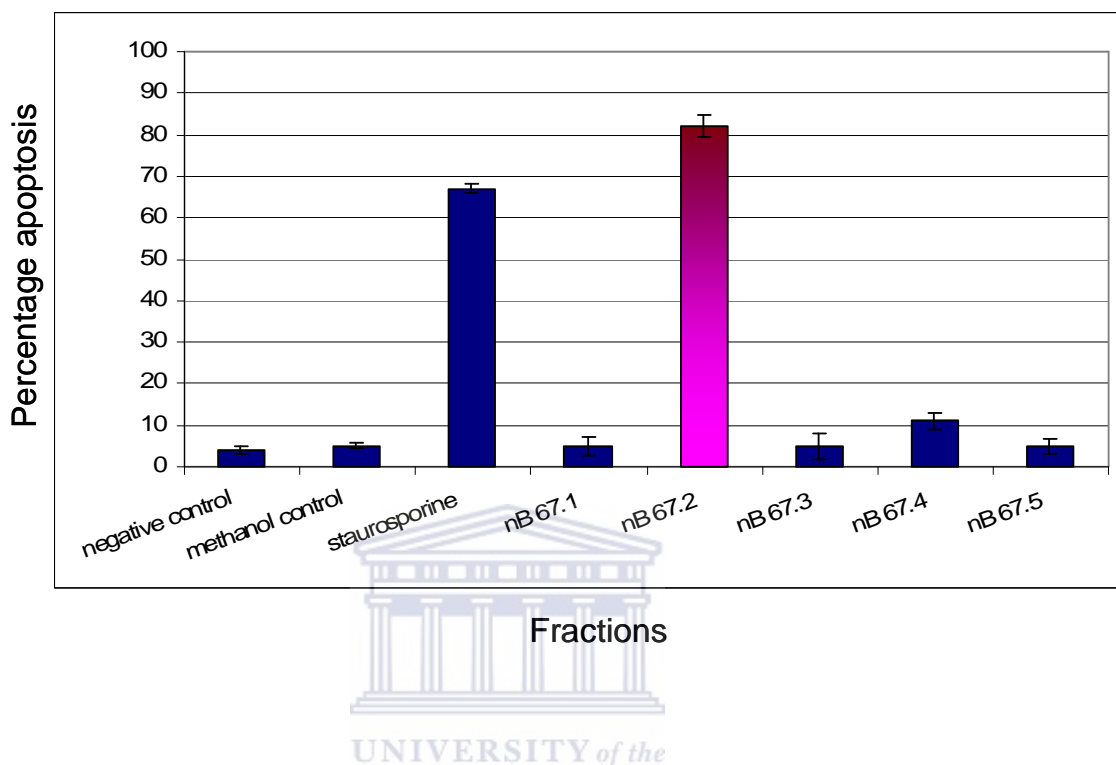


Figure 5.4. Flow cytometric analysis of the TLC fractions by APOPercentage™ staining. CHO cells were treated for 24 h with 0.250 mg/ml of each TLC fraction. As a positive control, cells were treated with 1.3 μM staurosporine. The experiment was repeated in triplicate. The results were plotted on a bar graph with apoptosis activity on the Y-axis and the fractions on the X-axis. The reddish-pink bar indicates the fraction that displayed the highest pro-apoptotic activity.

compounds. With HPLC a sample is separated on the basis of polarity and the liquid phase mobilizes as a result of the liquid phase being pumped through the column at high pressure (Robards *et al.*, 1994). Samples were fractionated using the Beckman HPLC system in combination with the chromatography station with Windows Clarity™ DataApex and collected using the FOXY JR 202F20077 fraction collector.

Fraction nB 67.2 was further fractionated by HPLC as described in section 2.6.5. The HPLC fractions were dried by rotary evaporation and re-dissolved in 10% methanol. Cells were plated in 24-well tissue culture plates as described in section 2.5.4. The cells were treated with 0.025 mg/ml of each fraction for 24 h. After cells were treated and stained with APOPercentage™ dye, cells were analyzed on a FACScan instrument. The results were plotted as a bar graph with the apoptosis activity on the Y-axis and the fractions on the X-axis. [Figure 5.5](#) show that the untreated control induces apoptosis in less than 4 % of the cells, whilst staurosporine induces apoptosis in 67 % of the cells. The active nB 67.2 fraction was fractionated in 7 fractions by HPLC (Figure 5.6C). The fractions nB 67.2.1, nB 67.2.2, nB 67.2.3, nB 67.2.4, nB 67.2.5, nB 67.2.6 and nB 67.2.7 induced apoptosis in 2 %, 72 %, 39 %, 10 %, 7 %, 2 % and 3 % of the cells, respectively. Fraction nB 67.2.2 demonstrated the most significant apoptosis activity. Purification of the active fractions identified in this fractionation process can be monitored by HPLC, whilst the success of each fractionation step is screen by serial dilution (Cannell, 1998).

The *E. rhinocerotis* fractionation process was tracked by HPLC utilizing the parameters described in section 2.6.5. [Figure 5.6 A](#) represents the active organic

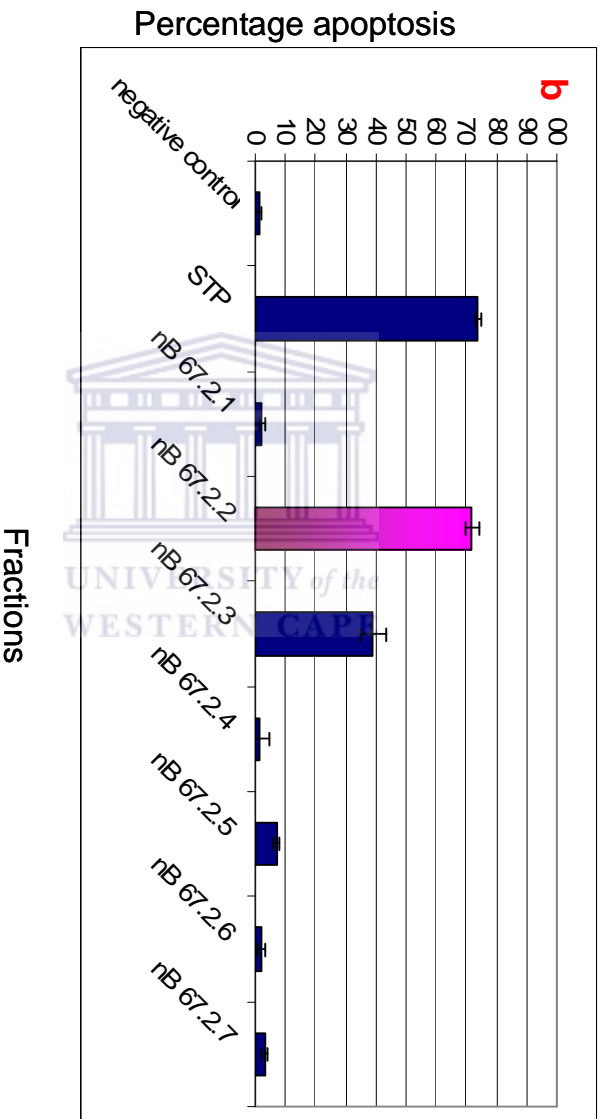
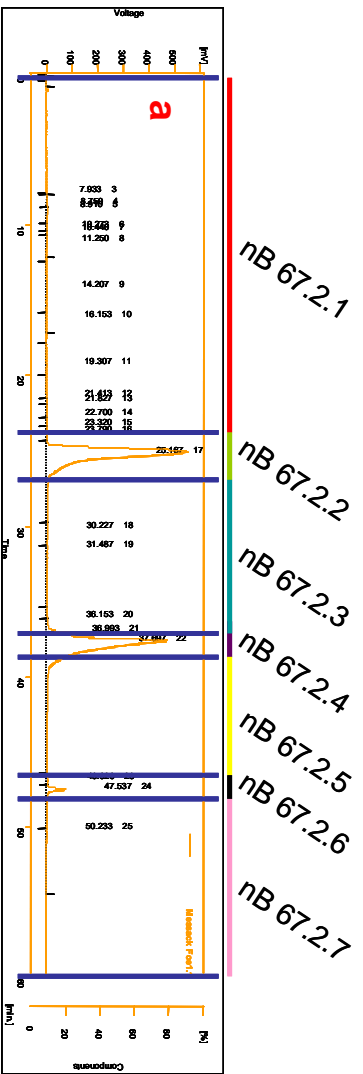
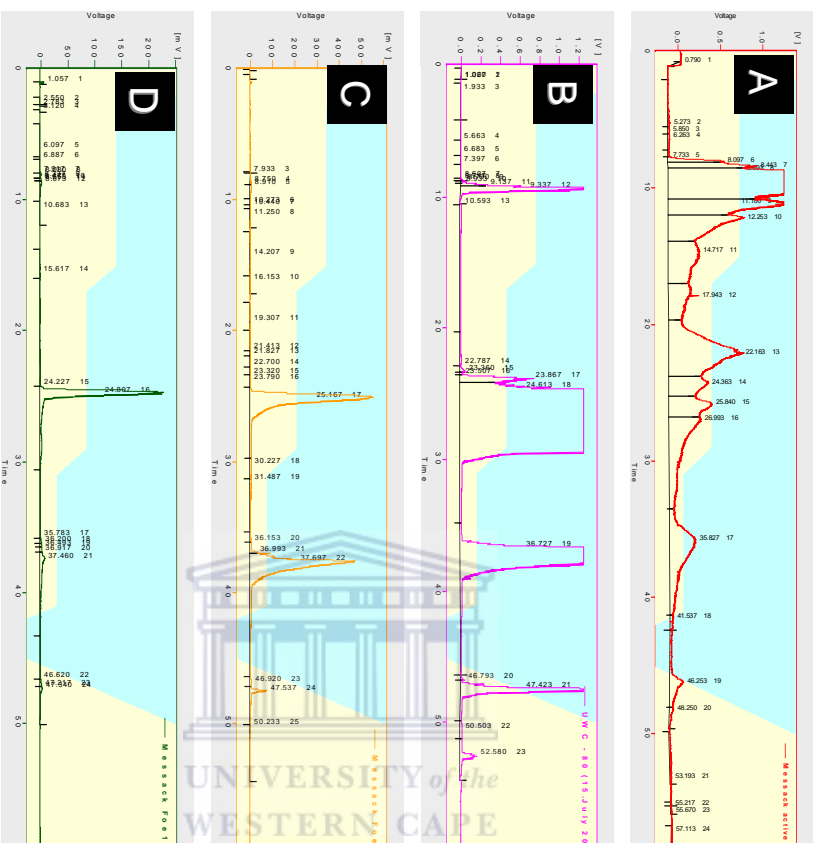


Figure 5.5 (a) A HPLC chromatograph representing the active TLC fraction, nB 67.2. HPLC was used to further fractionate the nB 67.2 fraction into seven fractions as indicated by the horizontal blue lines representing the start and end point of each fraction. **(b)** Flow cytometric analysis of the HPLC fractions by APOPercentage™ staining. CHO cells were treated for 24 h with 0.025 mg/ml of each HPLC fraction. As a positive control, cells were treated with 1.3 μM staurosporine. The results were plotted on a bar graph with apoptosis activity on the Y-axis and the fractions on the X-axis.



Active n-butanol

LCC → Apoptosis assay

Active LCC fraction 67

TLC → Apoptosis assay

Active TLC fraction 2

HPLC → Apoptosis assay

**Active HPLC fraction 2
'nB.67.2.2'**

Figure 5.6. Chromatographs illustrating the complexity of the active fractions identified in the purification process. The active fractions were the n-butanol (nB) fraction, LCC fraction 67 (nB.67), TLC fraction 3 (nB.67.2) and HPLC fraction 2 (nB.67.2.2) respectively.

fraction (nB). **B** represents the active LCC fraction (nB 67). **C** represents the active TLC fraction (nB 67.2.) **D** represents the active HPLC fraction (nB 67.2.2). The chromatograph traces provides a visual presentation of the complexity of the different subfractions. Figure 5.6 illustrates how the number of secondary metabolites is reduced during the chronological fractionation steps. The final fraction, nB 67.2.2 is a single peak that may not necessarily be pure as it may consist of a group of extremely similar compounds.

Serial dilutions of each active fraction identified in the bioactivity-guided fractionation process was tested to determine the concentration of extract required to induce apoptosis in 50 % of cells over a period of 24 h i.e. the LD₅₀. Cells were plated in 24-well tissue culture plates as described in section 2.5.4. The cells were treated with varying concentrations for 24 h. After cells were treated and stained with APOPercentage™ dye, the cells were analyzed on a FACScan instrument. It can be assumed that the aqueous extract contains 100 % of the bioactive units before fractionation. [Tables 5.1](#) show that during the successive fractionation steps the percentage of bioactive units in the total starting extract (one bioactive unit is equivalent to the LD₅₀ concentration) decreased from 100 % to 7.5 % in the active HPLC fraction nB 67.2.2. This is to be expected since it can be anticipated that at each fractionation step bioactive metabolites will be lost. In contrast, the LD₅₀ determined for each active fraction (results not shown) decreased from 3 mg/ml to 0.01 mg/ml, indicating an increase in bioactive unit concentration in the active fraction. This implies the successful fractionation and purification of the bioactive secondary metabolite(s).

Table 5.1 Serial dilutions of the active fractions used to verify the success of the purification process.

Level	Conc. of stock (mg/ml)	LD₅₀ (mg/ml)	Units of activity per 40 mg/ml	Volume (ml)	Total units	%active units retained
Aqueous extraction	40	3	13.3	2000	26667	100
Organic extraction	40	1	40	500	20000	75
LCC	20	0.05	400	40	16000	60
TLC	5	0.025	200	40	8000	30
HPLC	2	0.01	200	10	2000	7.5

The verification of a successful purification process by serial dilution and the HPLC chromatograph trace of fraction nB 67.2.2 displaying a single peak, warranted an attempt at structure determination by MS/NMR, similar to the strategy used by Sezik *et al.*, (Sezik *et al.*, 2005).

5.4) Structure Determination

The sample was sent to the Department of Chemistry, University of Stellenbosch, for structure determination. The sample was dissolved in CDCl₃ and the spectra run on a 600 MHz Varian Inova NMR spectrometer. The ¹H, ¹³C, ¹H-¹H COSY, ¹H-¹³C HSQC and ¹H-¹³C HMBC NMR spectra was collected. The sample concentration was low as can be seen from the ¹³C NMR spectrum (Figure 5.7) and the HMBC spectrum (Figure 5.8) in which only weak correlations were observed. The ¹H spectrum (Figure 5.9) appeared promising with an acid proton being observed at 12 ppm, a number of aromatic peaks between 6.5 and 7.5 ppm (which included a para-substituted phenyl ring) and probably methoxy CH₃'s slightly upfield of 4 ppm and peaks at 2.8, 3.1, and 5.4 ppm appeared to belong to a single spin system as seen from the COSY spectrum. However, integration of the ¹H spectrum indicated that it was probably unlikely that the para-substituted phenyl ring for instance would be in the same molecule as the spin system of the peaks at 2.8, 3.1, and 5.4 ppm. Integrations of other peaks also appeared anomalous. From the ¹H-¹³C HSQC spectrum (Figure 5.10) it was seen that though some of the signals in the ¹H spectrum that appeared to be due to single CH's (5.4 and 6.1 ppm for instance), they were infact due to at least two groups as they corresponded to two carbons in the ¹³C NMR spectrum. It is thus clear that a number

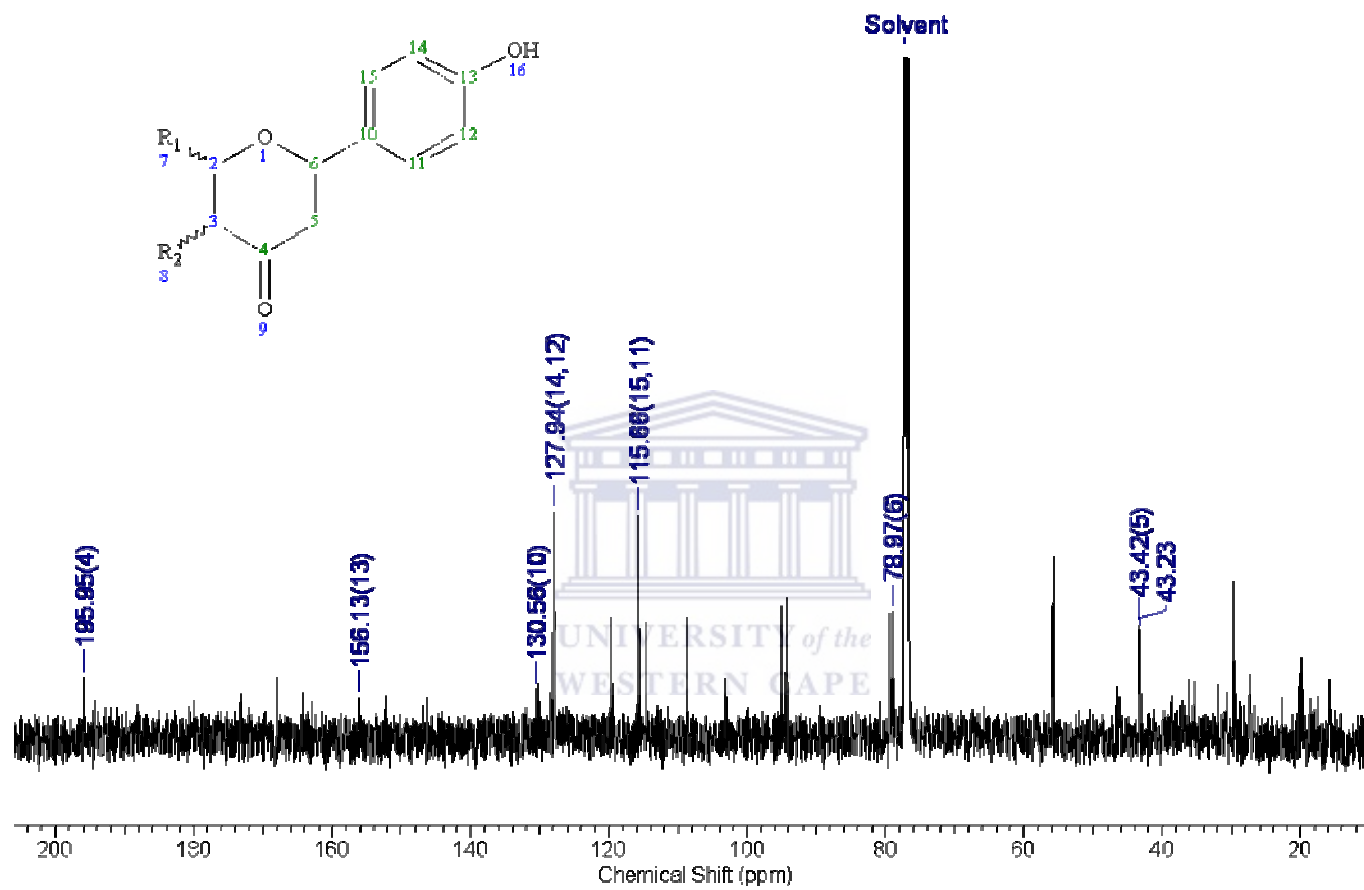


Figure 5.7: ^{13}C NMR spectrum

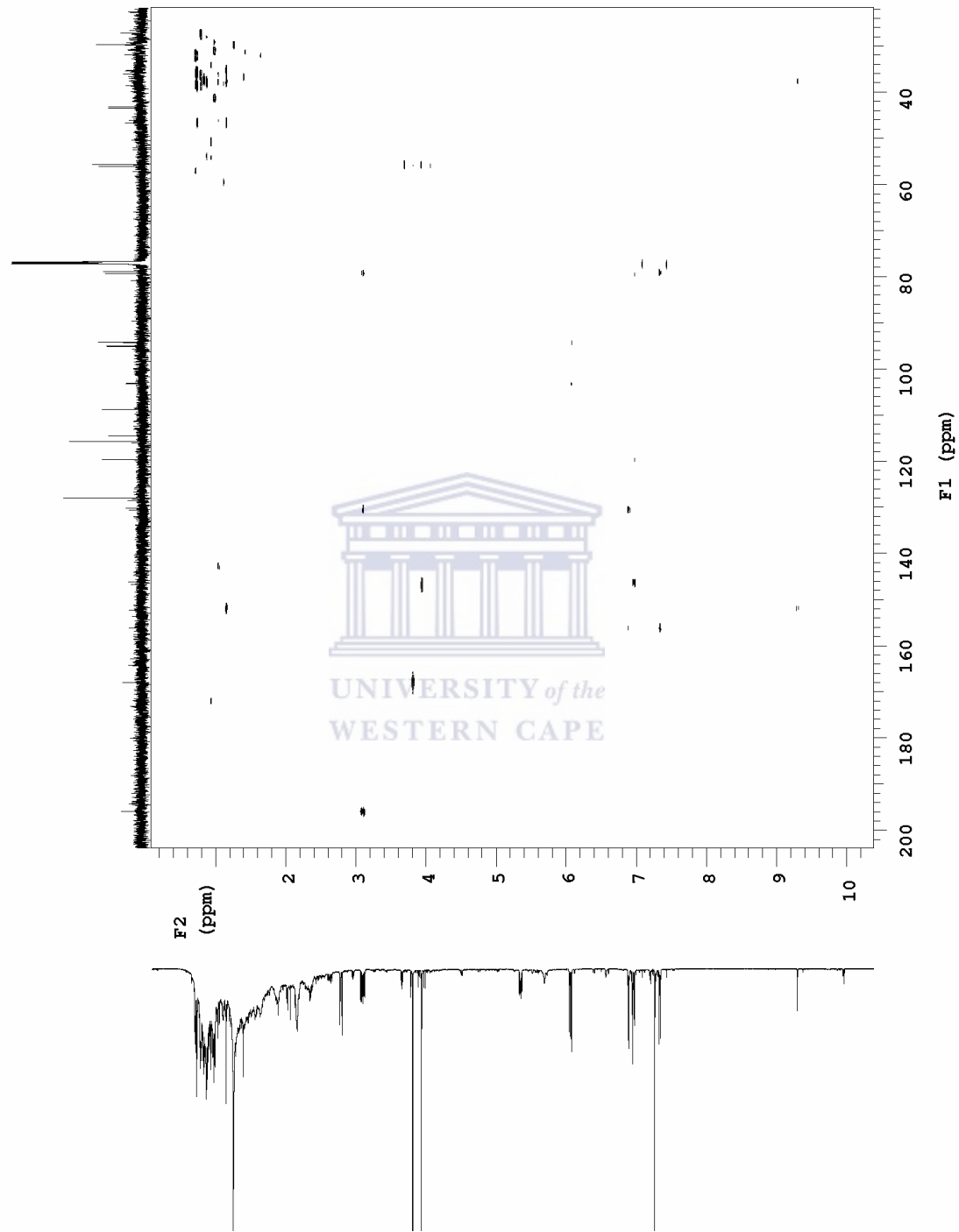


Figure 5.8: ^1H - ^{13}C hmbc NMR spectrum

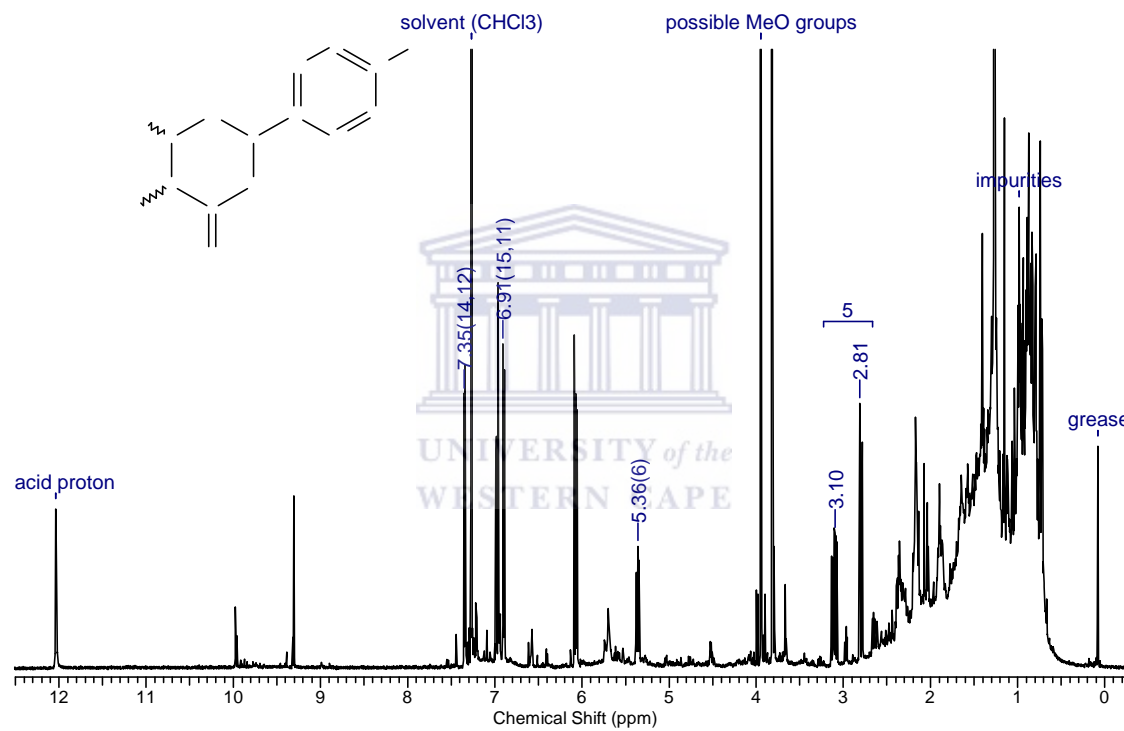


Figure 5.9: ^1H NMR spectrum

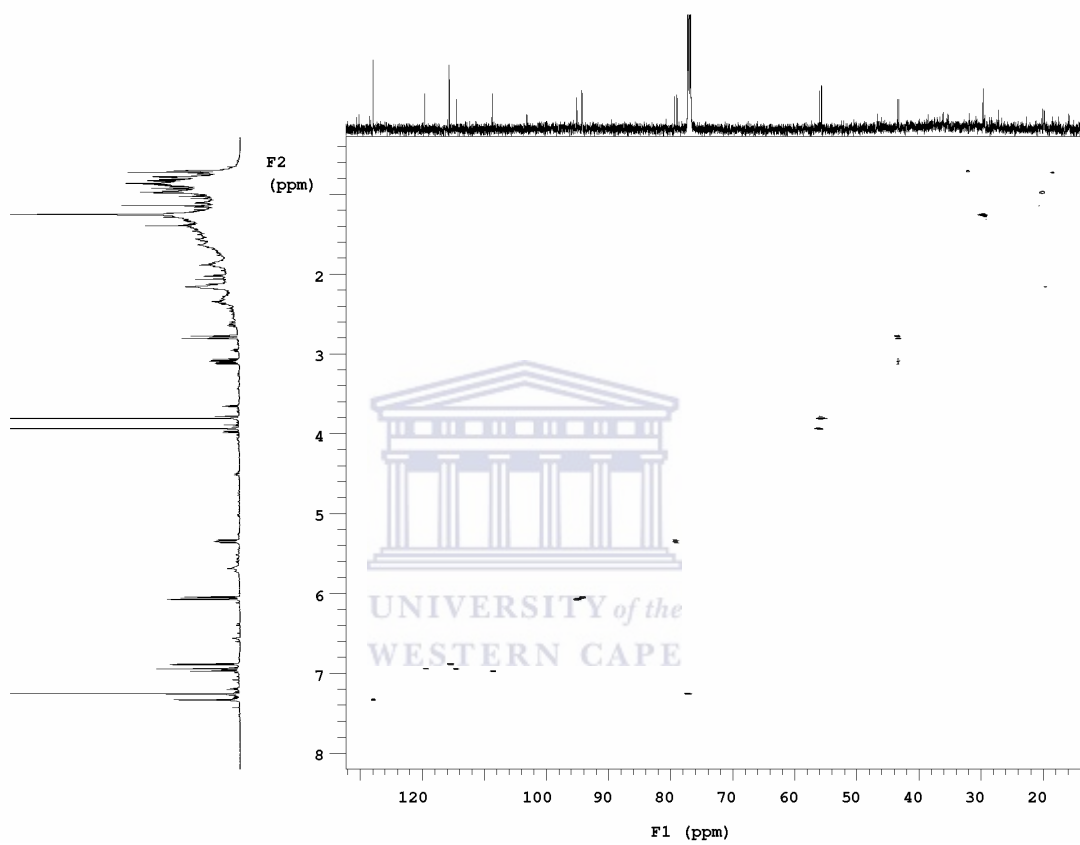


Figure 5.10: ^1H - ^{13}C hsqc NMR spectrum

of compounds were present in the sample. This should not necessarily be a barrier to elucidating structures of some of these compounds. However, it was found that the compounds were very similar resulting in overlapping peaks (especially in the ^1H spectrum) that made distinguishing the compounds from one another impossible. Also, the low concentration of the sample presented difficulties in that the HMBC spectrum did not show as many correlations as would be required to unambiguously assign the spectrum. Some attempt at structure elucidation was however carried out.

As mentioned above, the presence of a para-substituted phenyl ring was clearly observable from the ^1H spectrum. From the HSQC and HMBC spectra it was possible to identify the carbons on this ring as well (these have been indicated in the ^1H and ^{13}C spectra). The shift of one of the quaternary carbons on the ring was significantly downfield at 156 ppm indicated it was likely this carbon was connected to an electron withdrawing group such as an -OH. A long range correlation in the HMBC spectrum from the phenyl proton at 7.4 ppm to a peak in the ^{13}C spectrum at 79 ppm indicated the other substitution on the phenyl ring was a CH probably attached to an O atom (this region is typical of such carbons). The proton attached to this carbon resonates at 5.4 ppm in the ^1H spectrum (as determined from the HSQC spectrum). From the ^1H - ^1H COSY (Figure 5.11) this proton coupled to two diastereotopic protons 2.8 and 3.1 ppm. Their being diastereotopic was clear from the HSQC spectrum as they both showed correlations to the same carbon at 43.2 or 43.4 ppm. Two shifts are given here as this is an instance where two different compounds appeared to be resonating at the same position in the ^1H spectrum (indeed as mentioned above the integrals of the phenyl protons are not in the correct ratio to these protons). Two carbons are seen

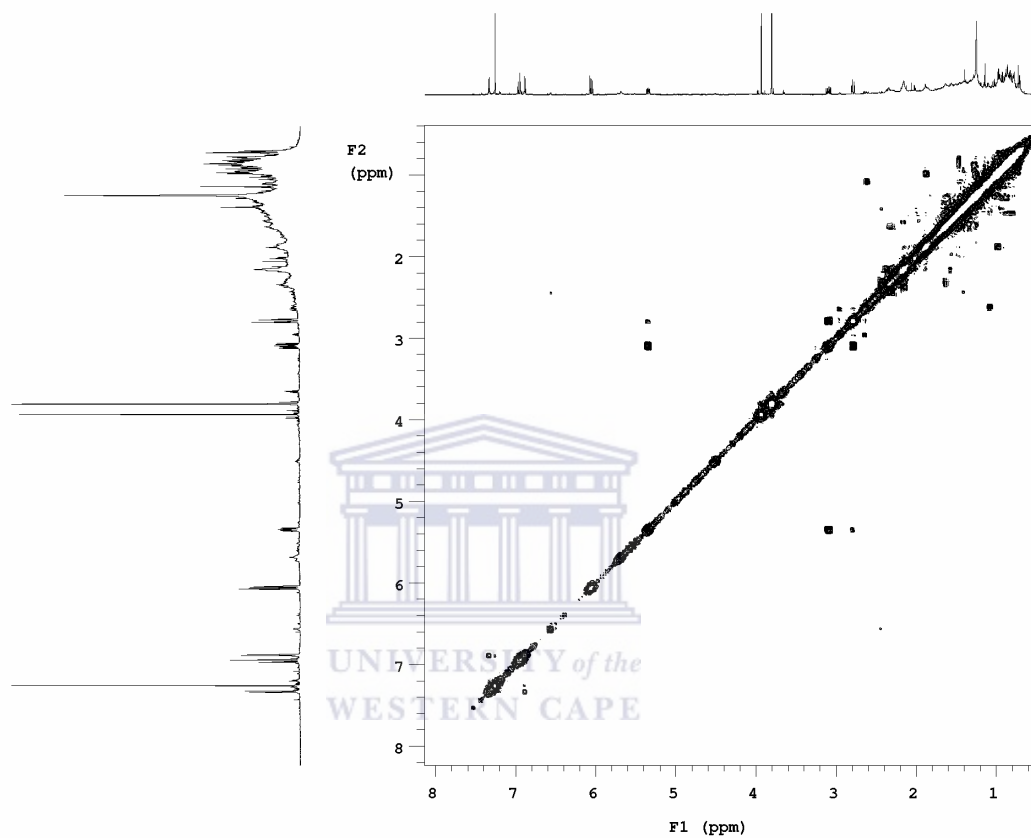


Figure 5.11: ^1H - ^1H cosy NMR spectrum

in the ^{13}C spectrum both correlating to both of the ^1H signals, i.e. two diastereotopic CH_2 groups due to similar molecules. The protons at 3.1 ppm showed a long range correlation to a $\text{C}=\text{O}$ peak in the HMBC spectrum, the ^{13}C chemical shift being 196 ppm. At this point no more correlations could be followed to complete the possible structure of this molecule in the mixture. Thus from the information gathered it appeared that a structure similar to the one given below was perhaps a possibility (numbering is arbitrary) (Figure 5.12). The predication that it would be a six-membered ring attached to the phenyl moiety rather than a branched chain is due to the chemical shift of C6 being downfield of what would be expected for a chain. Unfortunately, no other possible clear structures could be elucidated from the spectra especially as no mass spectral data could be obtained that could have been correlated with the NMR data.

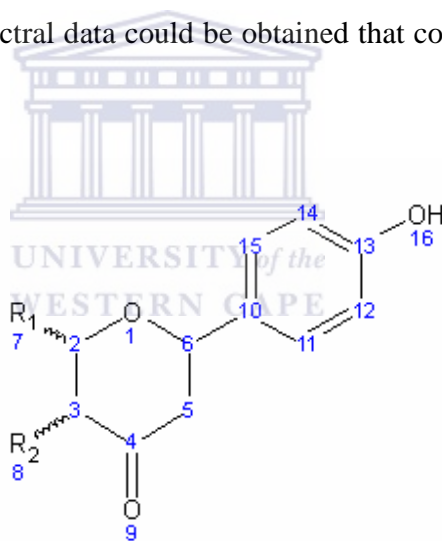


Figure 5.12: Compound structure 6-(4'-hydroxyphenyl)-2,3-di(R)tetrahydro-4H-pyran-4-one elucidated by NMR data.

Further purification is necessary for the assignment of two side chains and elucidation of the other compound/s. This may be possible by further purification of the active fraction by HPLC using a different column namely, the Thermo Hypersil-keystone

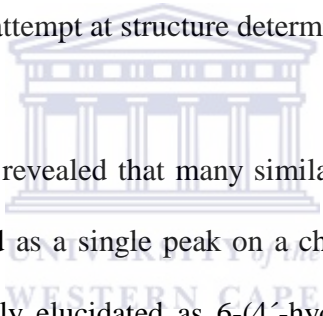
hypercarb (250 x 4.6 mm, 5 μ) or attempting to grow crystals from the active extract. Once these side chains are known, the apoptosis activity of this synthesized compound (if novel) or commercially available compound must be verified.

5.3) Summary

The aim of this section was to purify the pro-apoptotic secondary metabolite(s) in the aqueous extract of *E. rhinocerotis* by bio-activity guided fractionation.

These results demonstrated that the aqueous extract can be used as a platform from which the secondary metabolites can be fractionated on the basis of increasing polarity i.e. by organic extraction. The highest activity resided in the *n*-butanol fraction. *N*-butanol has a polarity index of 4, thus the active constituent(s) is non-polar. This active organic fraction was further fractionated by numerous chromatographic separation techniques namely LCC, TLC and HPLC respectively. The active *n*-butanol (nB) fraction was fractionated by LCC using ethyl acetate:hexane (1 : 3) as the mobile phase. The *n*-butanol fraction was fractionated into 9 fractions of which the successive fractions 6 and 7 were the most active fractions. The fractions were combined to form active fraction nB 67. The R_f of the active nB 67 fraction ranged between 0.1 and 0.44. Active LCC fraction nB 67 was further fractionated by TLC using ethyl acetate : hexane (1 : 9) as the mobile phase. The nB 67 fraction was fractionated into 5 fraction of which fraction nB 67.2 was the most active fraction. The R_f of the active nB 67.2 fraction ranged between 0.15 and 0.24. Active TLC fraction nB 67.2 was further fractionated by HPLC as described in

section 2.7.5. The nB 67.2 fraction was fractionated into 7 fractions of which fraction nB 67.2.2 was the most active fraction. The sequence of the chromatographic separation techniques is of utmost importance as a high yield of total aqueous extract is essential in ensuring that sample volume is sufficient for structure determination. Thus, the first chromatographic separation was by LCC which allows for the separation of a large volume of material, followed by TLC that separates a smaller volume but allows for the easy separation of dissimilar groups of compounds and HPLC that can further separate the similar compounds in the concentrated active TLC extract. This process has successfully transformed a complex mixture of secondary metabolites represented by numerous peaks on a chromatograph to a single peak. This single peak warranted an attempt at structure determination by NMR.



Integration of the spectra revealed that many similar compounds were present in the HPLC sample represented as a single peak on a chromatograph. However, only one structure could be partially elucidated as 6-(4'-hydroxyphenyl)-2,3-di(R)tetrahydro-4*H*-pyran-4-one, the mixture of compounds were very similar. Also, no quality MS data could be generated for correlation with the NMR data as a result of the mixture of compounds (MS data not shown). Further purification is necessary for the assignment of two side chains. This may be possible by purification of the active fraction by HPLC and /or the growing of crystals for structure determination by crystallography.

CHAPTER 6: GENERAL DISCUSSION

6.1) Introduction

The cell cycle is regulated by cell cycle check points. Genetic mutations that result in dysregulation of the cell cycle can lead to the uncontrolled growth of cells. Under normal physiological conditions the uncontrolled growth of cells that is tissue homeostasis is regulated by apoptosis. One of the physiological roles of apoptosis is to orchestrate the elimination of mutated or damaged cells. Cancer arises when cells escape the induction of apoptosis due to secondary mutations in genes that regulate apoptosis. It is therefore not surprising that the unifying concept for the mechanism of chemoprevention is the induction of apoptosis by chemotherapeutic drugs.

Many anti-cancer drugs are derived from natural sources, including marine, microbial origin and plants. FDA approved plant derived drugs include Combretastatin A-4 phosphate (*Combretum caffrum*), Taxol (*Taxus brevifolia*), Velban (*Catharanthus roseus*) etc. Thus, the aim of this study was to screen extracts of nine indigenous South African plants for the presence of pro-apoptotic compounds. Some of these plants are used in traditional medicine to treat cancer. The approach exploited was to extract the plant secondary metabolites by aqueous extraction followed by the screening of these aqueous extracts using a cytotoxicity assay and numerous apoptosis assays namely; the APOPercentageTM assay, Annexin V-PE Detection assay, Active Caspase-3 Detection assay and the TUNEL assay. Any secondary metabolite that has pro-apoptotic activity can be a potential anti-cancer agent. Hence,

the aqueous extract displaying the highest pro-apoptotic activity was selected for bioactivity guided fractionation. The fractionation or separation technology used includes organic extraction, LCC, TLC and HPLC.

6.2) Screening extracts of indigenous South African plants for the presence of anti-cancer compounds.

Pharmacological and phytochemical insights into several plants have led either to the discovery of novel chemicals and therefore novel drugs or to novel chemicals that served as lead compounds for the design of new drugs. In this study nine indigenous South African plants were screened; the poisonous *Cotyledon orbiculata*, *Oxalis pes-caprae*, *Echium plantagineum*, *Cissampelos capensis*, *Euphorbia mauritanica*, *Haemanthus pubescens*, *Cynanchum africanum* as well as the non-poisonous *Lessertia frutescens* and *Elytropappus rhinocerotis* for the ability to induce pro-apoptotic activity in the human cancer cell lines (MCF7 and HeLa), and the 'normal' hamster cell line (CHO).

Cytotoxicity and cell viability assays have been used extensively to screen potential anti-cancer drugs. These assays measure cell death or inhibition of cell growth. The rationale is that potential anti-cancer drugs will either inhibit cancer cell growth or kill cancerous cells (Cardellina *et al.*, 1993). Noteworthy is the fact that these assays do not discriminate between toxic cell death and cell death induced by apoptosis. As a consequence many potential anti-cancer drugs which start out as good candidate drugs based on cytotoxic and cell viability assays turn out to be too toxic to normal

cells and can therefore not be used as anti-cancer agents. This study did not only investigate the cytotoxic effects of the plant extracts, but also investigated their pro-apoptotic activity. In this study, apoptosis was detected and quantified by the APOPercentage™ assay whilst cytotoxicity was measured by the NR assay. *E. mauritanica*, *C. africanum*, *L. frutescens* and *E. rhinocerotis* displayed significant apoptosis activity but negligible cytotoxicity indicating that these plants would have been unduly eliminated as potential sources of anti-cancer agents if the initial preliminary screening process was based on cytotoxicity only.

The CHO cell line was more susceptible to the nine plant extracts, than the MCF7 and HeLa cell line. The results shows that *C. africanum* and *E. rhinocerotis* displayed the highest degree of activity in the MCF7 cell line. Also, *H. pubescens*, *L. frutescens* and *E. rhinocerotis* extracts are the most active apoptosis inducers for the HeLa cell line. The CHO cell line can be regarded as a 'normal' cell line. It is also known that cancer-derived cells such as MCF7 and HeLa are more resistant to cell death induced by various anti-cancer agents. This is most likely due to mutations in genes involved in the apoptotic pathways. For example, the MCF7 cell line in particular has been characterized with caspase-3 gene mutation and as a result these cells are not capable of activating apoptosis pathways via caspase-3 (Kurokawa *et al.*, 1999). The major apoptosis pathways converge at caspase-3, highlighting the reason why the presence of caspase-3 is recognized as a hallmark of apoptosis. This may account for the increased resistance to the MCF7 cell line to apoptosis induced by the plant extract. The HeLa cell line is a HPV infected cell line. The HPV genes produce the E6 and E7 proteins that bind to and inhibit p53 and Rb. Rb and p53 are important regulators of

the pathways (Scheffner *et al.*, 1991). Since, the *E. rhinocerotis* extract exhibited notable pro-apoptotic activity across all three cell lines, it is a good candidate extract for the bio-assay guided fractionation of secondary metabolites that can induce apoptosis.

Thus, *E. rhinocerotis* extract was further evaluated for specific markers of apoptosis such as phosphatidylserine externalization, activation of caspase-3 and DNA fragmentation. The study found that CHO cells treated for 6 h with the *E. rhinocerotis* extract showed externalization of phosphatidylserine and activation of caspase-3 in 71 % and 50 % of the cells, respectively. Externalization of phosphatidylserine also implies the possible involvement of tBid and AIF since it is known that tBid activates AIF and that AIF promotes the externalization of phosphatidylserine (Wang *et al.*, 2007). The fact that the *E. rhinocerotis* extract was able to induce the activation of caspase-3 in CHO cells and that the MCF7 cells which are caspase-3 negative is also susceptible to the *E. rhinocerotis* extract, suggests that the secondary metabolites in this extract has the ability to induce both caspase-3 dependent and caspase-3 independent pathways. The *E. rhinocerotis* extract also induced DNA fragmentation in 75 % of CHO cells treated for 48 h. The fragmentation of the genomic DNA is a late apoptotic event that results as a consequence of the active caspase-3 mediated cleavage of ICAD to activate CAD which in turn is responsible for the fragmentation of the genomic DNA (Sakahira *et al.*, 1998; Zhao *et al.*, 2001).

The *E. rhinocerotis* extract activated several markers of apoptosis. These extracts also induced significant apoptosis activity in all the cell lines tested. Hence, *E.*

rhinocerotis was selected for further study to identify the secondary metabolite responsible for the bioactivity.

6.3) Investigating whether the variation in bioactivity within the *E. rhinocerotis* species is associated with genetic variation

It is not uncommon for plants of the same species collected from different geographical locations or the same geographical location at different times to display variation in activity (Yang and Loopstra, 2005). *L. frutescens* collected from different geographical locations demonstrated variation in pro-apoptotic activity (Chinkwo, 2005). This prompted an investigation into whether *E. rhinocerotis* displays variation in bioactivity between isolates collected from different geographical locations. *E. rhinocerotis* was collected from various places in the Western Cape, namely Blaauwberg, Helderberg, Tygerberg, Kirstenbosch and Tulbagh. APOPercentage™ assay results indicate that the extracts of these five *E. rhinocerotis* samples display a notable variation in the degree of pro-apoptotic activity. The Kirstenbosch extract displayed the least activity (7%), whilst the Tulbagh extract displayed the most activity (71%). This is a 10 fold difference in bioactivity within the same plant species. The variation in the bioactivity of plant extracts within the same plant species from different geographical locations can be ascribed to differences in the plant chemistry, that is, the difference in the composition of the secondary metabolites present. It is possible that environmental factors can influence plant chemistry or that genetic event in the plant gives rise to genetic variants with different plant chemistry.

To investigate whether the variation in bioactivity within the *E. rhinocerotis* species is associated with genetic variation, the genetic relationships amongst the *E. rhinocerotis* samples were elucidated. Phylogenetic relationships among congeneric species and closely related genera in Asteraceae have been elucidated by DNA sequence analysis of the internal transcribed spacer (ITS) of nuclear ribosomal DNA (nrDNA) (Samuel *et al.*, 2003). Thus, to determine if this variation in pro-apoptotic activity is a consequence of genetic variation, the ITS1 sequences of these five *E. rhinocerotis* samples were amplified and sequenced. This represents the first study analyzing the ITS1 sequence of *E. rhinocerotis* since only the *trnL/F* spacer of *E. rhinocerotis* has been sequenced for phylogenetic studies to date (Bayer *et al.*, 2000). The sequence alignment of the five plants ITS1 region displayed 100 % to 98 % homology. It is worth noting that when comparing the genetic variation of the ITS1 sequences with their corresponding levels of apoptosis activity that is; Tulbagh (71%), Tygerberg (57%), Helderberg (51%), Blaauwberg (42%) and Kirstenbosch (7%); it is found that the apoptosis activity decreases as the sequence deviates from the root sequence.

This is still a preliminary study which may suggest a link between the genetic variation and apoptosis activity. However, a much bigger study is needed, along with a study on other *Elytropappus* species to establish biological significance of these findings.

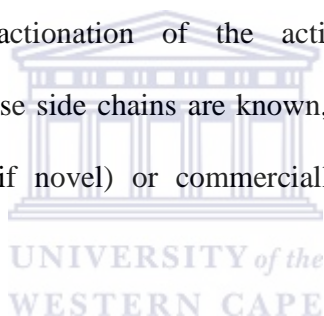
6.4) The partial purification of the pro-apoptotic secondary metabolite/s isolated from the extract of the *E. rhinocerotis* plant from Tulbagh

E. rhinocerotis plant material collected from Tulbagh was shown to have the highest pro-apoptotic activity and therefore most probably also contains more of the secondary metabolite/s responsible for the bioactivity. The aim therefore was to purify the pro-apoptotic secondary metabolite/s from the aqueous extract of *E. rhinocerotis* from Tulbagh by the bio-activity guided fractionation process and to attempt to characterize these secondary metabolites.

The aqueous extract was used as a platform for the organic fractionation of the secondary metabolites.. The major activity resided in the chloroform and *n*-butanol extracts. The *n*-butanol fraction was further fractionated by numerous chromatographic separation techniques namely LCC, TLC and HPLC. The success of each fractionation step was ascertained by serial dilution as described by Cannell (Cannell, 1998). The results displayed a decrease in the percentage of bioactive units after each fractionation step and an increase in bioactive units concentration in the active fraction. This signifies the successful fractionation and purification of the pro-apoptotic secondary metabolite(s). The *E. rhinocerotis* fractionation process was also tracked by HPLC chromatographic traces. The chromatograph traces provides a visual presentation of a complex mixture represented by numerous peaks on a chromatograph transformed into the active single peak, nB67.2.2. A single peak represents a single compound or a group of highly analogous compounds. Thus, the single peak warranted an attempt at structure determination by MS and NMR.

The sample was sent to the Department of Chemistry, University of Stellenbosch, for structure determination. The ^1H , ^{13}C , ^1H - ^1H COSY, ^1H - ^{13}C HSQC and ^1H - ^{13}C HMBC NMR spectra was collected. Integration of these spectra revealed that many similar compounds were present in the HPLC sample represented as a single peak on the chromatograph. A structure was partially elucidated as 6-(4'-hydroxyphenyl)-2,3-di(R)tetrahydro-4*H*-pyran-4-one. However, other possible clear structures could not be elucidated from the spectra especially as mass spectral data could not be obtained that could have been correlated with the NMR data.

Further purification is necessary for the elucidation of two side chains. This may be possible by further fractionation of the active fraction by HPLC and/or crystallography. Once these side chains are known, the pro-apoptotic activity of this synthesized compound (if novel) or commercially available compound must be verified.



6.5) Summary

In this study nine indigenous South African plants extracts were screened for their ability to induce cytotoxicity and pro-apoptotic activity in the human cancer cell lines (MCF7 and HeLa), and the 'normal' hamster cell line (CHO). This research illustrates that the cytotoxicity test is not a reliable preliminary screen for anti-cancer agents, and it also demonstrates that the *APOPercentage*TM assay coupled with acquisition and analysis by flow cytometry provides a means to measure pro-apoptotic activity directly and provide accurate quantification of the degree of pro-apoptotic activity.

Inducers of pro-apoptotic activity are considered good lead compounds for the development of anti-cancer drugs. This study verified that of the nine plant extracts screened, *C. africanum*, *H. pubescens*, *L. frutescens* and *E. rhinocerotis* displayed the most notable pro-apoptotic activity and therefore this study also lends support to claims by traditional healers that extracts of *L. frutescens* and *E. rhinocerotis* possess anti-cancer properties. The *E. rhinocerotis* extract was selected for the purification of a pro-apoptotic compound/s that may serve as a lead compound or a future anti-cancer drug. Also, *C. africanum* and *H. pubescens* are highlighted as future prospects for the purification process.

The research described here demonstrates the efficient streamlining of the screening process of plant extracts for anti-cancer compound/s. It also demonstrates a successful bio-activity guided fractionation process. NMR spectra revealed that the single peak was not pure. However, a structure was partially elucidated as 6-(4'-hydroxyphenyl)-2,3-di(R)tetrahydro-4H-pyran-4-one. In the near future, the complete elucidation of this pro-apoptotic compound may serve as a novel anti-cancer drug or lead compound.

REFERENCES

- Adamson, A.W., Beardsley, D.I., Kim, W.J., Gao, Y., Baskaran, R., and Brown, K.D. (2005). Methylator-induced, mismatch repair-dependent G2 arrest is activated through Chk1 and Chk2. *Molecular biology of the cell* 16, 1513-1526.
- Alnemri, E.S., Livingston, D.J., Nicholson, D.W., Salvesen, G., Thornberry, N.A., Wong, W.W., and Yuan, J. (1996). Human ICE/CED-3 protease nomenclature. *Cell* 87, 171.
- Alvarez, I., and Wendel, J.F. (2003). Ribosomal ITS sequences and plant phylogenetic inference. *Molecular phylogenetics and evolution* 29, 417-434.
- BabyCenter (2007). Fetal Development, // www.babycenter.com/pregnancy-fetal-development-index, ed.
- Barbetti, P., Grandolini, G., Fardella, G., and Chiappini, I. (1987). Indole Alkaloids from *Quassia amara*. *Planta medica* 53, 289-290.
- Bayer, R.J., Puttock, C.F., and Kelchner, S.A. (2000). Phylogeny of South African Gnaphalieae (Asteraceae) based on two noncoding chloroplast sequences. *Am J Bot* 87, 259-272.
- Belizario, J.E., Alves, J., Occhiucci, J.M., Garay-Malpartida, M., and Sesso, A. (2007). A mechanistic view of mitochondrial death decision pores. *Brazilian journal of medical and biological research = Revista brasileira de pesquisas medicas e biologicas / Sociedade Brasileira de Biofisica* [et al 40, 1011-1024.

- Belloc, F., Belaud-Rotureau, M.A., Lavignolle, V., Bascans, E., Braz-Pereira, E., Durrieu, F., and Lacombe, F. (2000). Flow cytometry detection of caspase 3 activation in preapoptotic leukemic cells. *Cytometry* 40, 151-160.
- Bleyer, W.A., Sather, H.N., Nickerson, H.J., Coccia, P.F., Finklestein, J.Z., Miller, D.R., Littman, P.S., Lukens, J.N., Siegel, S.E., and Hammond, G.D. (1991). Monthly pulses of vincristine and prednisone prevent bone marrow and testicular relapse in low-risk childhood acute lymphoblastic leukemia: a report of the CCG-161 study by the Childrens Cancer Study Group. *J Clin Oncol* 9, 1012-1021.
- Bodmer, J.L., Holler, N., Reynard, S., Vinciguerra, P., Schneider, P., Juo, P., Blenis, J., and Tschopp, J. (2000). TRAIL receptor-2 signals apoptosis through FADD and caspase-8. *Nature cell biology* 2, 241-243.
- Borenfreund, E., and Puerner, J.A. (1985). Toxicity determined in vitro by morphological alterations and neutral red absorption. *Toxicology letters* 24, 119-124.
- Brockmann, B., Geschke, E., Schmidt, U.M., and Ebeling, K. (1991). [Therapeutic results and toxic side effects of the cytostasan, adriamycin and vincristine combination as second line therapy in metastatic breast cancer]. *Geburtshilfe und Frauenheilkunde* 51, 383-386.
- Cannell, R.J.P. (1998). How to approach isolation of natural products. In *Methods in Biotechnology: Natural Products Isolation*, R.J.P. Cannell, ed. (New Jersey, Humana Press Inc.), pp. 1-51.
- Cardellina, J.H., 2nd, Munro, M.H., Fuller, R.W., Manfredi, K.P., McKee, T.C., Tischler, M., Bokesch, H.R., Gustafson, K.R., Beutler, J.A., and Boyd,

- M.R. (1993). A chemical screening strategy for the dereplication and prioritization of HIV-inhibitory aqueous natural products extracts. *Journal of natural products* 56, 1123-1129.
- Carpentieri, U., and Lockhart, L.H. (1978). Ataxia and athetosis as side effects of chemotherapy with vincristine in non-Hodgkin's lymphoma. *Cancer treatment reports* 62, 561-562.
 - Chang, H.Y., and Yang, X. (2000). Proteases for cell suicide: functions and regulation of caspases. *Microbiol Mol Biol Rev* 64, 821-846.
 - Chapuis, J.C., Sordat, B., and Hostettmann, K. (1988). Screening for cytotoxic activity of plants used in traditional medicine. *Journal of ethnopharmacology* 23, 273-284.
 - Chinkwo, K.A. (2005). *Sutherlandia frutescens* extracts can induce apoptosis in cultured carcinoma cells. *Journal of ethnopharmacology* 98, 163-170.
 - Chinnaiyan, A.M., Chaudhary, D., O'Rourke, K., Koonin, E.V., and Dixit, V.M. (1997). Role of CED-4 in the activation of CED-3. *Nature* 388, 728-729.
 - Clarke, D.J., Johnson, R.T., and Downes, C.S. (1993). Topoisomerase II inhibition prevents anaphase chromatid segregation in mammalian cells independently of the generation of DNA strand breaks. *Journal of cell science* 105 (Pt 2), 563-569.
 - Cordell, G.A., Beecher, C.W., and Pezzuto, J.M. (1991). Can ethnopharmacology contribute to the development of new anticancer drugs? *Journal of ethnopharmacology* 32, 117-133.
 - Cragg, G.M., Boyd, M.R., Cardellina, J.H., 2nd, Newman, D.J., Snader, K.M., and McCloud, T.G. (1994). Ethnobotany and drug discovery: the experience

of the US National Cancer Institute. Ciba Foundation symposium 185, 178-190; discussion 190-176.

- Crooks, P.A., and Rosenthal, G.A. (1994). Use of L-canavanine as a chemotherapeutic agent for the treatment of pancreatic cancer (United States The University of Kentucky Research Foundation).
- Degli-Esposti, M. (1998). Apoptosis: who was first. *Cell Death Diff* 5, 719.
- Edwards, A., Atma-Ram, A., and Thin, R.N. (1988). Podophyllotoxin 0.5% v podophyllin 20% to treat penile warts. *Genitourinary medicine* 64, 263-265.
- Eisenhut, M., Omari, A., and MacLehose, H.G. (2005). Intrarectal quinine for treating Plasmodium falciparum malaria: a systematic review. *Malaria journal* 4, 24.
- Engert, A., Franklin, J., Eich, H.T., Brillant, C., Sehlen, S., Cartoni, C., Herrmann, R., Pfreundschuh, M., Sieber, M., Tesch, H., *et al.* (2007). Two cycles of doxorubicin, bleomycin, vinblastine, and dacarbazine plus extended-field radiotherapy is superior to radiotherapy alone in early favorable Hodgkin's lymphoma: final results of the GHSG HD7 trial. *J Clin Oncol* 25, 3495-3502.
- Eschenfeldt, W.H., and Berger, S.L. (1987). Purification of large double-stranded cDNA fragments. *Methods in enzymology* 152, 335-337.
- Fadok, V.A., Voelker, D.R., Campbell, P.A., Cohen, J.J., Bratton, D.L., and Henson, P.M. (1992). Exposure of phosphatidylserine on the surface of apoptotic lymphocytes triggers specific recognition and removal by macrophages. *J Immunol* 148, 2207-2216.

- Fischer, H., Koenig, U., Eckhart, L., and Tschachler, E. (2002). Human caspase 12 has acquired deleterious mutations. *Biochemical and biophysical research communications* 293, 722-726.
- Freie, B.W., Ciccone, S.L., Li, X., Plett, P.A., Orschell, C.M., Srour, E.F., Hanenberg, H., Schindler, D., Lee, S.H., and Clapp, D.W. (2004). A role for the Fanconi anemia C protein in maintaining the DNA damage-induced G2 checkpoint. *The Journal of biological chemistry* 279, 50986-50993.
- Gill, C., Meyer, M., FitzGerald, U., and Samali, A. (2006). The role of heat shock proteins in the regulation of apoptosis. In *Stress response: a molecular biology approach*, K. India, ed. (India, Research Signpost), pp. 1-25.
- Groninger, E., Meeuwse-de Boer, T., Koopmans, P., Uges, D., Sluiter, W., Veerman, A., Kamps, W., and de Graaf, S. (2005). Vincristine pharmacokinetics and response to vincristine monotherapy in an up-front window study of the Dutch Childhood Leukaemia Study Group (DCLSG). *Eur J Cancer* 41, 98-103.
- Hadfield, J.A., Ducki, S., Hirst, N., and McGown, A.T. (2003). Tubulin and microtubules as targets for anticancer drugs. *Progress in cell cycle research* 5, 309-325.
- Harris, C.C., and Hollstein, M. (1993). Clinical implications of the p53 tumor-suppressor gene. *The New England journal of medicine* 329, 1318-1327.
- Hengartner, M.O. (2000). The biochemistry of apoptosis. *Nature* 407, 770-776.

- Henwood, J.M., and Brogden, R.N. (1990). Etoposide. A review of its pharmacodynamic and pharmacokinetic properties, and therapeutic potential in combination chemotherapy of cancer. *Drugs* 39, 438-490.
- Hitomi, J., Katayama, T., Taniguchi, M., Honda, A., Imaizumi, K., and Tohyama, M. (2004). Apoptosis induced by endoplasmic reticulum stress depends on activation of caspase-3 via caspase-12. *Neuroscience letters* 357, 127-130.
- Hutchins, J.B., and Barger, S.W. (1998). Why neurons die: cell death in the nervous system. *The Anatomical record* 253, 79-90.
- Jellinger, K.A. (2001). Cell death mechanisms in neurodegeneration. *Journal of cellular and molecular medicine* 5, 1-17.
- Johnson, J.D., Ahmed, N.T., Luciani, D.S., Han, Z., Tran, H., Fujita, J., Mislser, S., Edlund, H., and Polonsky, K.S. (2003). Increased islet apoptosis in Pdx1^{+/-} mice. *The Journal of clinical investigation* 111, 1147-1160.
- Jordan, M.A., and Wilson, L. (1998). Microtubules and actin filaments: dynamic targets for cancer chemotherapy. *Current opinion in cell biology* 10, 123-130.
- Julien, S., Jacoulet, P., Dubiez, A., Westeel, V., and Depierre, A. (1999). [Non-small-cell bronchial cancers: long-term survival after single drug chemotherapy with vinorelbine]. *Revue de pneumologie clinique* 55, 205-210.
- Kang, M.H., Kang, Y.H., Szymanska, B., Wilczynska-Kalak, U., Sheard, M.A., Harned, T., Lock, R.B., and Reynolds, C.P. (2007). Activity of vincristine, L-ASP, and dexamethasone against acute lymphoblastic leukemia is enhanced by the BH3-mimetic ABT-737 in vitro and in vivo. *Blood*.

- Kerr, J.F., Wyllie, A.H., and Currie, A.R. (1972). Apoptosis: a basic biological phenomenon with wide-ranging implications in tissue kinetics. *British journal of cancer* 26, 239-257.
- Kitagawa, R., Bakkenist, C.J., McKinnon, P.J., and Kastan, M.B. (2004). Phosphorylation of SMC1 is a critical downstream event in the ATM-NBS1-BRCA1 pathway. *Genes & development* 18, 1423-1438.
- Kroemer, G., Dallaporta, B., and Resche-Rigon, M. (1998). The mitochondrial death/life regulator in apoptosis and necrosis. *Annual review of physiology* 60, 619-642.
- Kurokawa, H., Nishio, K., Fukumoto, H., Tomonari, A., Suzuki, T., and Saijo, N. (1999). Alteration of caspase-3 (CPP32/Yama/apopain) in wild-type MCF-7, breast cancer cells. *Oncology reports* 6, 33-37.
- Li, L.Y., Luo, X., and Wang, X. (2001). Endonuclease G is an apoptotic DNase when released from mitochondria. *Nature* 412, 95-99.
- Lockshin, R.A., and Williams, C.M. (1964). Programmed cell death. II. Endocrine potentiation of the breakdown of the intersegmental muscles of silkmoths. *J Insect Physiol* 10, 643-649
- Long, B.H., and Fairchild, C.R. (1994). Paclitaxel inhibits progression of mitotic cells to G1 phase by interference with spindle formation without affecting other microtubule functions during anaphase and telephase. *Cancer research* 54, 4355-4361.
- Mailhos, C., Howard, M.K., and Latchman, D.S. (1993). Heat shock protects neuronal cells from programmed cell death by apoptosis. *Neuroscience* 55, 621-627.

- Matsuda, N., Tanaka, H., Yamazaki, S., Suzuki, J., Tanaka, K., Yamada, T., and Masuda, M. (2006). HIV-1 Vpr induces G2 cell cycle arrest in fission yeast associated with Rad24/14-3-3-dependent, Chk1/Cds1-independent Wee1 upregulation. *Microbes and infection / Institut Pasteur* 8, 2736-2744.
- Matthews, C.K., and Van Holde, K.E. (1990). *Biochemistry* (New York, Benjamin / Cummings Publishing Company, Inc.).
- McWhirter, A., Oakes, D., and Steyn, A. (1996). *Reader's Digest: Illustrated Encyclopedia of Essential Knowledge* (Cape Town, Reader's Digest Association (Pty) Limited).
- Meier, P., Finch, A., and Evan, G. (2000). Apoptosis in development. *Nature* 407, 796-801.
- Merad-Boudia, M., Nicole, A., Santiard-Baron, D., and Saille, C. (1998). Ceballos-Picot I. Mitochondrial impairment as an early event in the process of apoptosis induced by glutathione depletion in neuronal cells: relevance to Parkinson's disease. *Bioch Pharmacol* 56, 645-655.
- Miceli, N., Taviano, M.F., Giuffrida, D., Trovato, A., Tzakou, O., and Galati, E.M. (2005). Anti-inflammatory activity of extract and fractions from *Nepeta sibthorpii* Bentham. *Journal of ethnopharmacology* 97, 261-266.
- Morris, E.J., and Geller, H.M. (1996). Induction of neuronal apoptosis by camptothecin, an inhibitor of DNA topoisomerase-I: evidence for cell cycle-independent toxicity. *The Journal of cell biology* 134, 757-770.
- Ngan, V.K., Bellman, K., Hill, B.T., Wilson, L., and Jordan, M.A. (2001). Mechanism of mitotic block and inhibition of cell proliferation by the

semisynthetic Vinca alkaloids vinorelbine and its newer derivative vinflunine. *Molecular pharmacology* 60, 225-232.

- Nollen, E.A., and Morimoto, R.I. (2002). Chaperoning signaling pathways: molecular chaperones as stress-sensing 'heat shock' proteins. *Journal of cell science* 115, 2809-2816.
- Ohno, T., Nagatsu, A., Nakagawa, M., Inoue, M., Li, Y.M., Minatoguchi, S., Mizukami, H., and Fujiwara, H. (2005). New sesquiterpene lactones from water extract of the root of *Lindera strychnifolia* with cytotoxicity against the human small cell lung cancer cell, SBC-3. *Tetra Lett* 46, 8657-8660
- Page, J.E. (2005). Silencing nature's narcotics: metabolic engineering of the opium poppy. *Trends in biotechnology* 23, 331-333.
- Peter, M.E., and Krammer, P.H. (2003). The CD95(APO-1/Fas) DISC and beyond. *Cell death and differentiation* 10, 26-35.
- Phelps, W.C., Bagchi, S., Barnes, J.A., Raychaudhuri, P., Kraus, V., Munger, K., Howley, P.M., and Nevins, J.R. (1991). Analysis of trans activation by human papillomavirus type 16 E7 and adenovirus 12S E1A suggests a common mechanism. *Journal of virology* 65, 6922-6930.
- Puckree, T., Mkhize, M., Mgobhozi, Z., and Lin, J. (2002). African traditional healers: what health care professionals need to know. *International journal of rehabilitation research Internationale Zeitschrift fur Rehabilitationsforschung* 25, 247-251.
- Raff, M.C., Barres, B.A., Burne, J.F., Coles, H.S., Ishizaki, Y., and Jacobson, M.D. (1993). Programmed cell death and the control of cell survival: lessons from the nervous system. *Science (New York, NY)* 262, 695-700.

- Rathmell, J.C., and Thompson, C.B. (2002). Pathways of apoptosis in lymphocyte development, homeostasis, and disease. *Cell 109 Suppl*, S97-107.
- Ren, Y., and Savill, J. (1998). Apoptosis: the importance of being eaten. *Cell Death Differ* 5, 563-568.
- Robards, K., Haddad, P., and Jackson, P. (2002). Principles and practice of modern chromatographic methods (New York, Academic Press).
- Rothenberg, M.L., Liu, P.Y., Wilczynski, S., Nahhas, W.A., Winakur, G.L., Jiang, C.S., Moinpour, C.M., Lyons, B., Weiss, G.R., Essell, J.H., *et al.* (2004). Phase II trial of vinorelbine for relapsed ovarian cancer: a Southwest Oncology Group study. *Gynecologic oncology* 95, 506-512.
- Sakahira, H., Enari, M., and Nagata, S. (1998). Cleavage of CAD inhibitor in CAD activation and DNA degradation during apoptosis. *Nature* 391, 96-99.
- Samali, A., Cai, J., Zhivotovsky, B., Jones, D.P., and Orrenius, S. (1999). Presence of a pre-apoptotic complex of pro-caspase-3, Hsp60 and Hsp10 in the mitochondrial fraction of jurkat cells. *The EMBO journal* 18, 2040-2048.
- Samuel, R., Stuessy, T.F., Tremetsberger, K., Baeza, C.M., and Siljak-Yakovlev, S. (2003). Phylogenetic relationships among species of *Hypochaeris* (Asteraceae, Cichorieae) based on ITS, plastid trnL intron, trnL-F spacer, and matK sequences. *American J Botany* 90, 496-507.
- Savage, S.A., Burdett, L., Troisi, R., Douglass, C., Hoover, R.N., and Chanock, S.J. (2007). Germ-line genetic variation of TP53 in osteosarcoma. *Pediatric blood & cancer* 49, 28-33.
- Savill, J. (1996). Phagocyte recognition of apoptotic cells. *Biochemical Society transactions* 24, 1065-1069.

- Scheffner, M., Munger, K., Byrne, J.C., and Howley, P.M. (1991). The state of the p53 and retinoblastoma genes in human cervical carcinoma cell lines. *Proceedings of the National Academy of Sciences of the United States of America* 88, 5523-5527.
- Schiff, P.B., Fant, J., and Horwitz, S.B. (1979). Promotion of microtubule assembly in vitro by taxol. *Nature* 277, 665-667.
- Schiff, P.B., and Horwitz, S.B. (1980). Taxol stabilizes microtubules in mouse fibroblast cells. *Proceedings of the National Academy of Sciences of the United States of America* 77, 1561-1565.
- Schiff, P.B., and Horwitz, S.B. (1981). Taxol assembles tubulin in the absence of exogenous guanosine 5'-triphosphate or microtubule-associated proteins. *Biochemistry* 20, 3247-3252.
- Sezik, E., Aslan, M., Yesilada, E., and Ito, S. (2005). Hypoglycaemic activity of *Gentiana olivieri* and isolation of the active constituent through bioassay-directed fractionation techniques. *Life sciences* 76, 1223-1238.
- Shiraishi, H., Okamoto, H., Yoshimura, A., and Yoshida, H. (2006). ER stress-induced apoptosis and caspase-12 activation occurs downstream of mitochondrial apoptosis involving Apaf-1. *Journal of cell science* 119, 3958-3966.
- Singh, A., Ni, J., and Aggarwal, B.B. (1998). Death domain receptors and their role in cell demise. *J Interferon Cytokine Res* 18, 439-450.
- Sneller, M.C., Wang, J., Dale, J.K., Strober, W., Middleton, L.A., Choi, Y., Fleisher, T.A., Lim, M.S., Jaffe, E.S., Puck, J.M., *et al.* (1997). Clinical, Immunologic, and Genetic Features of an Autoimmune Lymphoproliferative

Syndrome Associated With Abnormal Lymphocyte Apoptosis. *Blood* 89 1341-1348.

- Solomon, M., Belenghi, B., Delledonne, M., Menachem, E., and Levine, A. (1999). The involvement of cysteine proteases and protease inhibitor genes in the regulation of programmed cell death in plants. *The Plant cell* 11, 431-444.
- Stokoe, C.T., Ogden, J., and Jain, V.K. (2001). Activity of infusional etoposide, vincristine, and doxorubicin with bolus cyclophosphamide (EPOCH) in relapsed Hodgkin's disease. *The oncologist* 6, 428-434.
- Studzinski, G.P. (1999). Overview of apoptosis. In *Apoptosis: A practical approach*, G.P. Studzinski, ed. (New York, Oxford University Press), p. 8.
- Swaffar, D.S., Ang, C.Y., Desai, P.B., and Rosenthal, G.A. (1994). Inhibition of the growth of human pancreatic cancer cells by the arginine antimetabolite L-canavanine. *Cancer research* 54, 6045-6048.
- Tai, J., Cheung, S., Chan, E., and Hasman, D. (2004). In vitro culture studies of *Sutherlandia frutescens* on human tumor cell lines. *Journal of ethnopharmacology* 93, 9-19.
- Taniguchi, T., Garcia-Higuera, I., Andreassen, P.R., Gregory, R.C., Grompe, M., and D'Andrea, A.D. (2002). S-phase-specific interaction of the Fanconi anemia protein, FANCD2, with BRCA1 and RAD51. *Blood* 100, 2414-2420.
- Thatte, U., Bagadey, S., and Dahanukar, S. (2000). Modulation of programmed cell death by medicinal plants. *Cellular and molecular biology (Noisy-le-Grand, France)* 46, 199-214.
- Uchida, J., Okada, H., Ohguchi, N., Kawa, G., Koyama, Y., Mikami, O., Kawamura, H., Ohhara, T., and Matsuda, T. (1997). [Comparison of side

effects caused by intra-arterial and intravenous infusion of M-VAC (methotrexate, vinblastine, adriamycin and cisplatin) for urothelial cancer]. *Hinyokika kiyo* 43, 637-640.

- Vacca, A., Ribatti, D., Iurlaro, M., Merchionne, F., Nico, B., Ria, R., and Dammacco, F. (2002). Docetaxel versus paclitaxel for antiangiogenesis. *Journal of hematotherapy & stem cell research* 11, 103-118.
- Van Cruchten, S., and Van Den Broeck, W. (2002). Morphological and biochemical aspects of apoptosis, oncosis and necrosis. *Anat Histol Embryol* 31, 214-223.
- van Luijk, I.F., Coens, C., van der Burg, M.E., Kobierska, A., Namer, M., Lhomme, C., Zola, P., Zanetta, G., and Vermorken, J.B. (2007). Phase II study of bleomycin, vindesine, mitomycin C and cisplatin (BEMP) in recurrent or disseminated squamous cell carcinoma of the uterine cervix. *Ann Oncol* 18, 275-281.
- Van Wyk, B.E., van Oudtshoorn, B., and Gericke, N. (2000). Medicinal plant of South Africa, Vol 1 (Pretoria, Briza Publications).
- Vermes, I., Haanen, C., Steffens-Nakken, H., and Reutelingsperger, C. (1995). A novel assay for apoptosis. Flow cytometric detection of phosphatidylserine expression on early apoptotic cells using fluorescein labelled Annexin V. *Journal of immunological methods* 184, 39-51.
- Vogelstein, B., Lane, D., and Levine, A.J. (2000). Surfing the p53 network. *Nature* 408, 307-310.
- Wang, X., Wang, J., Gengyo-Ando, K., Gu, L., Sun, C.L., Yang, C., Shi, Y., Kobayashi, T., Shi, Y., Mitani, S., *et al.* (2007). *C. elegans* mitochondrial

factor WAH-1 promotes phosphatidylserine externalization in apoptotic cells through phospholipid scramblase SCRM-1. *Nature cell biology* 9, 541-549.

- White, T.J., Bruns, T., Lee, S., and Taylor, J.W. (1990). Amplification and direct sequencing of fungal ribosomal RNA genes for phylogenetics. In *PCR Protocols: A Guide to Methods and Applications*, J. Gelfand, J. Sninsky, and T. White, eds. (New York, Academic Press, Inc.), pp. 315-322
- Wink, M. (1999). Introduction: Functions of plant secondary metabolites and their exploitation in biotechnology
- In *Annual Plant Reviews: Functions of plant secondary metabolites and their exploitation in biotechnology*, R. J., ed. (Sheffield, Sheffield Academic Press Ltd), pp. 1-16.
- Wu, J.Y., Fong, W.F., Zhang, J.X., Leung, C.H., Kwong, H.L., Yang, M.S., Li, D., and Cheung, H.Y. (2003). Reversal of multidrug resistance in cancer cells by pyranocoumarins isolated from *Radix Peucedani*. *European journal of pharmacology* 473, 9-17.
- Yamane, K., Taylor, K., and Kinsella, T.J. (2004). Mismatch repair-mediated G2/M arrest by 6-thioguanine involves the ATR-Chk1 pathway. *Biochemical and biophysical research communications* 318, 297-302.
- Yang, S.H., and Loopstra, C.A. (2005). Seasonal variation in gene expression for loblolly pines (*Pinus taeda*) from different geographical regions. *Tree physiology* 25, 1063-1073.
- Yoo, Y.D., Park, J.K., Choi, J.Y., Lee, K.H., Kang, Y.K., Kim, C.S., Shin, S.W., Kim, Y.H., and Kim, J.S. (1998). CDK4 down-regulation induced by

paclitaxel is associated with G1 arrest in gastric cancer cells. *Clin Cancer Res* 4, 3063-3068.

- Zhao, Y., Wu, M., Shen, Y., and Zhai, Z. (2001). Analysis of nuclear apoptotic process in a cell-free system. *Cell Mol Life Sci* 58, 298-306.

